

**DEVELOPMENT OF A RAPID TEST TO DETERMINE MOISTURE
SENSITIVITY OF HMA (SUPERPAVE) MIXTURES**

By

Harihar Shiwakoti

Submitted to the Department of Civil, Environmental, and Architectural Engineering
and the Graduate Faculty of the University of Kansas in partial fulfillment of the
requirements for the degree of Master's of Science.

Dr. Jie Han, Chairperson

Committee members

Dr. Robert L. Parsons

Dr. Steven D. Schrock

Date defended: _____

The Thesis Committee for Harihar Shiwakoti certifies

That this is the approved version of the following thesis:

DEVELOPMENT OF RAPID TEST TO DETERMINE MOISTURE SENSITIVITY
OF HMA (SUPERPAVE) MIXTURES

Committee:

Dr. Jie Han, Chairperson

Dr. Robert L. Parsons

Dr. Steven D. Schrock

Date approved: _____

Acknowledgement

First and foremost I would like to express my gratefulness to my advisor Dr. Jie Han for providing me opportunity to work in this interesting project and for his continuous encouragement and valuable suggestions throughout this research project. I would like to thank Dr. Robert L. Parsons and Dr. Steven D. Schrock for their support and time.

I got great cooperation from Mr. Chandra Manandhar, Ph.D. candidate in Kansas State University throughout the project and my friend Justin Clay during the entire process of sample preparation. This project would not have come to this stage without great support from our lab supervisor Mr. Jim Weaver. I express my special thanks to all of them.

I would also like to thank all of my fellow classmates in the KU Geotechnical Society who always helped and supported me when I needed. All my friends who encouraged me continuously and provided moral support also deserve my thanks.

Finally, I would like to express my emotional gratitude to my parents back home in Nepal for all the support, understanding, and encouragement they have provided to me.

Table of Contents

Abstract	vi
List of Tables	vii
List of Figures	viii
1. INTRODUCTION	1
1.1. Problem Statement	1
1.2. Objective	2
1.3. Organization.....	3
2. LITERATURE REVIEW	5
2.1. Mechanisms of Moisture Damage in HMA.....	5
2.2. Nature of Asphalt-aggregate Interaction.....	14
2.3. Test Methods to Predict Moisture Sensitivity in HMA	24
2.4. Techniques for Limiting Moisture Sensitivity	47
3. EXPERIMENTAL STUDY	51
3.1. Introduction.....	51
3.2. Test Equipment	57
3.2.1 Superpave Gyratory Compactor	57
3.2.2 Hamburg Wheel Testing Device.....	58
3.2.3 Asphalt Pavement Analyzer.....	59
3.3. Test Procedure	67
3.3.1 Sample preparation	67
3.3.2 Sample conditioning and testing.....	73

4. TEST RESULTS AND ANALYSIS	76
4.1. Introduction.....	76
4.2. Visual Observation of Stripping Phenomenon	76
4.3 Test Results and Analysis	79
4.3.1 District 2 (2G06015A -Wet 50°C).....	80
4.3.2 District 3 (3G06020A -Wet 50°C).....	84
4.3.3 District 5 (5G06016A -Wet 50°C).....	88
4.3.4 District 6 (6G06011A -Wet 50°C).....	92
4.3.7 District 6 (6G07002A -Wet 60°C).....	106
4.3.8 District 6 (6G07002A -Dry 50°C).....	107
4.3.9 District 6 (6G07002A –Dry 60°C).....	108
4.4 Comparisons of Test Results for District 6 - 6G07002A Mix	109
4.4.1 Wet vs. dry tests at 50°C	109
4.4.2 Wet vs. dry tests at 60°C	110
4.4.3 Wet tests at 50°C vs. 60°C	111
4.4.4 Dry tests at 50°C vs. 60°C.....	112
4.4.5 Samples prepared at KSU vs. KU.....	112
5. CONCLUSIONS AND RECOMMENDATIONS.....	119
5.1. Conclusions.....	119
5.2. Recommendations.....	120
Appendix – APA Test Data	133

Abstract

Existing test methods to determine moisture sensitivity in hot mix asphalt are time consuming and inconsistent. This research focused on wheel tracking devices to develop a rapid test method to evaluate moisture sensitivity. The Asphalt Pavement Analyzer (APA) and the Hamburg Wheel Tracking Device (HWTD) were used for this research. Compacted cylindrical samples were fabricated using the Superpave Gyrotory Compactor. Results show that although most mixes without any additive show stripping behavior, APA results do not indicate any stripping inflection points. The HWTD results show stripping inflection points. The APA results show wet tests are severe at lower temperatures whereas dry tests show high rut depth at higher temperatures. The HWTD results show improvement in the performance by the use of anti-stripping agents at later stage. Further studies should be carried out using HWTD to relate number of passes for stripping inflection point with severity of stripping. Lab results should be correlated with field performance.

List of Tables

Table 2-1 Gibbs free energy per unit mass (ergs/gm \times 103) (Cheng et al. 2002)	19
Table 2-2 Moisture sensitivity tests on loose samples (Solaimaninan et al., 2003)	25
Table 2-3 Moisture sensitivity tests on compacted samples (Solaimaninan et al., 2003)	25
Table 2-4 Summary of test parameters for AASHTO T283 (Aschenbrener 1996)	32
Table 2-5 Summary of ECS test procedure (Ashenbrener 1996)	34
Table 2-6 CalTrans low environmental risk zone	50
Table 2-7 CalTrans moderate and high environmental risk zones	50
Table 3-1 Samples made for APA and Hamburg tests	52
Table 3-2 Project Information	54
Table 4-1 Summary of tests carried out on different mixes.	77
Table 4-2 Aggregate-binder types D2: 2G06015A	80
Table 4-3 Aggregate-binder types D3: 3G06020A	84
Table 4-4 Aggregate-binder types D5: 5G06016A	88
Table 4-5 Aggregate-binder types D6: 6G06011A	92
Table 4-6 Aggregate-binder types D6: 6G06016A	96
Table 4-7 Aggregate-binder types D6: 6G07002A	100
Table 5-1 Summary of test results	115

List of Figures

Figure 2-1 Factors considered in moisture damage analysis.....	12
Figure 2-2 Interpretation of ECS Modular Curve.....	36
Figure 3-1 Pine Superpave Gyrotory Compactor Control Panel	58
Figure 4-1 Stripping in samples without additive (Left) and non stripping with additive (right)	78
Figure 4-2 Close up view of the left sample in Figure 4-1	78
Figure 4-3 Rut depth vs. number of cycles from the APA tests of D2-2G06015A mix (50°C wet).....	81
Figure 4-4 Rut depth vs. number of cycles from the HWTD tests of D2-2G06015A mix (50°C wet).....	82
Figure 4-5 Rut depth vs. number of cycles from the APA and the HWTD Tests of D2-2G06015A mix (50°C wet).....	83
Figure 4-6 Rut depth vs. number of cycles from the APA tests of D3-3G06020A mix (50°C wet).....	85
Figure 4-7 Rut depth vs. number of cycles from the HWTD tests of D3-3G06020A mix (50°C wet).....	86
Figure 4-8 Rut depth vs. number of cycles from the APA and the HWTD tests of D3- 3G06020A mix (50°C wet).....	87
Figure 4-9 Rut depth vs. number of cycles from the APA tests of D5-5G06016A mix (50°C wet).....	89

Figure 4-10 Rut depth vs. number of cycles from the HWTD tests of D5-5G06016A mix (50°C wet).....	90
Figure 4-11 Rut depth vs. number of cycles from APA and the HWTD tests of D5-5G06016A mix (50°C wet).....	91
Figure 4-12 Rut depth vs. number of cycles from the APA tests of D6-6G06011A mix (50°C wet).....	93
Figure 4-13 Rut depth vs. number of cycles from the HWTD tests of D6-6G06011A mix (50°C wet).....	94
Figure 4-14 Rut depth vs. number of cycles from the APA and the HWTD tests of D6-6G06011A mix (50°C wet).....	95
Figure 4-15 Rut depth vs. number of cycles from the APA tests of D6-6G06016A mix (50°C wet).....	97
Figure 4-16 Rut depth vs. number of cycles from the HWTD tests of D6-6G06016A mix (50°C wet).....	98
Figure 4-17 Rut depth vs. number of cycles from the APA and the HWTD tests of D6-6G06016A mix (50°C wet).....	99
Figure 4-18 Rut depth vs. number of cycles from the APA tests of D6-6G07002A mix (samples prepared at KSU, 50°C wet).....	102
Figure 4-19 Rut depth vs. number of cycles from the APA tests of D6-6G07002A mix (samples prepared at KU, 50°C wet).....	103
Figure 4-20: Rut vs. number of cycles from the HWTD tests of D6-6G07002A mix (samples prepared at KSU, 50°C wet).....	104

Figure 4-21 Rut depth vs. number of cycles from the APA and the HWTD tests of D6-6G07002A mix (50°C wet).....	105
Figure 4-22: Rut depth vs. number of cycles from the APA tests of D6-6G07002A mix (60°C wet).....	106
Figure 4-23 Rut depth vs. number of cycles from the APA tests of D6-6G07002A mix (50°C dry)	107
Figure 4-24 Rut depth vs. number of cycles from the APA tests of D6-6G07002A mix (60°C dry)	108
Figure 4-25 Rut depths for samples tested under wet 50°C vs. dry 50°C.....	109
Figure 4-26 Rut depths for samples tested under wet 60°C vs. dry 60°C.....	111
Figure 4-27 Wet tests at 50°C vs. 60°C.....	111
Figure 4-28 Dry tests at 50°C vs. 60°C.....	112
Figure 4-29: Samples made at KSU vs. KU	113

1. INTRODUCTION

1.1. Problem Statement

The Kansas Department of Transportation (KDOT) is increasingly using Superpave mixtures. The moisture susceptibility or stripping which causes loss of bonding between aggregate and binder is currently evaluated by the Kansas Standard Test Method KT-56. KT-56 is similar to the American Association of State Highway Transportation Officials (AASHTO) T-283 procedure adopted during the Superpave research but has minor modifications in the conditioning procedure. According to current KDOT specifications for Superior Performing Asphalt Pavements (Superpave) mixes, this KT-56 test at best takes 4 days to run and takes two failing tests to shut down the production. This requirement potentially can result in eight days of Superpave mixture production that could be susceptible to stripping. Another criticism on the current test procedure is that the use of anti-stripping agents could rectify the low Tensile Strength Ratio (TSR) or make the mixture meet the minimum TSR requirements. Instead of increasing the conditioned strength, the current test procedure lowers the tensile strength of the anti-stripping treated unconditioned specimen. This problem with the AASHTO T-283/KDOT KT-56 procedure has been recognized at the national level and the National Cooperative Highway Research Program (NCHRP) Project 9-34 - Improved Conditioning Procedure for Predicting the Moisture Susceptibility of Hot Mix Asphalt (HMA) Pavements looked into the

conditioning procedure of the AASHTO T-283. This project investigated the possibility of correlating the moisture sensitivity of paving mixes measured with the Environmental Conditioning System (ECS)/dynamic modulus (from the Simple Performance Tester) combination to (a) the known field performance of the mixes and (b) their moisture sensitivity measured with the Hamburg Wheel Tracking Device (HWTd) test method and the ASTM method D 4867 (moisture sensitivity test). The study showed that the HWTd identified moisture susceptibility of six Superpave mixtures out of eight tested (75% success rate). Some state agencies have already adopted “wheel tracking” type tests like the HWTd and the Asphalt Pavement Analyzer (APA) to evaluate moisture sensitivity of Superpave mixtures. Notables are Texas, Colorado, and Georgia. Research at Kansas State University (Gogula et al., 2003) demonstrated that the HWTd is capable of identifying moisture sensitivity of Superpave mixtures in Kansas.

1.2. Objective

Moisture sensitivity (also known as “stripping”) is one of the major problems in HMA pavements, potentially leading to premature pavement distress. Moisture damage in asphalt pavements can occur either by adhesive fracture, i.e. failure at the aggregate-mastic interface or cohesive fracture, i.e. failure within the mastic. Tests to determine moisture sensitivity suffer from inconsistency and the results from laboratory tests may not correlate well with field experiences. Extensive research is

still needed for wheel tracking devices such as the HWTD and the APA before they can be considered as rapid tests useful in evaluating moisture susceptibility. The objective of the present research is to develop a rapid test to determine moisture sensitivity of HMA (Superpave) mixtures. In cooperation with KDOT, research was carried out jointly at the University of Kansas (KU) and the Kansas State University (KSU). Six superpave mixtures were selected for evaluation. HWTD tests were conducted at KSU. APA tests were conducted at KU. The results obtained from these tests are analyzed to evaluate how well they can detect moisture sensitivity.

1.3. Organization

This thesis contains five chapters:

Chapter 1 presents the statement of the problem, the objective of the research and the organization of the thesis.

Chapter 2 provides a literature review of the mechanisms of water induced damage in hot mix asphalt pavements, the state of the research to evaluate the moisture damage, and the techniques for remedying the stripping damage.

Chapter 3 documents the experimental study carried on for the present research, which includes the use of the equipment, the preparation of the samples, and the test procedures.

Chapter 4 presents the test results obtained from the experimental study using APA and Hamburg test methods. Analysis and comparison of these test results are provided.

Chapter 5 summarizes the test results and makes conclusions and recommendations based on this research.

Data of the APA tests are presented in the Appendix at the end of this thesis.

2. LITERATURE REVIEW

2.1. Mechanisms of Moisture Damage in HMA

Asphalt mixtures lose their strength and durability due to effects of moisture, termed as moisture damage. This damage can occur due to loss of bond between asphalt cement or the mastic (asphalt cement plus the mineral filler minus 74 μm and smaller aggregate) and the fine and coarse aggregate. When water permeates, the mastic is weakened so that it is more susceptible to damage during cyclic traffic loading.

Little and Jones (2003) identified six contributing mechanisms to moisture damage: detachment, displacement, spontaneous emulsification, pore pressure-induced damage, hydraulic scour, and the effects of the environment on the aggregate-asphalt system.

2.1.1 Detachment

Detachment is the separation of an asphalt film from an aggregate surface by a thin film of water without an obvious break in the film (Majidzadeh and Brovold, 1968). According to Majidzadeh and Brovold (1968), if a three-phase interface consisting of aggregate, asphalt, and water exist, water reduces the free energy of the system more than asphalt to form a thermodynamically stable condition of minimum surface energy. Little and Jones (2003) indicated that the aggregate surface has a strong

preference for water over asphalt. Water has lower viscosity and surface tension than asphalt. Thus it is a better wetting agent.

Little and Jones (2003) also concluded that most asphalts have relatively low polar activity and the bond between the aggregate and asphalt is mainly due to relatively weak dispersion forces. Water molecules are, on the other hand, highly polar and can replace the asphalt at the asphalt–aggregate interface.

2.1.2 Displacement

Displacement differs from detachment because it involves displacement of asphalt at the aggregate surface through a break in the asphalt film (Tarrer and Wagh, 1991). Displacement often results from incomplete coating of the aggregate surface, rupture of the film at sharp aggregate corners or edges, pinholes originating in the asphalt film because of aggregate coatings.

The process of displacement can proceed through the changes in the pH value of the water at the aggregate surface, which enters through the point of disruption. These changes alter the type of adsorbed polar groups, which lead to the buildup of opposite, and negatively charged electrical double layers on the aggregate and asphalt surfaces. The drive to reach equilibrium attracts more water and leads to physical separation of the asphalt from the aggregate (Tarrer and Wagh 1991).

2.1.3 Spontaneous emulsification

Spontaneous emulsification is an inverted emulsion of water droplets in asphalt cement. Fromm (1974) demonstrated how an emulsion forms and the adhesive bond is broken once the emulsion formation penetrates the substrata. Literature indicates that the formation of such emulsions is further aggravated by the presence of emulsifiers such as clays and asphalt additives. Fromm (1974) observed that spontaneous emulsification occurs when asphalt films are immersed in water and that the rate of emulsification depends on the nature of the asphalt and the presence of additives. Organic amines, which are basic nitrogen compounds, can bond strongly to aggregates in the presence of water (Robertson 2000). Kiggundu (1986) demonstrated how the rate of emulsification is dependent on the nature and viscosity of asphalt, with AC-5 asphalt emulsifying in distilled water much faster than AC-10 asphalt. Kiggundu (1986) also demonstrated that this process is reversible upon drying.

2.1.4 Pore pressure

Pore pressure is developed under traffic loading when water is entrapped in asphalt concrete. Stresses imparted to the entrapped water from repeated traffic load applications will worsen the damage as the continued buildup in pore pressure disrupts the asphalt film from the aggregate surface or can cause the growth of microcracks in the asphalt mastic. Bhairampally et al. (2000) used a tertiary damage

model developed by Tseng and Lytton (1987) to demonstrate that well-designed asphalt mixtures tend to “strain harden” on repeated loading. Little and Jones (2003) indicated that this “strain hardening” differs from the classical strain hardening occurring when metals are cold-worked to develop interactive dislocations to prevent slip, instead, strain hardening seen in asphalt concrete is due to the “locking” of the aggregate matrix caused by densification during repeated loading.

Some mixtures also exhibit microcracks in the mastic under heavy repeated loading. The formation of cracks results in progressive cohesive or adhesive failure, or both. In the presence of water, the rate of formation of cracks increases due to the pore pressure in the microcracks voids. Terrel and Al-Swailmi (1994) described the concept of pessimum air voids, i.e., the range of air void contents within which most asphalt mixtures are typically compacted (between about 8% and 10%). Above this level the air voids become interconnected and moisture can flow out under a stress gradient developed by traffic loading. Below this value the air voids are disconnected and are relatively impermeable and thus do not become saturated with water. Within the pessimum range, water can enter the voids but cannot escape freely. The presence of such water causes the increase in pore pressure when subjected to loading.

2.1.5 Hydraulic scour

Hydraulic scour occurs from the action of tires on a saturated pavement surface. Water is sucked under the tire into the pavement by the tire action. Osmosis and pullback have been suggested as possible mechanisms of scour (Fromm, 1974). Fromm (1974) indicated that osmosis occurs in the presence of salts or salt solutions in aggregate pores and creates an osmotic pressure gradient that actually sucks water through the asphalt film. Fromm (1974)'s explanation is in agreement with Mack's (1964) while Thelen (1958) pointed out that osmosis is a slow process so that it cannot be the reason. However, several factors affect the potential occurrence of this mechanism including the facts that some asphalt is treated with caustics during manufacture, some aggregates possess salts (compositionally), and asphalt films are permeable. Cheng et al. (2002) demonstrated that the diffusion of water vapor through asphalt cement itself is considerable and asphalt mastics can hold a rather surprisingly large amount of water. Cheng et al. (2002) have shown that the amount of water held by asphalt is related to the level of moisture damage that occurs in the mixtures using that asphalt.

2.1.6 pH instability

Little and Jones (2003) mention Scott (1978) and Yoon (1987) demonstrated that asphalt–aggregate adhesion is strongly influenced by the pH value of the contact water. Kennedy et al. (1984) investigated the effect of various sources of water on

the level of damage that occurred in a boiling test. Scott (1978) observed that the value of interfacial tension between asphalt and glass peaked at intermediate pH values, up to about 9, and then dropped as pH increased. Yoon (1987) found that the pH of contact water was aggregate-specific and increased with duration of contact then stabilized after approximately 5 to 10 minutes of boiling. Yoon (1987) determined that the coating retention in boiling tests decreased as pH increased. Kiggundu and Roberts (1988) pointed out that stabilization of the pH sensitivity at the asphalt–aggregate interface can minimize the potential for bond breakage, provide strong, durable bonds, and reduce stripping.

Tarrer (1996) concluded that (a) the bond between asphalt and aggregate depends on surface chemical activity, (b) water at the aggregate surface (in the field) has a high pH, (c) some liquids used as anti-stripping agents require a long curing period (in excess of about 3 hours) to achieve resistance to loss of bond at higher pH levels, and (d) it is possible to achieve a strong chemical bond between aggregate and asphalt cement that is resistant to pH shifts and a high pH environment. This strong chemical bond can be achieved by the formation of insoluble organic salts (such as calcium-based salts), which form rapidly and are not affected by high pH levels or pH shifts.

Little and Jones (2003) indicated that pH values as high as 9 or 10 do not dislodge amines from the acidic surfaces of aggregates, nor do they affect hydrated lime.

Values of pH greater than 10 are not normally developed in asphalt mixtures unless a caustic such as lime is added. However, pH values below approximately 4 can dislodge amines from an aggregate surface and can dissolve lime depending on the type of acid used; these low pH values are not found in hot-mix asphalt.

2.1.7 Environmental effects on the aggregate–asphalt system

Terrel and Shute (1989) reported that factors such as temperature, air, and water have a profound effect on the durability of asphalt concrete mixtures. In mild climates, when good-quality aggregates and asphalt cements are available, the major contribution to deterioration is traffic loading. Premature failure may occur when poor materials and traffic are coupled with severe weather. Terrel and Al-Swailmi (1994) identified a number of environmental factors of concern: water from precipitation or groundwater sources, temperature fluctuations (including freeze–thaw conditions), and aging of the asphalt. They considered traffic and construction techniques as important factors external to the environment.

Cohesion in the mastic is influenced by the rheology of the filled binder. Kim et al. (2002) described how the resistance of mastic to microcracks development is strongly influenced by the dispersion of mineral filler. Cohesive strength of asphalt concrete mastic is controlled by the combination and interaction of both asphalt cement and the mineral filler. Water can affect cohesion in different ways including weakening

of the mastic due to moisture saturation and void swelling or expansion. Cohesion properties would logically influence the properties in the mastic beyond the region where interfacial properties dominate. The Schmidt and Graf (1972) studies showed that an asphalt mixture can lose approximately 50 percent of its modulus upon saturation. This loss may continue with time, but upon drying, the modulus can be completely recovered. Cheng et al. (2002) described the severe weakening of asphalt mixtures when they are subjected to moisture conditioning. They indicated that this strength loss is predictable when one compares the wet adhesive bond strength between the asphalt and the aggregate with the much higher dry adhesive bond strength. But Cheng et al. (2002) also demonstrated that the rate of damage in various mixtures is related to the diffusion of water into the asphalt mastic and the asphalts holding the greater amount of water accumulate damage at a faster rate.

Factors considered in moisture damage analysis are shown in **Figure 2.1**.

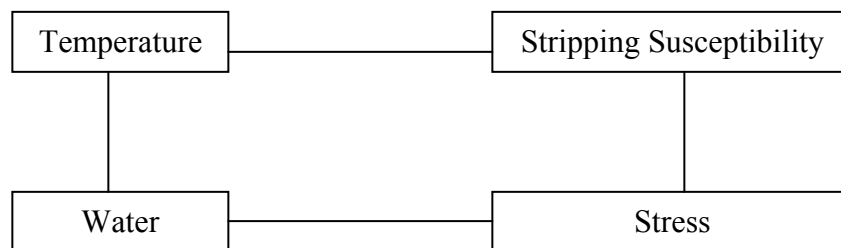


Figure 2-1 Factors considered in moisture damage analysis.

Essential ingredients to promote stripping are:

- Air voids
- Presence of water
- High stress
- High temperature

Saturation is the main cause of the problem and stripping is the outcome. The degree of saturation of pavements and asphalt layers is a critical element in the appraisal of stripping failures. If subsurface drainage of the pavement is inadequate, moisture and/or moisture vapor can move upwards due to capillary action and saturate the asphalt courses. Thermal pumping of moisture may occur if trafficking does not reduce the permeability of typical dense-graded HMA, and saturation may follow. If the HMA is not permeable for capillary flow, then there is no saturation and less chance of scouring. However, if saturation exists, stripping is highly likely and results from the hydraulic scouring of the binder from the aggregate surface due to extreme cyclic pore water pressure generated by heavy traffic.

To simulate the actual field condition, laboratory samples should be submerged under water then tested by applying repeated pulses of water pressure.

2.2. Nature of Asphalt-aggregate Interaction

2.2.1 Adhesive failure versus cohesive failure

Moisture damage (stripping) in asphalt pavements can occur in two ways: (1) adhesive fracture or failure. In this process, damage occurs at the aggregate-mastic interface, (2) cohesive fracture or failure. In this process, damage occurs within the mastic. The actual type of failure depends on the nature of the mastic and the relative thickness of the mastic around the coarse and fine aggregate.

Little and Jones (2003) mention that Lytton (2002) used micromechanics to assess the “thickness” of the asphalt film at which adhesive failure gives way to cohesive failure. It was explained that asphalt mixtures with thin asphalt films fail in tension by adhesive bond rupture, while those with thicker asphalt films (or mastic films) fail because of damage within the mastic (cohesive failure) as opposed to interfacial debonding. The film thickness that differentiates these two types of failure is dependent on the rheology of the asphalt (or mastic), the amount of damage for the asphalt or mastic to withstand prior to failure, the rate of loading, and the temperature at the time of testing.

2.2.2 Effect of aggregate characteristics

It is generally believed that acidic aggregates are hydrophobic while basic aggregates are hydrophilic. However, no aggregate can completely resist the stripping action of

water. Tarrer and Wagh (1991) listed several factors that influence the asphalt–aggregate bond: surface texture, penetration of pores and cracks with asphalt, aggregate angularity, aging of the aggregate surface through environmental effects, adsorbed coatings on the surface of the aggregate, and the nature of dry aggregates versus wet aggregates.

Maupin (1982) demonstrated that surface texture of the aggregate affects its ability to be properly coated, however, a good initial coating is necessary to prevent HMA from stripping. Calculating from basic surface energy measurements of the asphalt and aggregate, Cheng et al. (2002) demonstrated that the adhesive bond between certain granites and asphalt was higher than that between limestone aggregate and asphalt when the bond was quantified as the energy per unit of surface area. However, when the bond was quantified as energy per unit of aggregate mass, the bond energy was far greater for the calcareous aggregates than for the siliceous. These results clearly demonstrate the importance of the interaction of the physical and the chemical bonds. Gzernski et al. (1968) determined that stripping is severe in more angular aggregates because the angularity may promote bond rupture of the binder or mastic, leaving a point of intrusion for the water. Cheng et al. (2002) substantiated this argument that, regardless of the strength of the bond between the asphalt and aggregate, the bond between water and aggregate is considerably stronger. Cheng et al. (2002) also showed that the bond between water and aggregates is at least 30% stronger than that for any of the asphalts.

A freshly crushed aggregate surface would have a greater free energy than an uncrushed aggregate surface. This phenomenon is because broken bonds due to fracture should substantially increase the internal energy even though such broken bonds have a counter-effect on randomness (entropy increase). However, Tarrer and Wagh (1991) pointed out that sometimes newly crushed faces tend to strip faster than stockpiled aggregates. They stated that it is characteristic of many aggregates that one or more layers of water molecules become strongly adsorbed on the aggregate surface as a result of electrochemical attractions.

Tarrer and Wagh (1991) indicated that heating aggregates may remove free water and the outermost adsorbed water molecules on the aggregates and reduce the interfacial tension between the aggregate and the asphalt so that the stripping potential is reduced. Little and Jones (2003) explained that heating reduces asphalt viscosity, allows better penetration of asphalt into the aggregate surface, and promotes a more effective physical bond.

According to Tarrer and Wagh (1991), the asphalt–aggregate bond can be enhanced by three processes: (a) preheating the aggregate, (b) weathering the aggregate, and (c) removing aggregate coatings. When the aggregate surface is heated, the outermost adsorbed water layer is removed so as to improve the state of interfacial tension between the asphalt and aggregate and, in turn, to improve the bond between asphalt

and aggregate. The weathering process results in a replacement of the adsorbed water layer with organic fatty acids from the air. This process results in an improved asphalt–aggregate bond (Fromm, 1974). A dust coating on the aggregate surface promotes stripping by preventing intimate contact between the asphalt and aggregate and creating channels through which water can penetrate (Castan, 1968).

2.2.3 Material properties for accessing distress processes on HMA

Surface energy can be related to material processes and failure mechanisms. From this relationship, Little and Jones (2003) established a set of principles that can be used to measure material properties needed for assessing the basic distress processes of HMA. These principles are listed as follows:

- Both asphalt and aggregate have surface energies.
- Surface energies have different components: permanent deformation distress, fatigue failure process, cohesive strength reduction, and adhesive failure (stripping) in the presence of moisture.
- The theory of adhesive and cohesive bonding has been developed and used reliably in industrial surface chemistry and chemical engineering.
- Fracture and healing involve both chemical and mechanical properties. Neither fracture nor healing can be properly described without the use of both

properties: *chemical*—surface energies; *mechanical*—modulus, tensile strength and their change with age.

- The presence of moisture at the asphalt–aggregate interface interrupts the bond and accelerates the rate of fracture damage. The presence of moisture in the mastic reduces cohesive strength and fracture resistance, therefore, it reduces the healing potential for microcracks in the mastic.
- On the basis of surface energy characteristics, calculations may be performed to determine appropriate combinations of aggregate and asphalt to ensure them bond and heal well.

Little and Jones (2003) suggested in selecting materials for an asphalt pavement mixture among several available alternatives, the best combination of all of the available aggregate and asphalt should be selected to resist fracture, heal and bond them well, and resist moisture damage. Prediction of HMA performance requires the measurement of physical properties.

Cheng et al. (2002) determined the free energy per unit mass for different aggregates and binders as shown in **Table2-1**. They used two types of binder AAM and AAD which were used by Strategic Highway Research Program (SHRP). They described that the AAM asphalt bonds strongly with either the limestone or granite aggregate than the AAD asphalt. The AAD asphalt has more water holding capacity than the

AAM asphalt, which leads to a higher level of damage. Limestone has a higher value of energy per unit mass than granite. Thus the bonding energy of limestone with the binder is greater than that of granite.

Table 2-1 Gibbs free energy per unit mass (ergs/gm $\times 10^3$) (Cheng et al. 2002)

Binder	Georgia Granite	Texas Limestone	Colorado Limestone
AAD-1	158	614	375
AAM-1	206	889	536
Rubber asphalt	219	819	497
Aged rubber asphalt	178	714	435

Asphalt molecules are comprised primarily of carbon and hydrogen (between 90% and 95%) by weight. Remaining atoms, called heteroatoms, are very important to the interaction of asphalt molecules as well as their performance. These heteroatoms consist of oxygen, nitrogen, sulfur, nickel, vanadium, and iron.

Asphalt atoms are linked together to form molecules. Aliphatic carbon-carbon chain saturated with hydrogen bonds is the simplest form. The carbon-carbon bonds can

also form rings saturated with hydrogen. These carbon atoms saturated by hydrogen atoms in asphalt molecules are non-polar and interact primarily through relatively weak Van der Waals forces. A second class of asphalt molecules involves aromatics. This molecule has six carbon atoms in the form of a hexagonal ring. This ring possesses a unique bond with alternating single and double bonds between carbon atoms (Little and Jones, 2003).

2.2.4 Asphalt chemistry and adhesion

Polarity or separation of charge within the organic molecules promotes attraction of polar asphalt components to the polar surfaces of aggregates. Even though neither asphalt nor aggregate has a net charge, their components have non-uniform charge distributions, and both behave as if they have charges that attract the opposite charge of the other material (Little and Jones, 2003). Curtis et al. (1992) showed that aggregates vary widely in terms of surface charge and are influenced by environmental changes.

Robertson (2000) pointed out that adhesion between asphalt and aggregate arises between the polar nature of the asphalt and the polar surface of the aggregate and polarity alone in asphalt is not sufficient to achieve good adhesion in pavements because asphalt is affected by the environment. Robertson (2000) further stated that

asphalt has the capability of incorporating and transporting water. Cheng et al. (2002) showed that a substantial quantity of water can diffuse and be retained in a film of asphalt cement or asphalt mastic so as to change the rheology of the binder. Curtis (1992) found acidic groups, carboxylic acids, and sulfoxides had the highest adsorptions, while ketone and nonbasic nitrogen groups had the least. However, the sulfoxide and carboxylic acids were more susceptible to desorption in the presence of water. According to Curtis (1992), the general trend of desorption potential of polar groups from aggregate surfaces is as follows: sulfoxide > carboxylic acid > nonbasic nitrogen \geq ketone > basic nitrogen > phenol.

2.2.5 Effect of aggregate properties on adhesion

Various aggregate properties affect the adhesive bond between asphalt and aggregate, which include size and shape of aggregate, pore volume and size, surface area, chemical constituents at the surface, acidity and alkalinity, adsorption size surface density, and surface charge or polarity. The asphalt–aggregate bond is affected by aggregate mineralogy, adsorbed cations on the aggregate surface, surface texture, and porosity. Asphalt must be able to wet and permeate the aggregate surface. The ability of bonding asphalt to aggregate is dynamic and changes with time. This ability is largely affected by the shift in pH at the aggregate–water interface, which can be

triggered by dissociation of aggregate minerals near the surface or by the nature of the pore water (cation type and concentration).

2.2.6 Requirements of moisture sensitivity tests

For successful moisture susceptibility test procedure for mix design and field quality control, the following criteria must be satisfied (Solaimanian et al., 2003):

1. It is representative of the mechanisms that cause moisture damage in the field and produce results that match those occurring in the field under similar conditions
2. It is capable of distinguishing between poor and good performers in regard to stripping. Even when the lab test does not replicate the mechanisms of failures in the field, it can still discriminate between the high and low moisture susceptible mixtures using any other parameters, however, the results must still be tied to field performance.
3. It is repeatable and reproducible, with the allowable variance depending on the constraint of the fourth criterion.
4. It is feasible, practical, and economical enough that it can be included in routine mix design practice.

2.2.7 Summary

Several processes contribute simultaneously to the moisture damage in asphalt pavements. The literature review shows that neither asphalt nor aggregate has a net charge, but their components have non-uniform charge distributions. Asphalt and aggregate both behave as if they have charges that attract the opposite charged materials. By treating asphalt with additives, more tenacious and long lasting bonds can be developed. The most durable bonds appear to be formed by interaction of phenolic groups and nitrogen bases from the bitumen, which form insoluble salts and have less chance to be affected by water. Since sulfoxides and carboxylic acids have a greater affinity for the aggregate surfaces, they are most susceptible to dissolution on water.

Along with adhesive failure, moisture damage is also associated with the weakening of cohesive strength of the mastic due to moisture infiltration. The literature review shows that water can diffuse into asphalt of mastics, weaken the asphalt mixture in a long run, and make it more susceptible to damage. Hence, the deleterious effects of moisture on the adhesive and cohesive properties, both of which influence asphalt mixture performance, must be considered. Little and Jones (2003) indicated that the propensity for either adhesive or cohesive failure in an asphalt mixture is dependent on the thickness of mastic cover. Since the distribution of aggregates on asphalt as

well as the thickness of asphalt matrix varies considerably within the mixture, the statistical distribution will determine the controlling mechanism (Jones and Little, 2003). Thicker asphalt matrix will lead to cohesive failure in asphalt (separation of film) whereas thin asphalt matrix will lead to the adhesive bond failure in aggregate-asphalt interface.

2.3. Test Methods to Predict Moisture Sensitivity in HMA

Various test methods to predict moisture sensitivity have been developed. Tests may be carried out in loose samples as well as on compacted specimens. These test methods are presented in **Table 2-2** for loose samples and **Table 2-3** for compacted specimens.

2.3.1 Boiling Water Test

ASTM D 3625 (Boiling Water Test) has been used to predict moisture sensitivity of hot mix asphalt pavements. This test is used primarily as an initial screening test of a HMA mix. The test involves immersion of samples in boiling water for 10 minutes and the retained coated area is determined. Usually more than 95% of retained coated area is required.

Table 2-2 Moisture sensitivity tests on loose samples (From Solaimanian et al., 2003)

Test	ASTM	AASHTO	Other
Methylene Blue			Technical Bulletin 145, International Slurry Seal Association
Film Stripping			(California Test 302)
Static Immersion	D1664*	T182	
Dynamic Immersion			
Chemical Immersion			Standard Method TMH1 (Road Research Laboratory 1986, England)
Surface Reaction			Ford et. al. (1974)
Quick Bottle			Verginia Highway and Transportation Research Council (Maupin 1980)
Boiling	D3625		Tex 530-C, Kennedy et.al. (1984)
Rolling bottle			Isacson and Jorgensen, Sweden,
Net adsorption			SHRP A-341 (Curtis et al. 1993)
Surface energy			Thelen (1958) and HRB Bulletin 192
Pneumatic pull-off			Youtcheff and Aurilio (1997)

* no longer available as an ASTM standard.

Table 2-3 Moisture sensitivity tests on compacted samples (From Solaimanian et al., 2003)

Test	ASTM	AASHTO	Others
Moisture vapor susceptibility			California Test 307 Developed in late 1940s
Immersion-	D1075	T165	ASTM STP 252 (Goode, 1959)
Marshal Immersion			Stuart 1986
Freeze-thaw pedestal			Kennedy et. al. 1982
Original Lottman Indirect tension			NCHRP Report 246 (Lottman, 1982); Transportation Research Record 515 (1974)
Modified Lottman indirect tension		T 283	NCHRP Report 274 (Tunncliff and Root, 1984), Tex 531-C

Tunnicliff-Root	D 4867		NCHRP Report 274 (Tunnicliff and Root, 1984)
ECS with resilient modulus			SHRP-A-403 (Al-Swailmi and Terrel, 1994)
Hamburg wheel			1993 Tex-242-F
Asphalt Pavement Analyzer			
ECS/ SPT			NCHRP 9-34 2002-03
Multiple freeze-thaw			

2.3.2 Texas Boiling Water Test

The Texas Boiling Water Test (TBWT) is to visually determine the degree of stripping after the sample is placed in the boiling water. Asphalt cement is heated at 325°F (163°C) for 24 hours to 26 hours. One hundred grams or 300 grams of unwashed aggregate is heated at the same temperature for 1 to 1.5 hours. The aggregate and asphalt are mixed and allowed to cool for two hours. A 1000 ml beaker is filled half-way with distilled water and boiled. The mixture is placed in boiling water for 10 minutes. Asphalt cement that is floating is skimmed off the top. The water is cooled to room temperature and then poured off. The mixture is emptied onto a paper towel and graded. A same panel of observers grade the mixture at that time and again the next day, when the mixture is dry. A mixture that retains 65% to 75% of the asphalt cement is favorable for use in the field (Kennedy et al., 1984).

2.3.3 Texas Freeze-Thaw Pedestal Test

The Texas Freeze-Thaw Pedestal Test (TFTPT) is conducted on a HMA mix with uniform aggregate sizes. Since a uniform aggregate size is used, the effects of mechanical properties of the aggregate are minimized in the test. Thus, the effects of bonding are maximized. To perform this test, asphalt and aggregate are mixed using the Texas Mixture Design Procedure. After initial mixing, the mixture is reheated and mixed for two additional times.

A cylindrical mold is used to form the specimen, which has a height of 19.05 mm (0.75 in) and a 41.3 mm (1.6 in.) diameter. A constant load of 27.6 kN (6200 lbs) is applied for 20 minutes. The specimen is cured at ambient temperature for three days. Thermal cycling is performed on the specimen. The specimen is placed on a stress pedestal in a jar and covered with 12.7 mm (0.5 in) of distilled water. It is cycled through -12°C (-10°F) for 12 hours then 49°C (120°F) for 12 hours. The number of freeze-thaw cycles to induce cracking indicates moisture susceptibility of the HMA. Kennedy et al. (1984) found that mixes susceptible to moisture survived less than 10 cycles. Mixtures that were not susceptible to moisture survived more than 20 cycles.

2.3.4 Static Immersion Test

Static Immersion Test (AASHTO T-182) is a subjective test. An HMA mix sample is immersed in a distilled water bath at 77°F (25°C). The mix is left in the water bath

for 16 to 18 hours. Similar to the Boiling Water Test, the percentage of total visible area that remains coated with asphalt cement is estimated as above or below 95% (Solaimanian 2003)

2.3.5 The Lottman Test

Lottman (1982) developed this test at the University of Idaho. Nine specimens are used in the laboratory procedure. They are compacted to the field air void content. The nine cores are split into three groups. Group one is the control group, in which no conditioning is done. In the second group, the cores are vacuum-saturated with water for 30 minutes up to 660mmHg. Group two reflects the field performance of the HMA mix for the first four years of life. The third group is also vacuum-saturated but the cores are then subjected to a freeze-thaw cycle. Group three cores are frozen at 0°F (-18°C) for 15 hours. Then they are thawed at 140°F (60°C) for 24 hours. Group three is designed to reflect the field performance from the fourth to the twelfth year (Lottman, 1982; Roberts et al., 1996)

The Resilient Modulus (M_R) Test and/or the Indirect Tensile Strength Test (ITS) are performed on each core after the prescribed conditioning has been completed. These tests can be performed at either 55°F (13°C) or 73°F (23°C). ITS is determined using a loading rate of 0.065 in/min. The retained tensile strength (TSR) is calculated for the cores in groups of two and three. The TSR is equivalent to the ITS of the

conditioned specimens divided by the ITS of the control specimens. TSR greater than 0.7 is typically recommended. However, field cores showed visual stripping when TSR value was 0.8. (Lottman, 1982; Roberts et al., 1996)

The indirect tensile strength is defined as the maximum stress from a diametrical vertical force that a specimen can withstand and can be expressed as follows:

$$\sigma_t = 2000 \frac{P}{\pi t D} \quad (3-1)$$

where, σ_t = tensile strength (kPa)

P = maximum load carried by the specimen (N)

t = thickness of specimen (mm), and

D = diameter of specimen (mm).

The Tensile Strength Ratio (TSR) was first suggested by Lottman (1982) and has been used as a parameter to identify moisture sensitive mixtures. TSR is defined as the ratio of the strength of conditioned (wet) specimens to the strength of unconditioned specimens and can be expressed as:

$$TSR = \frac{\sigma_t(\text{conditioned specimen})}{\sigma_t(\text{unconditioned specimen})} \quad (3-2)$$

where σ_t = tensile strength.

Other parameters may also be used, such as: the flexural stiffness and the fatigue life. The flexural stiffness is the repeated flexural stress divided by the corresponding strain. The flexural stiffness ratio (FSR) is defined as the ratio of conditioned to unconditioned stiffness values:

$$FSR = S_{\text{conditioned}} / S_{\text{unconditioned}} \quad (3-3)$$

where FSR = flexural stiffness ratio,

$S_{\text{conditioned}}$ = stiffness of conditioned specimens,

$S_{\text{unconditioned}}$ = stiffness of unconditioned specimens.

The fatigue life is defined as the number of cycles to reach 50 percent of the initial flexural stiffness of the beam specimen and can be expressed as follows:

$$FLR = FL_{\text{conditioned}} / FL_{\text{unconditioned}} \quad (3-4)$$

where FLR = flexural stiffness ratio,

$FL_{\text{conditioned}}$ = fatigue life of conditioned specimens,

$FL_{\text{unconditioned}}$ = fatigue life of unconditioned specimens.

2.3.6 The Tunicliff and Root Conditioning

The Tunicliff and Root conditioning is a strength test that utilizes ITS. Six specimens are produced with air voids between 6 and 8 percent. The six samples are split into two groups of three. The first group is the control group without any conditioning. The second group is vacuum-saturated at 28.6 in. Hg for five minutes. Saturation limits for the specimens are 55 to 80 percent. After saturation, group two cores are placed in a 140°F (60°C) water bath for 24 hours. The ITS test is performed at 77°F (25°C) with a loading rate of 2 in/min. The minimum acceptable TSR used is 0.7 to 0.8 (ASTM D4867, “Standard Test Method for Effect of Moisture on Asphalt Concrete Paving Mixtures,”).

2.3.7 The Modified Lottman Test (AASHTO T-283)

AASHTO accepted the Modified Lottman Test (AASHTO T-283) in 1985. It is the combination of the Lottman Test and the Tunicliff and Root Test. Six specimens are produced with air voids between six and eight percent. The higher percentage of air voids helps accelerate moisture damage on the cores. Two groups of three specimens

are used. The first group is the control group. The second group is saturated between 55 and 80 percent with water and placed in the freezer (0°F or -18°C) for 16 to 18 hours. The frozen cores are moved to a water bath at 140°F (60°C) for 24 hours. After conditioning, the Resilient Modulus test and/or Indirect Tensile Strength (ITS) test are performed. The ITS test is performed at 77°F (25°C) with a loading rate of 2 in/min. The minimum acceptable TSR is 0.7 (Roberts et. al., 1996). The test procedure is summarized in **Table 2-4**.

Table 2-4 Summary of test parameters for AASHTO T283 (Aschenbrener 1996)

Test Parameter	Test Requirement
Short Term Aging	Loose mix: 16 hours at 60°C Compacted mix: 72-96 hours at 25°C
Air Voids	6-8 percent
Sample Grouping	Average air voids of two subsets should be equal
Saturation	55 to 80 percent
Swell Determination	Not required
Freeze	Minimum 16 hours at -18°C (optional)
Hot Water Soak	24 hours at 60°C
Strength Property	Indirect Tensile Strength
Loading Rate	51 mm/min at 25°C
Precision Statement	None

2.3.8 Immersion-Compression Test

The immersion-Compression Test (AASHTO T-165) utilizes six cores. Each core is four inches in diameter and four inches in height. The cores are compacted with a double plunger at 3,000 psi (20.6 MPa) for two minutes. An air void content of 6 percent is attained. The six cores are split into two groups. The first group is the control group. The second group is conditioned in a water bath at 120°F (49°C) for four days or at 140°F (60°C) for one day.

After conditioning, the unconfined compressive strength of each core is determined. A testing temperature of 77°F (25°C) and a loading rate of 0.2 in/min (5 mm/min) are used. The retained compressive strength is calculated. A retained strength of 70 percent is specified by many agencies (Roberts et al., 1996).

The Immersion-Compression Test has produced retained strengths close to 100 percent even when stripping is visually evident in cores. Thus, this test is not sensitive enough to measure damage induced by moisture. This problem is attributed to the internal pore water pressure that develops (Roberts et al., 1996).

2.3.9 Environmental Conditioning System (ECS)

The Environment Conditioning System (ECS) was developed at Oregon State University (OSU) as part of an Strategic Highway Research Program (SHRP) (Al-Swailmi and Terrel, 1992). The sample for ECS has 102 mm (4 in) in diameter by 102 mm in height and is membrane encapsulated. It is subjected to cycles of temperature, repeated loading, and moisture conditioning. The test procedure is summarized in **Table 2-5**.

Table 2-5 Summary of ECS Test Procedure (Aschenbrener, 1996)

Step	Description
1	Prepare test specimens per the SHRP protocol.
2	Determine the geometric and volumetric properties of the specimen. Determine the triaxial and diametrical modulus using a closed-loop, hydraulic test system.
3	Encapsulate specimen in a silicone sealant and latex rubber membrane and allow curing overnight.
4	Place the specimen in the ECS load frame between two perforated Teflon disks to determine air permeability.
5	Determine unconditioned (dry) triaxial resilient modulus.
6	Vacuum a condition specimen (subject to vacuum of 51 cm Hg for 10 minutes).
7	A wet specimen by pulling distilled water through specimen for 30 minutes using a 51 cm Hg vacuum.
8	Determine unconditioned water permeability.
9	Heat the specimen to 60°C for 6 hours under repeated loading as a hot cycle.
10	Cool the specimen to 25°C for at least 4 hours. Measure the triaxial resilient modulus and water permeability.

11	Repeat steps 9 and 10 for additional hot cycles.
12	Cool the specimen to -18°C for 6 hours without repeated loading as a freeze cycle. This procedure is optional.
13	Heat the specimen to 25°C for at least 4 hours and measure the triaxial resilient modulus and the water permeability.
14	Split the specimen and perform a visual evaluation of stripping.
15	Plot the triaxial resilient modulus and water permeability ratios.

Resilient modulus (M_R) is determined before or after conditioning in the ECS procedure. The ECS- M_R ratio (ratio of conditioned to unconditioned) and the visual observation of stripping from the split specimen after conditioning are the bases for evaluating moisture damage.

Aschenbrener (1996) suggested that the moisture resisting specimen requires the ECS- M_R ratio to be greater than 0.7 after the final conditioning cycle. The SHRP research suggested that additional insight to mixture behavior might be gained by evaluating plotted ECS- M_R ratio curves (Aschenbrener, 1996). **Figure 2-2** shows that the first ECS cycle shows more obvious moisture sensitivity while the later cycles show less effect. Aschenbrener (1996) that if the 3- or 4-cycle ECS- M_R ratio results are marginal (0.8 to 0.7), the ECS- M_R ratio could be supplemented by using the slope as a judgment factor to guide the engineer in the final selection process. Aschenbrener (1996) indicated that even though the slope or trend offers promise for future research, no definitive conclusion can be drawn yet.

The correlation between Tensile Strength Ratio (TSR) from AASHTO T283 with the ECS- M_R ratio after 4 cycles is expressed by the following regression equation (Aschenbrener 1996):

$$M_R = 0.96TSR + 0.23 \quad (3-5)$$

where $y = M_R$ ratio from ECS cycle after 4 cycles,

$x =$ TSR from AASHTO T 283.

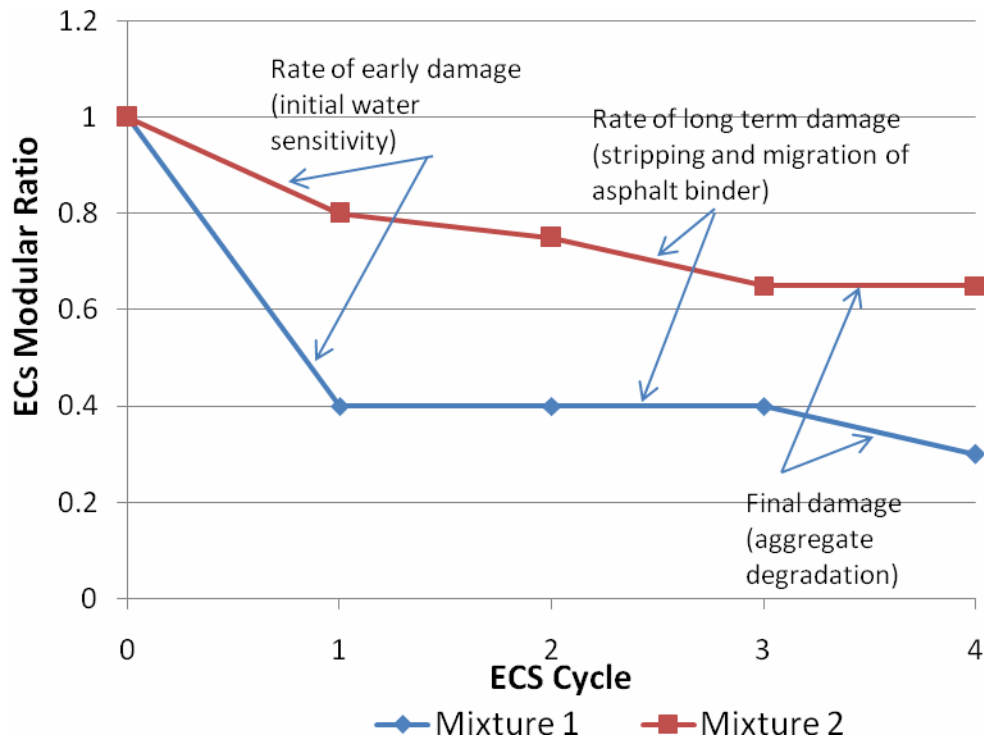


Figure 2-2 Interpretation of ECS Modular Curve

The coefficient of determination r^2 is 0.52. The slope of the regression is approximately 1.0 indicating a 1:1 relationship of the TSR and ECS- M_R . In addition, M_R is approximately 0.23 higher than the TSR.

The correlation between TSR from AASHTO T283 and the percent of asphalt coating from ASTM D 3625 is expressed by the following regression equation (Aschenbrener 1996):

$$y = 4.11x + 65 \quad (3-6)$$

where y = percent of asphalt coating from ASTM D 3625,

x = TSR from AASHTO T 283

The coefficient of determination r^2 is 0.003. There is no correlation between these two tests.

2.3.10 APA tests

The APA as shown in Figure 2-3 is a multifunctional loaded wheel tester used for evaluating permanent deformation (rutting), fatigue cracking, and moisture susceptibility of both hot and cold asphalt mixes. This machine is available at most

DOTs in the U.S. APA is a laboratory scale accelerated load wheel tester and modified from the version of the Georgia loaded wheel tester (GLWT). APA has a wheel running back and forth over a pressurized hose placed on top of the sample inside a chamber under a wide range of conditions. The APA machine and sample testing in APA machine are shown in **Figure 2-3** and **Figure 2-4**. Details of the APA machine used in the current study will be presented in Chapter 3.



Figure 2-3 Asphalt Pavement Analyzer machine

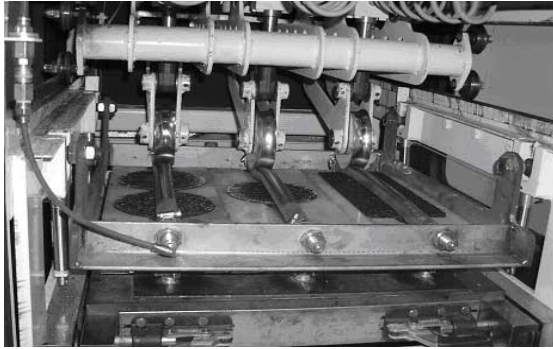


Figure 2-4 Sample testing in APA machine

Mohammad, N. (2001) mention that Georgia DOT used the APA to evaluate the permanent deformation characteristics of stone mastic asphalt mixture, large stone asphalt mix, and a heavy-duty conventional 19mm mix and they concluded that APA rut depth was consistent with the actual field rut depth.

Cross and Voth (2001) conducted APA tests in Kansas to evaluate the effects of sample preconditioning on rut depths and the suitability of APA for determining moisture susceptible mixtures. In their study, Cross and Voth (2001) measured rut depths at 500, 1000, 2000, 4000, and 8000 cycles. Eight different mixes from seven project sites were evaluated. Air and water bath temperatures were set at 40°C. Samples were tested using four different preconditioning procedures. First preconditioning was done by placing samples in APA at a chamber temperature of 40°C for 4 hours before running APA. This is referred as *40°C dry* condition state. Second preconditioning was done by soaking samples in a 40°C water bath for 2 hours before running the APA. The samples were tested while submerged in water at

40°C. This test procedure is referred as *40°C soak*. Third preconditioning was done by vacuum saturation of the samples in accordance with the AASHTO T283 and then placed in a 60°C water bath for 24 hours. Next the samples were placed in the APA's water bath at 40°C for two hours and then tested in APA while submerged in 40°C water. This procedure is referred as *40°C saturated*. Fourth preconditioning was done by vacuum saturation as in the third state, but freeze-thaw cycle following the AASHTO T283 was added. Then the samples were placed in water bath for 2 hours at 40°C and tested in APA submerged in water at 40°C. This procedure is referred as *40°C freeze*. Tests were conducted with or without anti-stripping additives and hydrated lime. Measured rut depth data were analyzed using two-way analysis of variance (ANOVA), in which rut depth was the response variable (Y-variable) and the project site and the condition state were two effects (X-variable). A statistical comparison using the Tukey-Kramer test was conducted.

The test results suggested that the AASHTO T-283 preconditioning had little effect upon the rutting results. 40°C soak preconditioning had the greatest rut depth followed by 40°C saturated, 40°C dry, and 40°C freeze, which had the least amount of rutting. Rut depths for the soak conditioning were greater than the freeze conditioning on all 8 sites, and greater than the saturated conditioning on 7 out of 8 sites. Cross and Voth (2001) suggested that pore pressure was likely created during the rut testing due to the vacuum saturated conditioning of the samples and this pore pressure could have provided some resistance to rutting. Therefore, testing of

samples with dry and soak conditioning may be all that is necessary for developing a test method for predicting moisture susceptibility with the APA. However, Cross and Voth (2001) could not establish good correlation between rut depths and the results obtained from other test methods like TSR values, methylene blue values, and sand equivalent. APA tests were able to detect the influence of liquid anti-strip agents but could not detect the influence of lime additives. APA tests were not able to identify all the sites with TSR values below 80%.

Cross and Voth (2001) also suggested that any potential test procedure for determining the moisture susceptibility of mixes should incorporate two or three tests, such as the loaded wheel test and a methylene blue test. A 2.0 mm and/or 50% increase in rut depth from samples with dry and soak conditioning appear to be threshold values that provide some correlation with conventional moisture sensitivity test results. They indicated that 50°C testing temperature could result in more definitive results.

2.3.11 Hamburg tests

The HWTD as shown in Figure 2-5 is originally manufactured by Helmut-Wind, Inc of Hamburg, Germany. Test samples are typically 260 mm (10.2 in) wide, 320 mm (12.6 in) long, and 40 mm (1.6 in) thick and they are compacted at approximately 7 percent air voids using a plate compactor. Two samples are tested simultaneously.

The samples are commonly submerged under water at 50°C (122°F) even though the temperature can vary from 25°C to 70°C (77°F to 158°F). A steel wheel, 47 mm (1.85 in) wide and loaded under 705 N (158 lb) makes 50 passes over each sample per minute. The maximum velocity of the wheel is 340 mm/sec (1.1 ft/sec) in the center of the sample. Each sample is loaded for 20,000 passes or until 20 mm of deformation occurs. Approximately 6-1/2 hours are required for one test.



Figure 2-5 Hamburg Wheel Tracking Device

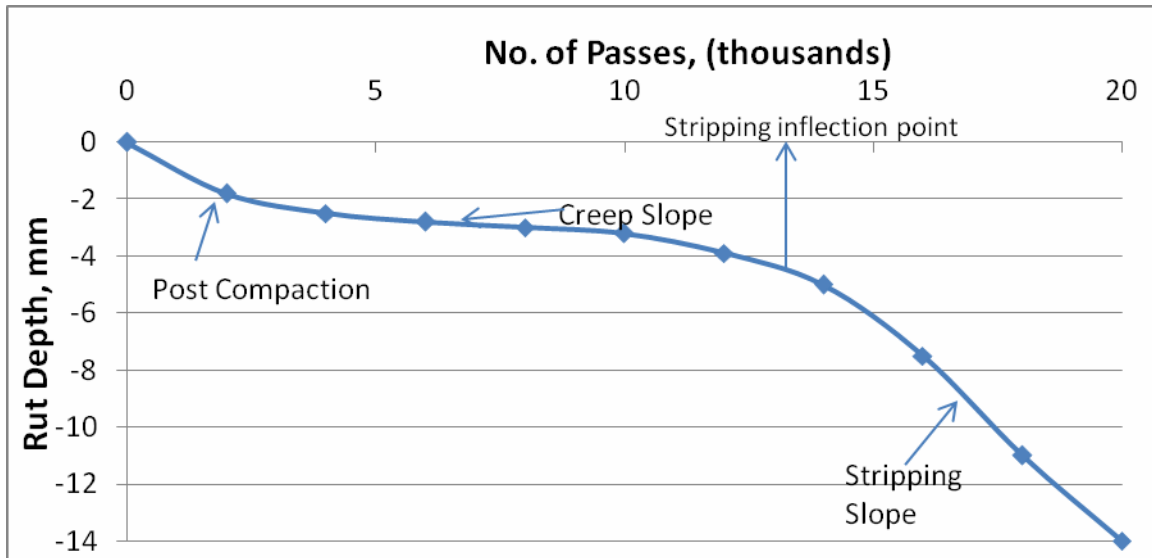


Figure 2-6 Results from Hamburg Wheel Tracking Device (Aschenbrener, 1996)

As shown in **Figure 2-6**, the typical results from the Hamburg wheel tracking device include the creep slope, stripping slope, and stripping inflection point. The creep slope relates to rutting from plastic flow and is the inverse of the rate of deformation in the linear region of the deformation curve after the post-compaction and before the onset of stripping. The stripping slope is the inverse of the rate of deformation in the linear region of the deformation curve after the stripping inflection point and until the end of the test. The stripping slope would then represent the number of passes required to create a 1 mm impression from stripping. The stripping slope is related to the severity of moisture damage. The stripping inflection point is the number of passes at the intersection between the creep slope and the stripping slope, which is related to the resistance of the HMA to moisture damage (Aschenbrener, 1996).

The manufacturer, Hamburg in Germany, specifies a rut depth of less than 4 mm after 20,000 passes. Based on the studies in Colorado, Aschenbrener (1996) indicated that the 4 mm specification is too severe and he suggested that a rut depth of less than 10 mm after 20,000 passes should be used instead.

Aschenbrener (1996) tested HMA mixes used in the pavements of known stripping performances using the HWTD. Seven good pavements (sites 1 to 7), five pavements requiring high maintenance (sites 8 to 12), and eight pavements that lasted less than 1 year (sites 13 to 20) were tested. Aschenbrener (1996) found excellent correlation between the stripping inflection point and the known stripping performance. Good pavements (sites 1 to 7) had stripping inflection points generally greater than 10,000 passes. The high-maintenance pavements (sites 8 to 12) had stripping inflection points generally between 5,000 and 10,000 passes. The pavements that lasted less than 1 year (sites 13 to 20) had stripping inflection points less than 3,000 passes. Based on these tests, Aschenbrener (1996) concluded:

- The HWTD has the potential to distinguish pavements of varying field stripping performance.
- The HWTD results are sensitive to aggregate properties including clay content, high dust to asphalt ratios, and dust coating on aggregates.
- An increase of the asphalt cement stiffness at the same testing temperature makes the stripping inflection point to occur at a larger number of passes.

Using the same grade of asphalt cement but reducing the testing temperature, the stripping inflection point would occur at a larger number of passes. Moisture resistance improves as asphalt cement stiffness is increased and when temperature is decreased.

- The HWTD results are sensitive to the amount of short-term aging. As short-term aging time increases, the samples become more resistant to moisture damage.
- The HWTD results are sensitive to the crude oil source and refining process. Even for the same AC-10 or PG 58-22 grading asphalt cement, it may have different adhesion properties. The HWTD results are affected by the components and quality of asphalt cement.
- Liquid anti-stripping additives can increase the passes required for the stripping inflection point from the Hamburg for most aggregates. Hydrated lime can increase more passes as compared to all other additives.
- Samples compacted in the laboratory using the linear kneading compactor (steel wheel) gave slightly better results than samples compacted with the French plate compactor (pneumatic tire) in the field. In general, the laboratory–compacted samples performed similarly. The field compacted samples did significantly worse than the laboratory compacted samples. This result may be due to higher air voids in field samples or lower compaction efforts.

- When the target density of the HMA samples was achieved at a higher temperature during compaction, the HWTD wheel-tracking device would produce higher passes of the stripping inflection point.

2.3.12 Fatigue testing

This test is carried out on the apparatus positioned in a temperature control cabinet under conditions prescribed in the Austroads standard (Rickards, 2003). This test uses a constant stress test regime in the belief that it can best replicate the field condition. The standard testing temperature and stress frequency are 20°C and 10 Hz, respectively. A constant stress required to achieve a strain of approximately 400 microstrain is calculated as 1200 kPa (Rickards, 2003). Fatigue life is calculated as the number of cycles at which the modulus of the beam is reduced to half its initial modulus. The field validation has suggested that this test is extremely severe.

This test postulates that stripping damage would occur (even in the most compatible system), if the asphalt is at or near saturation and the pavement temperature and traffic loading are high. Rickards (2003) indicated that “In a heavily trafficked high temperature environment even the best asphalt systems will fail if near saturation. In this case the problem is saturation, not stripping.”

2.4 Techniques for Limiting Moisture Sensitivity

2.4.1 Liquid anti-stripping agents

Liquid anti-stripping agents are chemical compounds containing amines. According to Tunicliff et al. (1984), these compounds reduce surface tension between the asphalt and aggregate in a mixture. The reduction of surface tension increases the adhesion of the asphalt to the aggregate. Anti-stripping agents are surface active agents. These anti-stripping agents can be added with the asphalt by heating the asphalt to a liquid state or by adding the additive directly to the aggregate prior to the addition of binder.

Liquid anti-stripping agents are added directly to the asphalt binder either at the refinery or asphalt terminal, or at the contractor's asphalt facility during production of the mix with an in-line blending system. Liquid anti-stripping agents are commonly used in cold-applied, asphalt-bound patching materials, asphalt binders for chip seals, and the binder for pre-coating the aggregates in chip seals.

2.4.2 Lime additives

Lime can reduce the potential for moisture to disrupt the adhesive bond that exists between asphalt binder and aggregate. The contribution of lime is to change the surface chemistry or molecular polarity of the aggregate surface.

Lime can be added to the aggregate either dry or as lime slurry. When dry lime is used, a fixed percent of hydrated lime (by dry weight of aggregate) is added to pre-wetted aggregate (for example, 5% water added to aggregate and then 1.5% dry hydrated lime added to aggregate). On the other hand, lime slurry can also be used, in which a fixed percent of hydrated lime (for example, 1.5% by dry weight of aggregate) is introduced in form of a lime –water slurry mixed in a fixed ratio (for example, 1 to 3 by weight).

Lime-aggregate is cured (1 or 2 days to 1 or 2 months) to allow for pozzolanic reaction to take place between lime and aggregates.

The T283 tests have showed that lime treatment increases the strength value and tensile strength ratio (Shatnawi, 1995). The strength improvement can be computed by the following formula:

$$SI = [(\sigma_{\tau_{CL}} - \sigma_{\tau_{CNL}})/\sigma_{\tau_{CNL}}] \times 100\% \quad (3-7)$$

where SI = strength improvement (%),

$\sigma_{\tau_{CL}}$ = tensile strength of conditioned lime treated specimens, and

$\sigma_{\tau_{CNL}}$ = tensile strength of unconditioned specimens without lime treatment.

The analysis has showed that lime treatment can extend the performance life of HMA pavements by an average of 3 years (Martin et al. 2003), which is equivalent to an average increase of 38% in the expected pavement life. Percentage increase in the pavement life of 38% compares favorably with the percent increase in the cost of HMA mixtures of 6% (\$2/ton) by the use of lime treatment.

California Department of Transportation (CalTrans) pre-coated all the aggregates with lime slurry when they were mixed at the plant (Martin et al., 2003). The pre-coated aggregate was stockpiled for a maximum marination period of 24 hours to 21 days for chemical reaction to take place on the aggregate surface. The AASHTO T 283 test was used initially and a TSR of 80% or above was required. But the industry claimed that the results of the T 283 tests were not consistent and had high variability. Then CalTrans District 02 discontinued the T 283 test, instead, made it mandatory to lime treat all the aggregates for all asphalt concrete for all major projects.

Recommendations for low, moderate, and high environmental risk zones are presented in **Tables 2-6** and **Table 2-7** (Martin et al., 2003).

Table 2-6 CalTrans low environmental risk zone (Martin et al., 2003)

TSR	Mix Risk	Treatment	Required TSR after Treatment
>= 70	Low	None required	
51 – 69	Moderate	LAS, DHL, LSM	TSR >= 70
<= 50	High	DHL, LSM	TSR >= 70

Note: LAS= liquid anti-strip agent, DHL= dry hydrated lime with no marination, and LSM= lime slurry with marination

Table 2-7 CalTrans moderate and high environmental risk zone (Martin et al., 2003)

TSR	Mix Risk	Treatment	Required TSR after Treatment
>= 75	Low	None required	
61 – 74	Moderate	LAS, DHL, LSM	TSR >= 75
<= 60	High	DHL, LSM	TSR >= 70

3. EXPERIMENTAL STUDY

3.1. Introduction

This experimental study is part of the joint research efforts between the KU and KSU sponsored by KDOT through the Kansas Transportation Research and New-Developments (K-TRAN) program to develop a rapid test method for evaluating moisture sensitivity of HMA samples. APA tests were conducted at KU while HWTD tests were conducted at KSU. To eliminate possible variations of sample preparation, a series of test samples for APA and HWTD tests were prepared at KSU by the same members. These samples were tested parallel using APA and HWTD testers between KU and KSU. To extend the research scopes for the K-TRAN project, additional samples were prepared and tested at KU.

For this experimental study, Superpave HMA cylindrical samples were fabricated using Superpave gyratory compactors. The diameter of all the samples was 150 mm. **Table 3.1** provides the dimensions and volumes of these cylindrical samples. For APA tests, the height of samples was 75 mm whereas for HWTD tests it was 60 mm. Six samples were made with additive and six without additive for both APA and HWTD tests. Aggregate, binder, and additive were obtained from KDOT. One design mix each for Districts 2, 3 and 5 and three design mixes for District 6 were

used to prepare lab samples for the joint research portion between KU and KSU. Eight sets of additional samples (4 with additive and 4 without additive) were made at KU based on the D607002A mix of District 6 and will be further discussed later.

Table 3-1 Samples made for APA and Hamburg tests.

	APA	HWTD
Diameter of sample, d (mm)	150	150
Height of sample, h (mm)	75	60
Volume of 1 sample (cc)	1325.36	1060.29
Volume of 6 samples (cc)	7952.16	6361.73

Table 3.2 presents overall project information on the HMA mixes used in different districts, the name of county, and the contractor who was involved in the real project. Mixing and molding temperatures, aggregate type and ratio, binder type, additive type, and their amount each mix are also provided.

All samples used for the HWTD tests at KSU were soaked in water at 50°C. The delay time after the water reached 50°C was thirty minutes. Rut depth in the cylindrical sample vs. number of cycle was recorded automatically.

In case of the APA tests done at KU, samples were subjected to vacuum saturation (20in Hg) for six minutes before wet tests. Samples were soaked for one hour after the required temperature was reached. For APA tests, two sets of temperature were used. All those parallel samples using 50°C in HWTD were tested at same temperature in the APA too. Eight additional sets of samples were fabricated at KU.

Tests were conducted at 50°C dry and 60°C dry conditions as well to evaluate the effect of saturation and temperature on the samples. Manual measurements were taken using a steel plate and a dial gauge.

The analysis and discussion on the results of both Hamburg and APA tests are presented in Chapter 4.

Table 3-2 Project Information

KTRAN- KU-KSU Project	D2: 2G06015A	D3: 3G06020A	D5: 5G06016A	D6: 6G06011A	D6: 6G06016A	D6: 6G07002A
	District 2	District 3	District 5	District 6	District 6	District 6
Project No	106-KA-0349-01	183-82K-6377-01	42-106 KA-0285-0	54-60K-7411-01	54-60K-7411-01	54-88k-7283-01
County	Cloud-Jewell	Rooks	Barber-Kingman	Meade	Meade	Meade
Specs:	1990 Std.& 90 M-	1990 Std.& 90 M-	1990 Std.& 90 M-	1990 Std.& 90 M-	1990 Std.& 90 M-	1990 Std.& 90 M-
Contractor	US Asphalt Co.	APAC - Shears Division	APAC- Shears Division	APAC- Shears Division	APAC- Shears Division	J&R Sand Company, Inc.
Producer	US Asphalt Co.	Hays Branch	APAC- Shears, H.H	APAC- Shears, Dodge City	SEM- Muskogee	J&R Sand Company, Inc.
Combined Sp. Gr.	2.616	2.614	2.543	2.578		2.581
Project ESAL's (M)	1.2	1.9	0.5	7.9	7.9	6.10
Mixing temp range (F)	305 - 315	290-300	307-317	309-317	306-326	311-320
Molding temp range (F)	285 - 295	275-285	286-295	286-295	290-315	286-295
Mix Designation	SM - 9.5 A	SM - 19 A	SM - 9.5 A	SM - 19 A	SM - 19 A	SM - 19 A
% Air Void Design						
Specs Min	2	2	2	2	2	2
Specs Max	6	6	6	6	6	6
% VFA @ Design						
Specs Min	65	65	65	65	65	65
Specs Max	78	78	78	76	76	76
% VMA @ Design						
Specs Min	14	13	14	13		13
Dust/Binder ratio						

Table 3.2 Project information (continued)

K-TRAN-KU- KSU Project	D2: 2G06015A	D3: 3G06020A	D5: 5G06016A	D6: 6G06011A	D6: 6G06016A	D6: 6G07002A
	District 2	District 3	District 5	District 6	District 6	District 6
Specs Min	0.6	0.6	0.6	0.6	0.6	0.6
Specs Max	1.2	1.2	1.2	1.2	1.2	1.2
Tensile Strength Ratio (TSR)	80	80	80	80	80	80
Sand Equivalent (Min)	40	40	40	45	45	45
Uncompacted Voids (Min)	42	42	42	42	42	42
Course Aggr. Angularity						
1 Face	75	50	75	60	60	60
% Flat & Elongated Pieces (Max)	10	10	10	10	10	10
Aggregate type and ratio	CS 1A (40%)	CS 1 (23%)	CS 1A (20%)	CG 1 (20%)	CG 1 (18%)	CG 1 (15%)
	CS 1B (10%)	CS 1B (30%)	CS 1B (15%)	CG 2 (10%)	CG 2 (10%)	CG 2 (15%)
	CS 2 (15%)	CS 2C (12%)	CS 2A (20%)	CG 3 (10%)	CG 3 (27%)	CG 4 (15%)
	SSG 1 (10%)	SSG 1 (35%)	CS 2 (10%)	CG 4 (25%)	CG 4 (20%)	CG 5 (20%)
	SSG 2 (25%)		SSG 3 (35%)	SSG 2 (25%)	SSG 2 (25%)	SSG 1 (35%)
				SSG 4 (10%)		
Mass of each specimen (gm)	2950	2980	2900	2880	2950	2970
No. of samples with additive	6	6	6	6	6	6
No. of samples without additive	6	6	6	6	6	6
Total Mass	35400	35760	34800	34560	35400	35640
Binder type	PG 64-22	PG 64-22	PG 64-22	PG 64-22	PG 70-28	PG 64-22
Additive type	Arr-maz	Arr-maz	Arr-maz LA-2	Arr-Mazz, LA-2	Arr-Mazz, LA-2	AD-Here HP Plus
Design % Asphalt	5.5	5.1	6.75	5.15	5.00	4.70
Asphalt Source	Sinclair, Phillipsburg	Sinclair	Valero-Ark City	SEM Dodge City	SEM-Muskogee	SEM Mat. DC, KS

Table 3.2 Project information (continued)

KTRAN-KU- KSU Project	D2: 2G06015A	D3: 3G06020A	D5: 5G06016A	D6: 6G06011A	D6: 6G06016A	D6: 6G07002A
	District 2	District 3	District 5	District 6	District 6	District 6
Sp. Gr. of AC	1.0264					
Design % Additive	0.3	0.3	0.3	0.3	0.25	0.5
Expected Gmm	2.444	2.466	2.377	2.437	2.435	2.435
Obtained Gmm	2.454	2.461	2.341	2.433	2.428	2.402
Nini Gyration	7	7	7	8	8	8
Ndes Gyration	75	75	75	100	100	100
Nmax Gyration	115	115	115	160	160	160

3.2. Test Equipment

3.2.1 Superpave Gyratory Compactor

The Superpave gyratory compactor is a transportable device. It is used to fabricate test specimens by simulating the effect of traffic on an asphalt pavement. The specimens fabricated with the gyratory compactor can be used to determine the volumetric properties (air voids, voids in the mineral aggregate, and voids filled with asphalt) of Superpave mixes. Those properties, measured in the laboratory, indicate how well the mix will perform in the field. Thus, the gyratory compactor can be used for quality control/quality assurance. This equipment can also be set up at a job site to verify that the delivered asphalt mix meets the job mix volumetric specifications.

The Superpave gyratory compactor prepares specimens that represent actual in-service pavements in terms of compaction and traffic loads. The level or amount of compaction is dependent on the environmental conditions and traffic levels expected at the job site.

To create a mix with a high degree of internal friction and high shear strength, the Superpave mix design procedures include requirements for aggregate angularity and gradation. The design goal is the production of a strong stone skeleton which resists rutting, yet includes enough asphalt and voids to improve the durability of the mix.

Sample height, number of gyrations as well as pressure to be applied can be set in the Superpave gyratory compactor as shown in **Figure 3-1**. The sample height of 75 mm for APA tests and the sample height of 60 mm for HWTD tests were fixed in this study.



Figure 3-1 Pine Superpave Gyratory Compactor Control Panel

3.2.2 Hamburg Wheel Testing Device

The HWTD was used to evaluate the moisture sensitivity at KSU. Details of this testing device have been reviewed in Chapter 2.

3.2.3 Asphalt Pavement Analyzer

This APA machine available at KU was manufactured by Pavement Technology Inc., (PTI) Covington, GA. It is 2.03 m (6.5 ft) long, 0.9 m (2.9 ft) wide, and 1.78 m (5.7 ft) high. The total weight of this machine is 1358.4 kg (3000 lb). This machine has retractable legs with wheels to make it portable and anchored while in use. Importantly, although the air consumption is low, the minimum pressure of 827.4 kPa (120 psi) is critical to maintain the adequate hose inflation. Since the machine is normally operated from the front, a space of one meter in the front of the APA should be adequate for the operation, and a space of one meter is also needed on both sides of the machine to access the service door.

This following section briefly discusses the major parts of the APA machine, the calibration, and the data acquisition system:

Wheel tracking/loading system

The APA is designed to simulate a rolling wheel condition by rolling three concave metal wheels on three rubber hoses which can provide the pressure ranging from 0 kPa to 827kPa (120 psi) to simulate the effect of tire pressures. In this study, 0.44 kN (100 lb) loaded wheels on rubber hoses that have air pressures of 690 kPa (100 psi)

were used. The rubber hoses are part of a hose rack, **Figure 3-2**, which can be taken out from the main chamber.

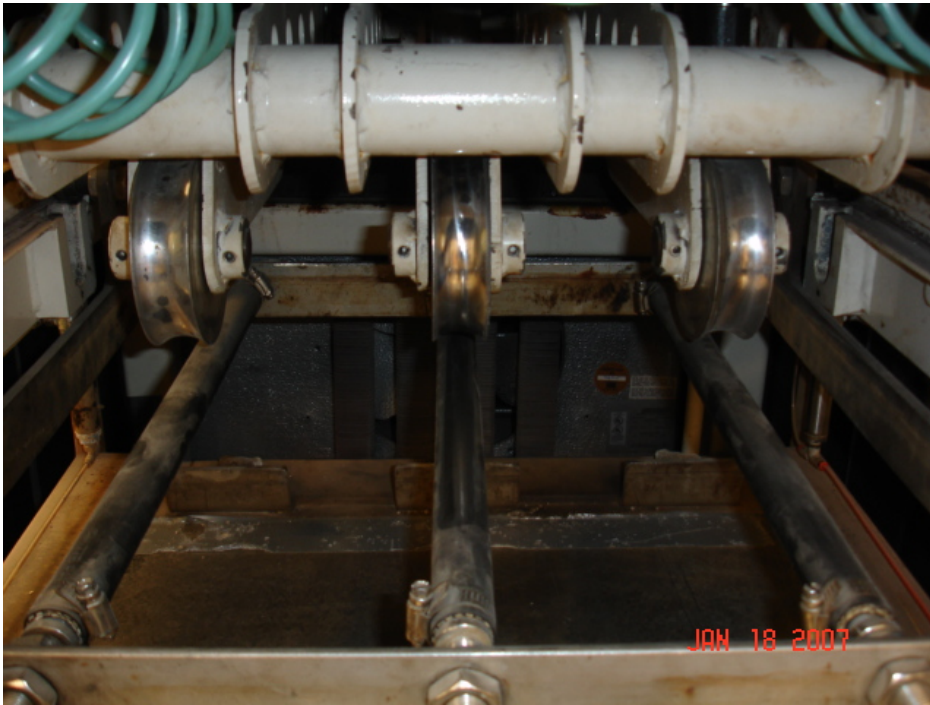


Figure 3-2 Three metal wheels on three rubber hoses

Sample holding assembly

The assembly holds the samples directly underneath the rubber hoses to allow the sample to be subjected to the wheel tracking action during the test. The tractable tray, **Figure 3-3**, allows the sample to be pulled out of the machine for manual measurements and sample installation. The tray can be locked by two toggle clamps

when it is fully pushed in. Three different sample molds are typically provided by the manufacturer: cylindrical rut test mold, beam rut test mold, and beam fatigue test mold. The cylindrical rut test mold **Figure 3-4** was used in this study.



Figure 3-3 Sample tray



Figure 3-4 Cylindrical mold for rutting tests

Temperature control

Heating and cooling of the main chamber are provided by four heat strips, two fans, and a cooling unit, which are regulated by a solid state based temperature controller. Cabin temperature as well as water temperature can be set to a desired test temperature. In this study, most tests were conducted at 50°C whereas a few additional tests were conducted at 60°C.

Water submerging system

The water submerging system allows the water to cover the test samples in the submerged-in-water tests. A water heater heats the water to a set temperature and a water pump circulates the water from the lower water tank (reservoir) to the upper water tank (where the sample is conditioned). For manual measurements, the upper water tank is lowered, then the sample tray is pulled out for data recording. When the water tray is lowered, the water is drained down to the lower water reservoir. The upper water tank can be raised again to continue the wet test.

Sample temperature conditioning shelf

The shelf is located inside the lower front doors. It allows the heat conditioning of extra samples.

Air regulator

This system consists of an air inlet regulator controlling the maximum air pressure to the APA, an electronic regulator controlling the hose pressure, three regulators controlling the left, middle, and right wheel cylinders, and the pressure booster regulator doubling the incoming air pressure.

Operating controls

The APA is controlled by a Programmable Logic Computer (PLC). The control panel is shown in **Figure 3-5**.



Figure 3-5 Control panel of APA

Calibration

The following items should be calibrated no less than once per year: (1) the wheel load, (2) calibration of the automated vertical measuring system, (3) the chamber temperature, and (4) the hose pressure. Instructions for each of these calibration procedures are included in this section. A load cell as shown in **Figure 3-6** was used

to calibrate each wheel load. The calibration of the wheel load followed the following steps:



Figure 3-6 Load cell for calibration

- (1) Remove the hose rack.
- (2) Connect the load cell to the load cell meter located on the APA front panel. Turn on the meter using the toggle switch and zero the load cell by pressing the zero buttons located at the right of the meter.
- (3) Lower and raise each wheel 20 times by switching to CAL to loosen up the cylinders.

- (4) Do not lock the sample tray in place (release the “Red Toggle Clamps). It must be able to move freely during the calibration so that the load cell always rests evenly on the sample tray.
- (5) Place the load cell on the table under the first wheel.
- (6) If all three wheels are used during the test, then place two empty specimen molds (turned upside down) under the other two wheels. This setup simulates the loading condition the carriage is under during the test.
- (7) Lower the wheels by switching each one to CAL (on control panel).
- (8) If adjustment needs to be made, raise the wheel that is being calibrated and turn the regulator up or down (The other two wheels should be left in the down position).
- (9) The final adjustment made to a regulator, should always be in a clockwise direction. The final adjustment should never be made in a counter clockwise direction to avoid a malfunction in the regulator.
- (10) Lower the wheel and allow the meter to stabilize.
- (11) All three wheels should be calibrated to within 5 pounds of each other.
- (12) Repeat steps 5-10 for each wheel.

Data acquisition

The APA system has automatic and manual measurements. The APA machine is connected to a computer. Software installed in this computer can automatically

perform data acquisition to take the measurements of the rut depth with the number of cycles. Automatic measurement was not taken in this study due to its malfunction.

All measurements for the present study were made manually. The measurement was recorded by using a steel plate and a dial gauge. The steel plate is fitted in the slot of the mold, and a dial gauge is placed on the top of the plate to take a measurement. It should be noted that there is a unique position for the plate to fit in the cylindrical mold so that the plate is at the same level for every measurement.

3.3. Test Procedure

3.3.1 Sample preparation

Cylindrical samples were prepared for the APA and the HWTD wheel tests. Diameter of all the samples was 150 mm. For the APA tests, the height of the sample was 75 mm whereas for the HWTD tests, the height of the sample was 60 mm. All samples for KDOT districts were prepared at KSU for uniformity in preparing samples. Design mixes provided by KDOT and shown in Table 3-2 for Districts 2, 3, 5 and 6 were used. One set of samples each for Districts 2, 3, and 5 were prepared whereas three sets were prepared for District 6. Each set consist of 6 cylindrical samples without any anti-stripping agent and 6 cylindrical samples with an anti-stripping agent for the APA tests and equal number of samples for the HWTD tests.

The contents of the asphalt binder used in this study were in the range of 4.7-6.75%.

The contents of additives were in the ratio of 0.25-0.5%.

Mix and compaction temperatures were selected based on the requirements of the KDOT design. Aggregate was weighed and heated in oven to the desired mix temperature, **Figure 3-7**. An asphalt heater as shown in **Figure 3-8** was used to heat the binder. Once the desired temperature was reached, aggregate was mixed with binder in an electrical mixer, **Figure 3.9**. A hand scoop was also used to mix and to make sure aggregate was mixed properly. When the additive was used, the required quantity of additive was added and mixed along with binder and aggregate. The mix was then again heated for two hours for short term aging as shown in **Figure 3-10**.



Figure 3-7 Heating of aggregate up to the required mixing temperature



Figure 3-8 Heating of asphalt binder up to the required mixing temperature



Figure 3-9 Mixing of aggregate and binder



Figure 3-10 Short term aging of Superpave mix

The Pine Superpave Gyrotory Compactor was used to fabricate the samples. Gyrotory molds, the mix pouring funnel, the scoop were all heated to match up the compaction temperature. After two hours of short term aging, the required quantity of mix for one sample was poured in the gyrotory mold using the sample pouring funnel as shown in **Figure 3-11**. The mold was then placed inside the gyrotory compactor chamber as shown in **Figure 3-12** and the door was closed. The number of gyrations, the sample height, and the required compaction pressure were set on the control panel. In this study, the compaction pressure was set at 600 kPa and the number of gyrations was set at 160. The base of the compactor inclined to 1.5° and the load was applied from upper and lower plates. The compactor stopped itself when either the set height or the number of gyrations was reached. Once the machine

self parked, the door was opened and the compacted sample was removed from the chamber and extruded using the hydraulic jack on the right side of the compactor as shown in **Figure 3-13**. Six cylindrical samples were prepared for APA tests in one batch as shown in **Figure 3-14**.



Figure 3-11 Pouring of hot mix in the Gyratory mold.



Figure 3-12 Mold with loose mix in the Superpave Gyratory Compactor



Figure 3-13 Extrusion of the compacted sample from the Gyratory mold



Figure 3-14 Compacted Samples ready for testing

3.3.2 Sample conditioning and testing

Before running an APA wheel test on wet samples, samples were subjected to 20in Hg vacuum saturation for six minutes each as shown in **Figure 3-15**. Three molds were used in one set of test. Each mold contained two samples. Hence six samples were tested in one set. Water temperature and cabin temperature were raised and samples were soaked in the APA machine before running the test. All the wet samples were pre-conditioned for at least one hour after the water and chamber temperatures reached the desired temperature. The number of required cycles was set

on the APA machine control panel. The air compressor was turned on and the required hose pressure was set on the control panel. The wheel load was applied on the cylindrical samples by switching the green button in the control panel as shown in **Figure 3-16**. All rut depths were measured manually for this study. The relationship of rut depth vs. number of cycles for each test is plotted in spreadsheet for analysis.



Figure 3-15 Vacuum saturation of a sample before wet testing



Figure 3-16 APA test

4. TEST RESULTS AND ANALYSIS

4.1. Introduction

A summary of APA tests carried on at KU is presented in **Table 4-1**. All tests from No. 1 to 12 were conducted using the samples prepared at KSU. The tests included the HWTD tests at KSU and the APA tests at KU. Since these samples were prepared under the same condition, their test results should compare well. The test results for these samples obtained from the HWTD tests as well as the APA tests are presented in this chapter. Additional samples were prepared at KU to carry out some dry tests as well as tests at higher temperature (60°C). The comparisons of results obtained from the HWTD and APA tests, between dry and wet tests, and between high and low temperatures are presented in the following sections.

4.2. Visual Observation of Stripping Phenomenon

After each test, samples were examined visually to inspect the degree of stripping. Most samples prepared without additive showed clear or some degree of stripping after the APA tests. The stripping exhibited in forms of debonding of binder and aggregate and washing out of particles as shown in **Figure 4-1**. The samples in Figure 4-1 had the same mix design except the use of the additive. Close up view of the striping is shown in **Figure 4-2**, in which free or washed out sand can be seen. In case of samples prepared with additive, there was no obvious stripping phenomenon.

The visual observation of the stripping phenomenon for each mix is provided in the summary of the test results later.

Table 4-1 Summary of tests carried out on different mixes.

No.	District	Design Number	Mix	Lab Designation Number	Type of test done
1	2	2G06015A	9.5 A	T3 (w/o additive)	Wet (50°C)
2	2	2G06015A	9.5 A	T5 (w additive)	Wet (50°C)
3	3	3G06020A	SM-19A	T13 (w/o additive)	Wet (50°C)
4	3	3G06020A	SM-19A	T15 (w additive)	Wet (50°C)
5	5	5G06016A	9.5 A	T7 (w/o additive)	Wet (50°C)
6	5	5G06016A	9.5 A	T11 (w additive)	Wet (50°C)
7	6	6G06011A	SM-19A	T18 (w/o additive)	Wet (50°C)
8	6	6G06011A	SM-19A	T20(w additive)	Wet (50°C)
9*	6	6G07002A	SM-19A	T23 (w/o additive)	Wet (50°C)
10**	6	6G07002A	SM-19A	T25 (w additive)	Wet (50°C)
11	6	6G06016A	SM-19A	T28 (w/o additive)	Wet (50°C)
12	6	6G06016A	SM-19A	T30 (w additive)	Wet (50°C)
13*	6	6G07002A	SM-19A	K1 (w/o additive)	Wet (50°C)
14	6	6G07002A	SM-19A	K2 (w/o additive)	Wet (60°C)
15	6	6G07002A	SM-19A	K5 (w/o additive)	Dry (60°C)
16	6	6G07002A	SM-19A	K6 (w/o additive)	Dry (50°C)
17**	6	6G07002A	SM-19A	K3 (w additive)	Wet (50°C)
18	6	6G07002A	SM-19A	K4 (w additive)	Wet (60°C)
19	6	6G07002A	SM-19A	K7 (w additive)	Dry (60°C)
20	6	6G07002A	SM-19A	K8 (w additive)	Dry (50°C)

No. 1-12: the KU-KSU joint project, all samples prepared at KSU, and HWTD tests conducted at KSU but APA tests at KU.

No. 13-20: additional samples prepared and tested using APA at KU.

* and **: repeated tests for the same mixes prepared at KSU and KU for comparison purposes



Figure 4-1 Stripping in samples without additive (Left) and non stripping with additive (right)



Figure 4-2 Close up view of the left sample in Figure 4-1

4.3 Test Results and Analysis

All manual readings taken for the APA tests are presented in the Appendix of this thesis. The test results from the HWTB tests were obtained and provided by KSU. The curves from the APA and the HWTB tests are presented and discussed in terms of samples for different districts in the following section.

4.3.1 District 2 (2G06015A -Wet 50°C)

The Superpave HMA mix used in Cloud Jewel County of Kansas District 2 was used to make lab samples. The estimated equivalent single axle load (ESAL) was 1.2 million. The temperature used for mixing of aggregate and binder was 305-315°F (151-157°C) whereas the molding temperature was 285-295°F (140-146°C). The design mix used for this project was 2G06015A. The aggregate type and ratio and the type of percent of binder and additive used for this mix are provided in **Table 4-2**.

Table 4-2 Aggregate-binder types of D2 - 2G06015A mix

K-TRAN-KU-KSU Project	D2 - 2G06015A
	District 2
Aggregate type and ratio	CS 1A (40%)
	CS 1B (10%)
	CS 2 (15%)
	SSG 1 (10%)
	SSG 2 (25%)
Binder type	PG 64-22
Additive type	Arr-maz
Design % Asphalt	5.5
Design % Additive	0.3
Mixing temp range (°F)	305 - 315
Molding temp range (°F)	285 - 295
Mix Designation	SM - 9.5 A

APA test results

APA tests were carried out on six samples with additive and six samples without additive. Samples were subjected to 6 min vacuum saturation and one hour soak in water at 50°C. **Figure 4-3** shows the measured rut vs. the number of cycles from the APA tests. Even though stripping was observed on the sample without additive, the rut depth was smaller for the mix without additive than that of the mix with additive. No definitive stripping inflection point exists for either curve.

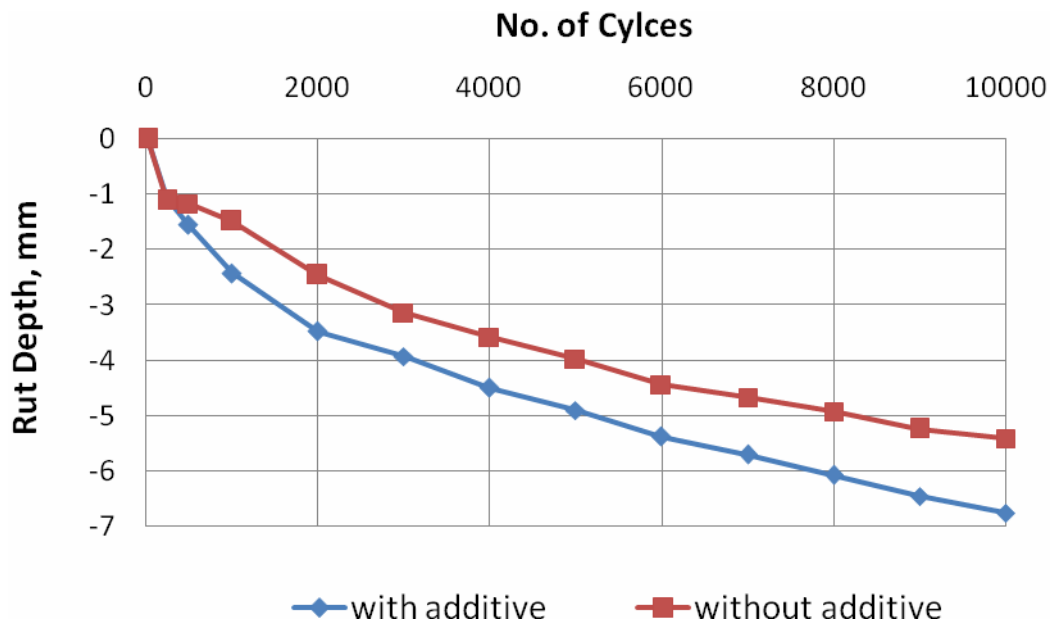


Figure 4-3 Rut depth vs. number of cycles from the APA tests of D2-2G06015A mix (50°C wet)

HWTD test results

HWTD tests were conducted on the same mixes at KSU. The measured rut vs. the number of cycles for this mix is shown in **Figure 4-4**. For the sample without additive, the stripping inflection point occurred around 1500 cycles. **Figure 4-4** shows that the use of the additive increased the number of cycles corresponding to the inflection point and reduced the rut depth.

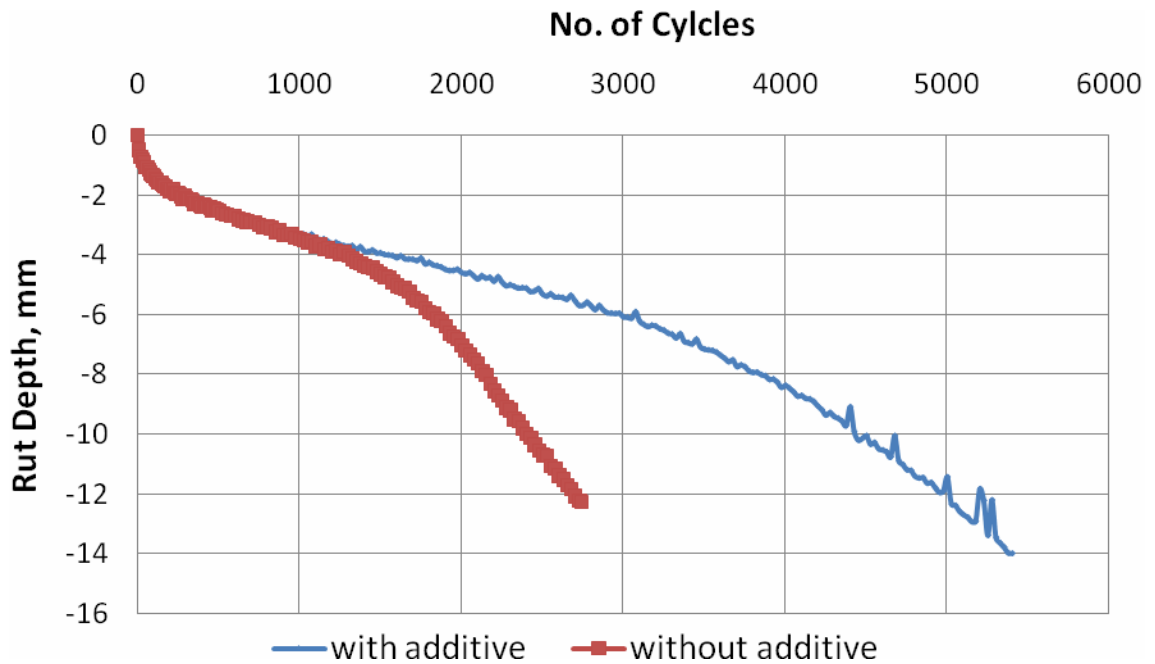


Figure 4-4 Rut depth vs. number of cycles from the HWTD tests of D2-2G06015A mix (50°C wet)

APA vs. HWTD test results

Figure 4-5 presents the comparison of rut depths obtained from the APA and the HWTD tests. From the curves, the APA tests could not identify the benefit of using additive whereas the HWTD tests could identify some benefits. The curves from the HWTD tests show stripping inflection points but those from the APA do not show any inflection points. Visual inspection show stripping in the sample after the APA tests. The HWTD results match with visual inspection. In addition, the overall rut depths from the HWTD tests are larger than those from the APA curves, therefore, the HWTD tests are more severe than the APA tests.

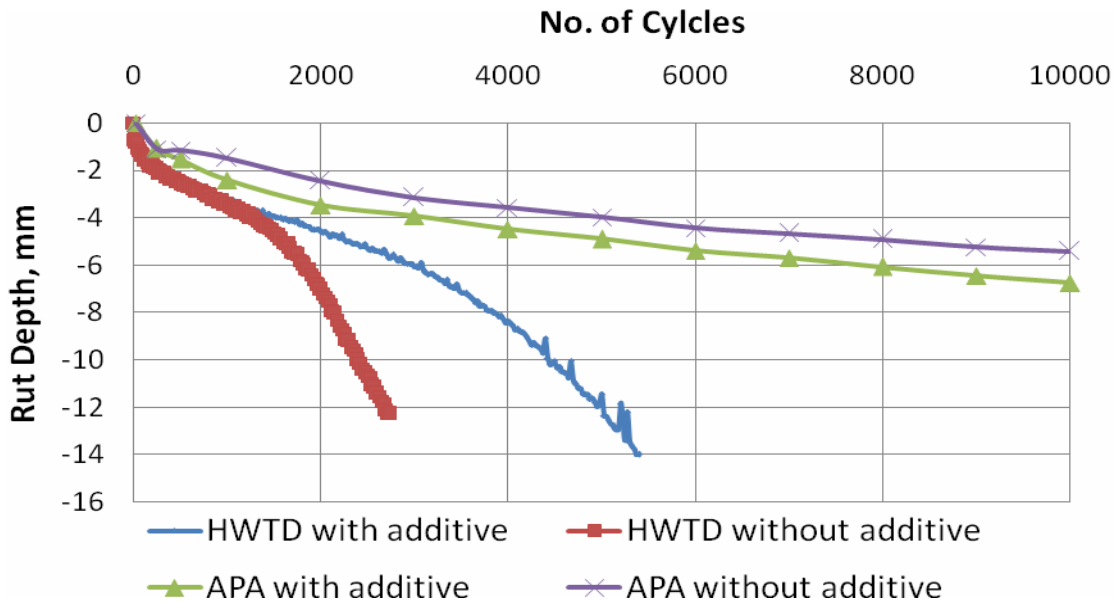


Figure 4-5 Rut depth vs. number of cycles from the APA and the HWTD Tests of D2-2G06015A mix (50°C wet)

4.3.2 District 3 (3G06020A -Wet 50°C)

The Superpave HMA mix used in Rooks County of Kansas District 3 was used to make the lab samples. The estimated ESAL was 1.9 million. The temperature used for mixing of aggregate-binder was 290-300°F (143-150° C) whereas the molding temperature was 275-285°F (135-140°C). The aggregate type and ratio and the type and percent of the binder and additive for this mix are provided in **Table 4-3**.

Table 4-3 Aggregate-binder types of D3 - 3G06020A mix

K-TRAN-KU-KSU Project	D3 - 3G06020A
	District 3
Aggregate type and ratio	CS 1 (23%)
	CS 1B (30%)
	CS 2C (12%)
	SSG 1 (35%)
Binder type	PG 64-22
Additive type	Arr-maz
Design % Asphalt	5.1
Design % Additive	0.3
Mixing temp range (°F)	290-300
Molding temp range (°F)	275-285
Mix Designation	SM - 19 A

APA test results

Figure 4-6 presents the measured rut depth vs. number of cycles for the APA tests on D3-3G06020A at 50°C. The measured curves for samples with and without additive virtually overlap. Even though the number of cycles for the sample with additive was continued up to 20000, no definitive stripping inflection point occurred in either curve.

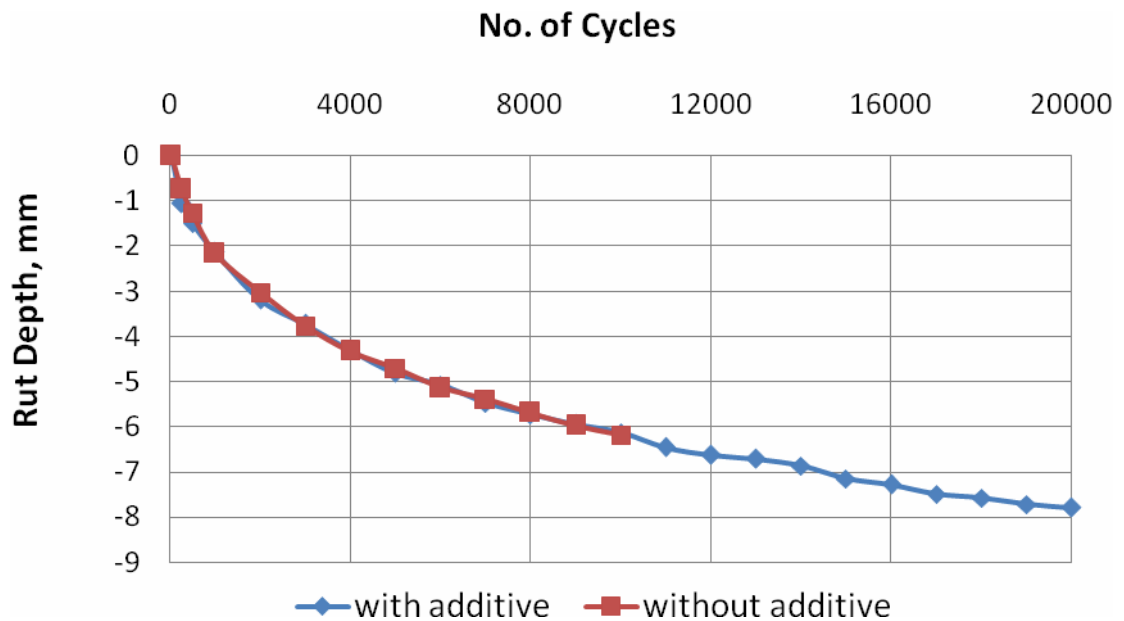


Figure 4-6 Rut depth vs. number of cycles from the APA tests of D3-3G06020A mix (50°C wet)

HWTD test results

The rut depth vs. number of cycles from the HWTD tests at KSU is shown in **Figure 4-7**. For the sample without additive, the stripping inflection point occurred around 4500 cycles. The use of additive yielded larger rut depth at the beginning up to 6500 cycles but showed long term benefit after this level.

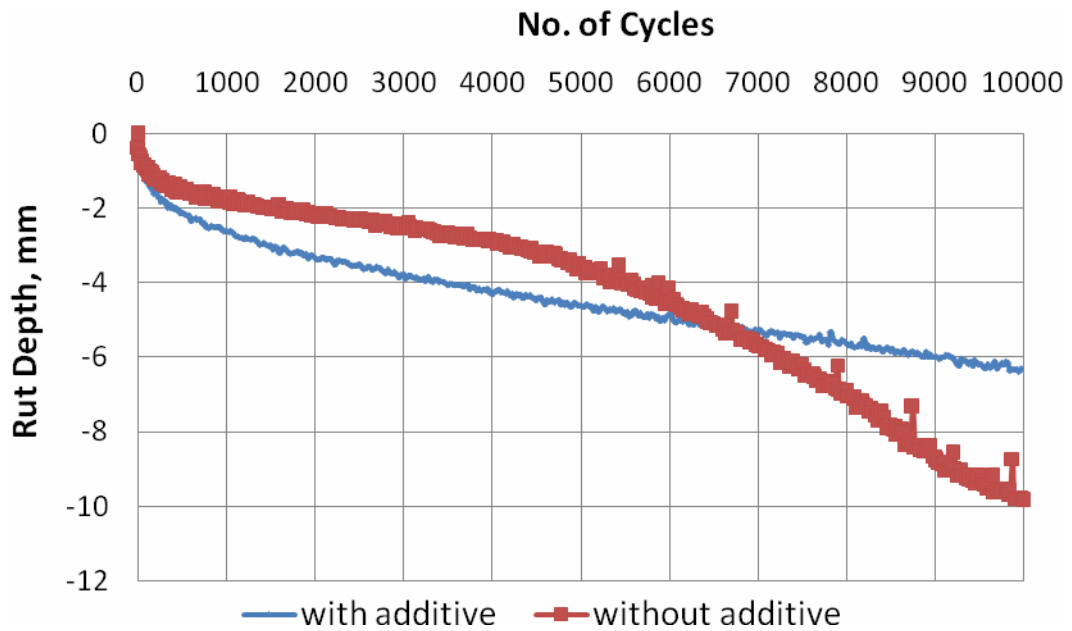


Figure 4-7 Rut depth vs. number of cycles from the HWTD tests of D3-3G06020A mix (50°C wet)

APA vs. HWTD test results

Figure 4-8 shows the comparison of rut depths obtained from the APA and the HWTD tests. The curves from the APA tests do not identify the benefit of using additive whereas the curves from the HWTD tests identify some benefits after a higher number of cycles. The curve from the HWTD test on the sample without additive shows the stripping inflection point. However, the curves from the APA tests do not show any inflection point for both cases. Visual inspection show stripping in the sample after APA tests. HWTD results match with visual inspection. Curves from the APA tests, both with and without additive overlap with curve from the HWTD test with additive. Rut depth is larger for the HWTD curve without additive which shows stripping as well.

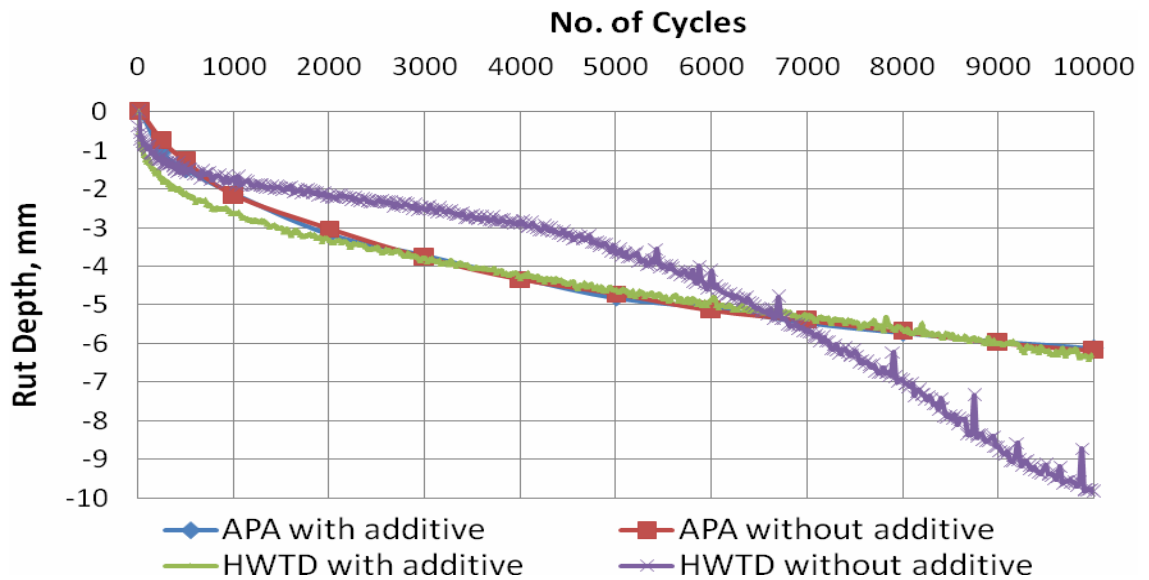


Figure 4-8 Rut depth vs. number of cycles from the APA and the HWTD tests of D3-3G06020A mix (50°C wet)

4.3.3 District 5 (5G06016A -Wet 50°C)

The Superpave HMA mix used in Barber-Kingman County of Kansas District 5 was used to make the lab samples. The estimated ESAL was 0.5 million. The temperature used for mixing of aggregate and binder was 307-317°F (153-158°C) whereas the molding temperature was 286-295°F (141-146°C). The aggregate type and ratio and the type and percent of binder and additive used for this mix are provided in **Table 4-4**.

Table 4-4 Aggregate-Binder types of D5 - 5G06016A mix

K-TRAN-KU-KSU Project	
	District 5
Aggregate type and ratio	CS 1A (20%)
	CS 1B (15%)
	CS 2A (20%)
	CS 2 (10%)
	SSG 3 (35%)
Binder type	PG 64-22
Additive type	Arr-maz LA-2
Design % Asphalt	6.75
Design % Additive	0.3
Mixing temp range (F)	307-317
Molding temp range (F)	286-295
Mix Designation	SM - 9.5 A

APA test results

Figure 4-9 presents the measured rut depth vs. number of cycles from the APA tests. Similar to District 2 samples, the APA tests did not detect any benefit of using additive. Even though the visual inspection showed that the sample without additive had more obvious stripping behavior than that with additive. The rut depth for the sample with additive was larger than that without additive. In addition, there is no obvious stripping inflection point for either curve.

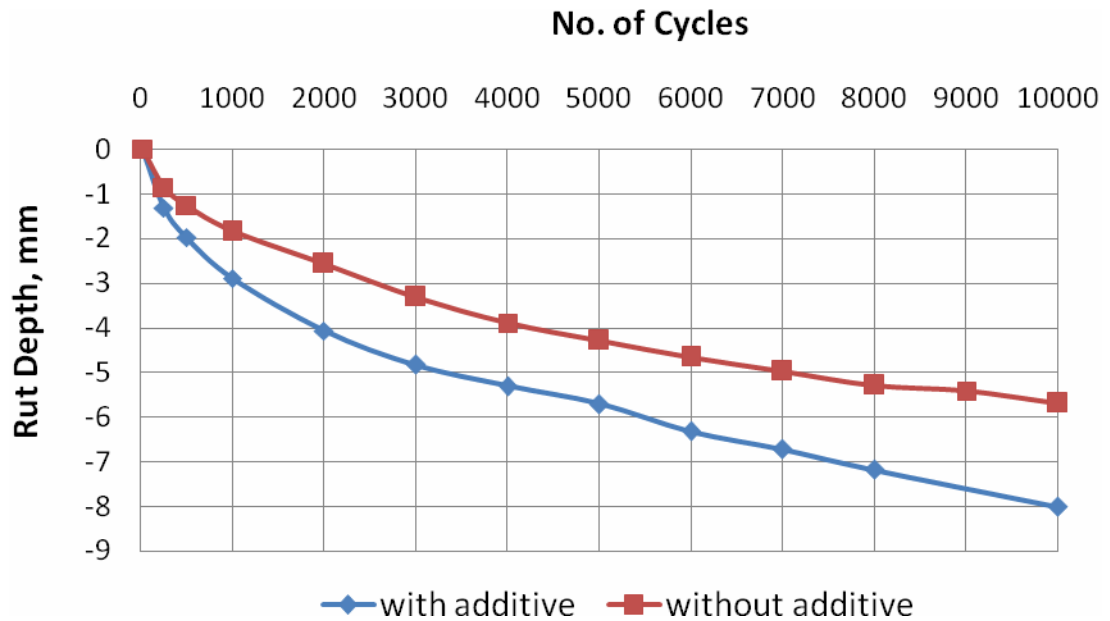


Figure 4-9 Rut depth vs. number of cycles from the APA tests of D5-5G06016A mix (50°C wet)

HWTD test results

The measured rut depth vs. number of cycles from the HWTD tests is shown in **Figure 4-10**. The curve for the sample without additive shows a stripping inflection point while that with additive does not show a clear inflection point. The use of additive increased the rut depth at the beginning but reduced the rut depth after about 2100 cycles.

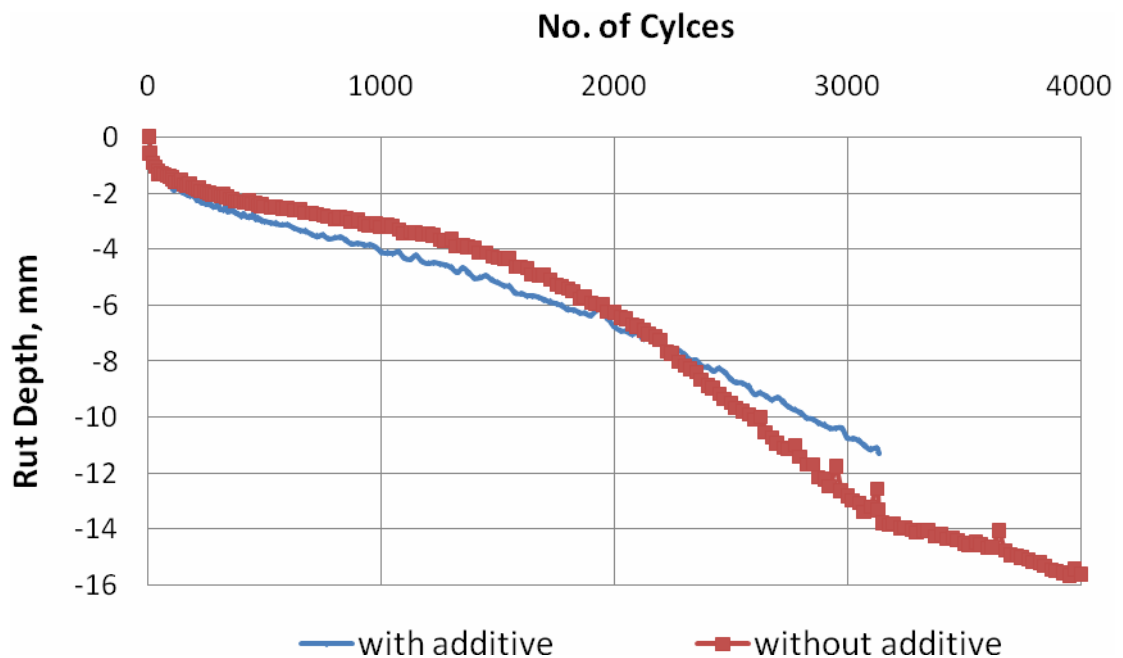


Figure 4-10 Rut depth vs. number of cycles from the HWTD tests of D5-5G06016A mix (50°C wet)

APA vs. HWTD test results

Figure 4-11 shows the comparison of rut depths obtained from the APA and the HWTD tests for this mix. The curves from the APA tests do not identify the benefit of using additive in the reduction of rut depth whereas the curves from the HWTD tests identify some benefit at the higher number of cycles. The curve for the sample without additive from the Hamburg test shows a stripping inflection point but the curves from the APA tests do not show any inflection point. Visual inspection show stripping in the sample after the APA tests. The HWTD results match with visual inspection. Again, the overall rut depths in the Hamburg tests are larger than those in the APA tests.

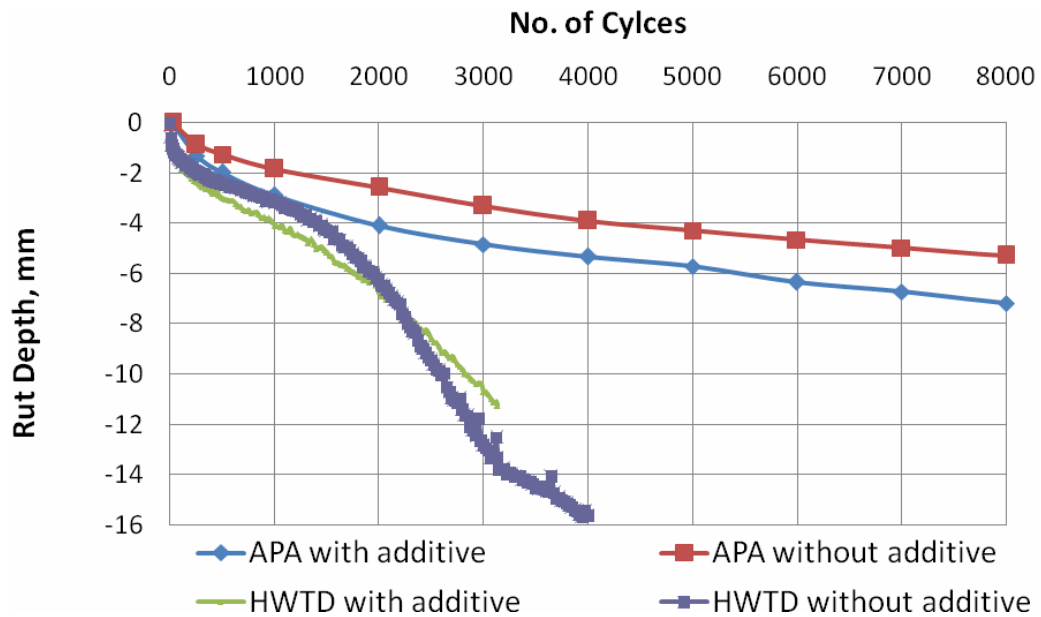


Figure 4-11 Rut depth vs. number of cycles from APA and the HWTD tests of D5-5G06016A mix (50°C wet)

4.3.4 District 6 (6G06011A -Wet 50°C)

The Superpave HMA mix used in Meade County of Kansas District 6 was used to make lab samples in this study. The estimated ESAL for this mix was 7.9 million. The temperature used for mixing of aggregate and binder was 311-320°F (155-160°C) whereas the molding temperature was 286-295°F (141-146°C). The aggregate type and ratio and the type and percent of binder and additive used for this mix are as in **Table 4-5**.

Table 4-5 Aggregate and binder types of D6 - 6G06011A mix

K-TRAN-KU-KSU Project	
	District 6
Aggregate type and ratio	CG 1 (20%)
	CG 2 (10%)
	CG 3 (10%)
	CG 4 (25%)
	SSG 2 (25%)
	SSG 4 (10%)
Binder type	PG 64-22
Additive type	Arr-Mazz, LA-2
Design % Asphalt	5.15
Design % Additive	0.3
Mixing temp range (°F)	311-320
Molding temp range (°F)	286-295
Mix Designation	SM - 19 A

APA test results

Figure 4-12 presents the measured rut depth vs. number of cycles from the APA tests, which shows unusually large rut depth for the sample with additive. No curves show stripping inflection point. Additive in this case might have helped the binder to be softer hence larger rut depth.

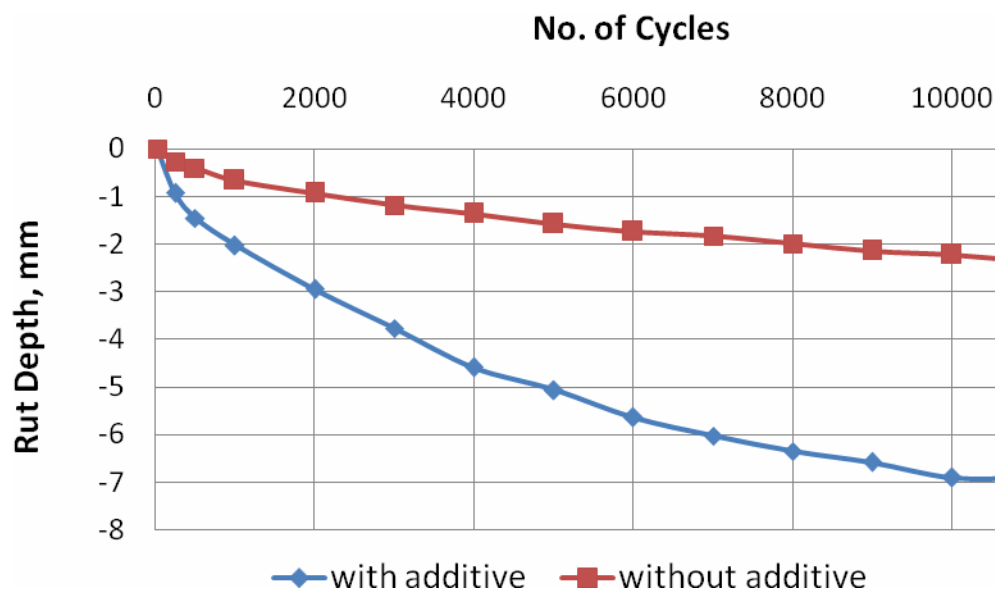


Figure 4-12 Rut depth vs. number of cycles from the APA tests of D6-6G06011A mix (50°C wet)

Hamburg test results

The measured rut depth vs. number of cycles from the HWTD tests is shown in **Figure 4-13**. Curves for this test do not show stripping inflection point. Similar to the APA tests, rut depth for sample with additive is much larger than that without additive. Additive in this case might have helped the binder to be softer and hence higher rut depth.

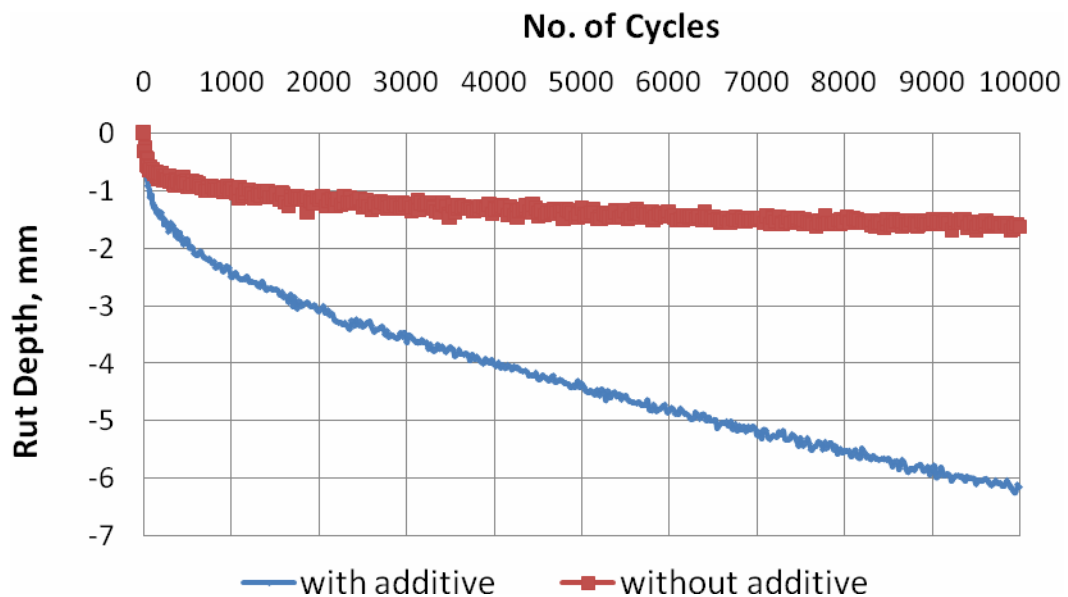


Figure 4-13 Rut depth vs. number of cycles from the HWTD tests of D6-6G06011A mix (50°C wet)

APA vs. Hamburg test results

Figure 4.14 shows comparison of curves obtained from the APA and the HWTD tests. Both APA and HWTD tests do not show stripping inflection point. Visual inspection after APA tests shows that the samples do not have stripping. Test results match with visual inspection results. Both tests show larger rut depths in samples using additive. This unexpected behavior may be due to binder softening.

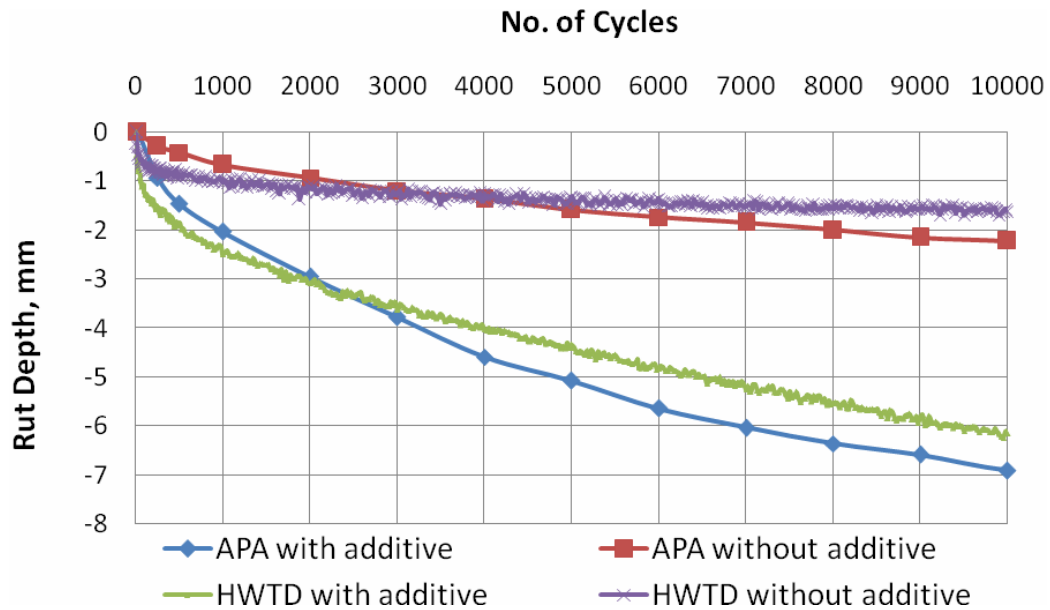


Figure 4-14 Rut depth vs. number of cycles from the APA and the HWTD tests of D6-6G06011A mix (50°C wet)

4.3.5 District 6 (6G06016A -Wet 50°C)

The Superpave HMA mix used in Meade County of Kansas District 6 was used to make lab samples. The estimated ESAL was 7.9 million. The temperature used for mixing of aggregate and binder was 309-317°F (154-158°C) whereas the molding temperature was 286-295°F (141-146°C). The aggregate type and ratio and the type and percent of binder and additive for this mix are listed in **Table 4-6**.

Table 4-6 Aggregate and binder types of D6 - 6G06016A

K-TRAN-KU-KSU Project	D6: 6G06016A
	District 6
Aggregate type and ratio	CG 1 (18%)
	CG 2 (10%)
	CG 3 (27%)
	CG 4 (20%)
	SSG 2 (25%)
Binder type	PG 70-28
Additive type	Arr-Mazz, LA-2
Design % Asphalt	5.00
Design % Additive	0.25
Mixing temp range (F)	309-317
Molding temp range (F)	286-295
Mix Designation	SM - 19 A

APA test results

Figure 4-15 presents the rut depth vs. number of cycles from the APA tests for this mix. It is shown that the samples with and without additive basically performed equally. No obvious stripping inflection point can be identified in either curve.

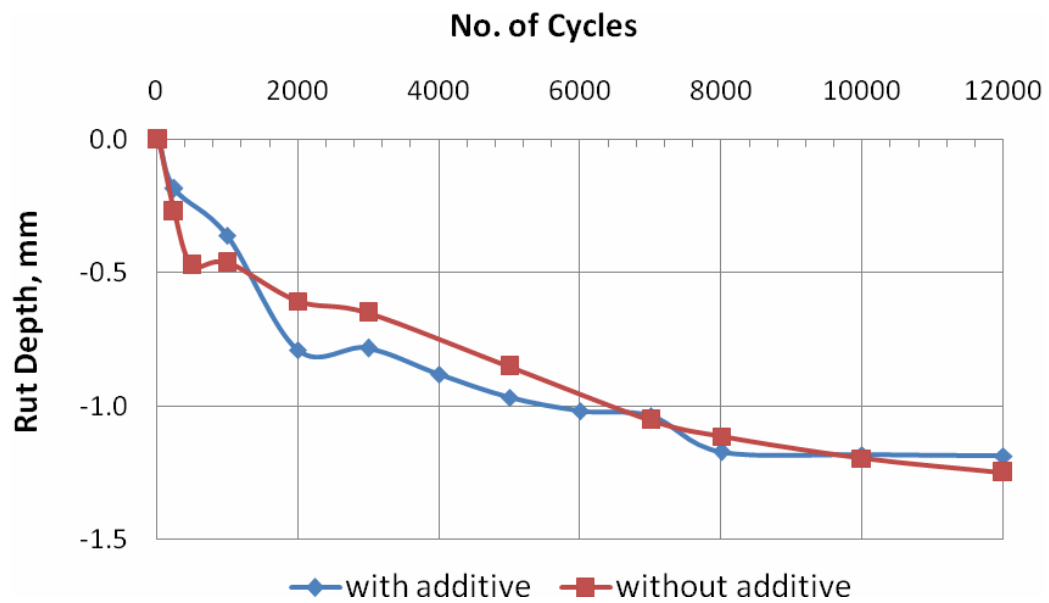


Figure 4-15 Rut depth vs. number of cycles from the APA tests of D6-6G06016A mix (50°C wet)

Hamburg test results

The measured rut depth vs. number of cycles from the HWTD tests is shown in **Figure 4-16**. Curves for this test do not show stripping inflection point. Use of additive has shown benefit against rut depth.

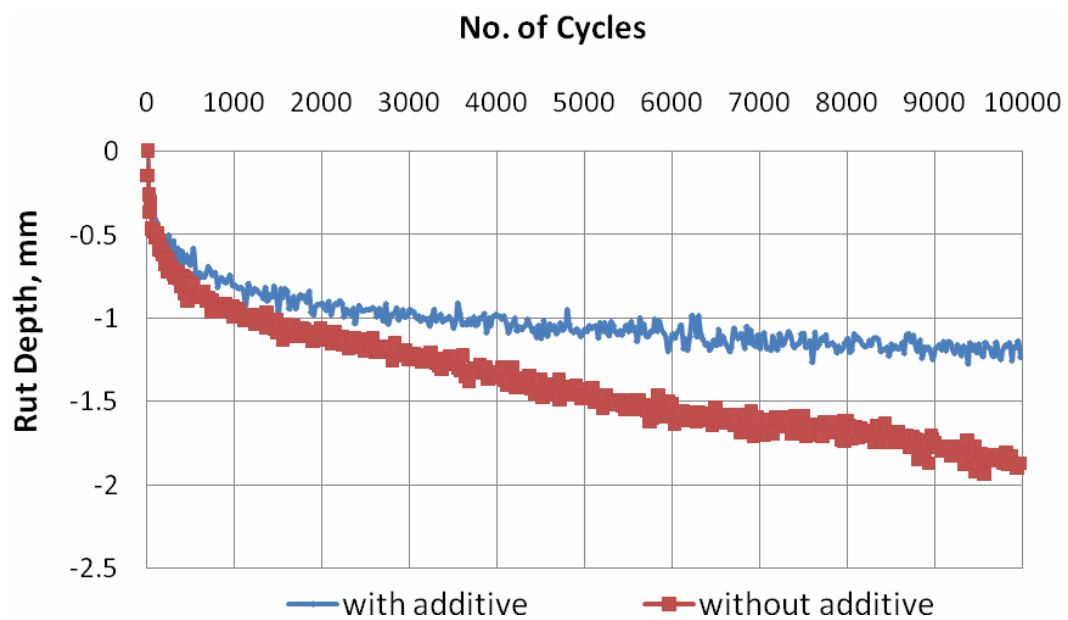


Figure 4-16 Rut depth vs. number of cycles from the HWTD tests of D6-6G06016A mix (50°C wet)

APA vs. HWTD test results

Figure 4.17 show comparison of results from the APA and the HWTD for this mix. Both tests do not show stripping inflection point. Visual inspection after the APA tests show that the samples do not have stripping. Test results match with visual inspection results. The HWTD results show smaller rut depth in samples with additive whereas the APA results show both curves almost overlap each other. Sample with additive tested in the HWTD almost overlap with curves obtained from APA tests. Hence rut depth obtained from the HWTD and the APA match reasonably well.

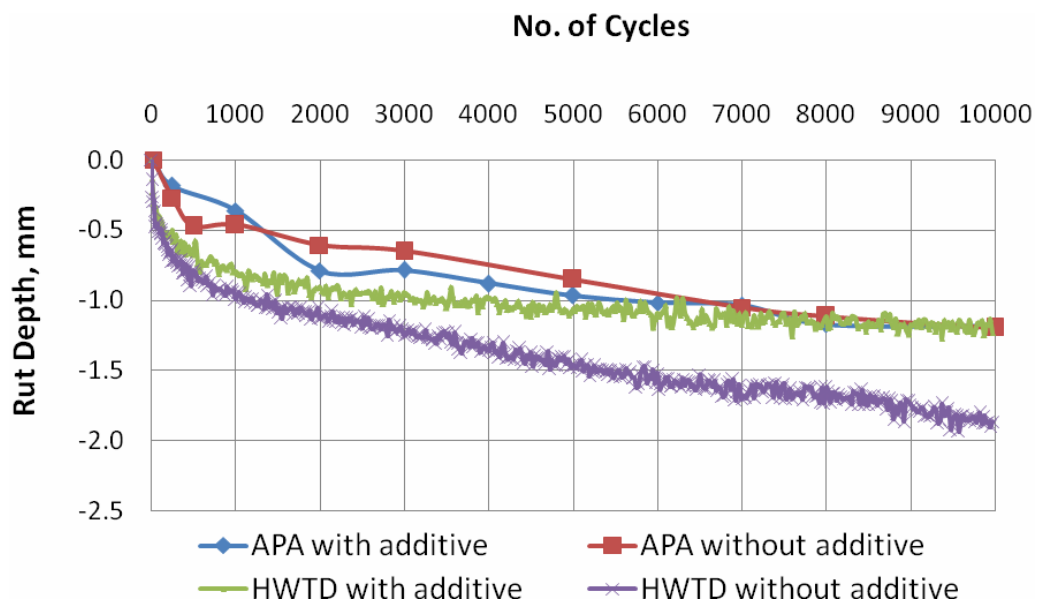


Figure 4-17 Rut depth vs. number of cycles from the APA and the HWTD tests of D6-6G06016A mix (50°C wet)

4.3.6 District 6 (6G07002A -Wet 50°C)

The Superpave HMA mix used in Meade County of Kansas District 6 was used to make lab samples. The estimated ESAL was 6.1 million. The temperature used for mixing of aggregate and binder was 306-326°F (152-158°C) whereas the molding temperature was 290-315°F (143-157°C). The aggregate type and ratio and the type and percent of binder and additive used for this mix are presented in **Table 4-7**.

Table 4-7 Aggregate and binder types of D6 - 6G07002A mix

	D6: 6G07002A
K-TRAN-KU-KSU Project	District 6
Aggregate types and ratio	CG 1 (15%)
	CG 2 (15%)
	CG 4 (15%)
	CG 5 (20%)
	SSG 1 (35%)
Binder type	PG 64-22
Additive type	AD-Here HP Plus
Design % Asphalt	4.70
Design % Additive	0.5
Mixing temp range (F)	306-326
Molding temp range (F)	290-315
Mix Designation	SM - 19 A

Six samples with additive and six without additive were prepared at KSU for the APA tests. The same mix was used to prepare an equal number of samples at KU to investigate possible effect of sample preparation at two different labs. In addition, extra samples were prepared at KU using this mix to run APA tests under different preconditioning (dry vs. wet) and test conditions (60°C vs. 50°C). The test results of these extra tests will be presented in the later sections.

APA test results

Figure 4-18 presents the measured rut depth vs. number of cycles from the APA tests on samples prepared at KSU. It is shown that the samples without any additive had slightly larger rut depth than those with the additive. To investigate the stripping inflection point, the APA tests were run up to 20,000 cycles, which are commonly used for the HWTD tests. However, no stripping inflection point was observed even up to 20,000 cycles.

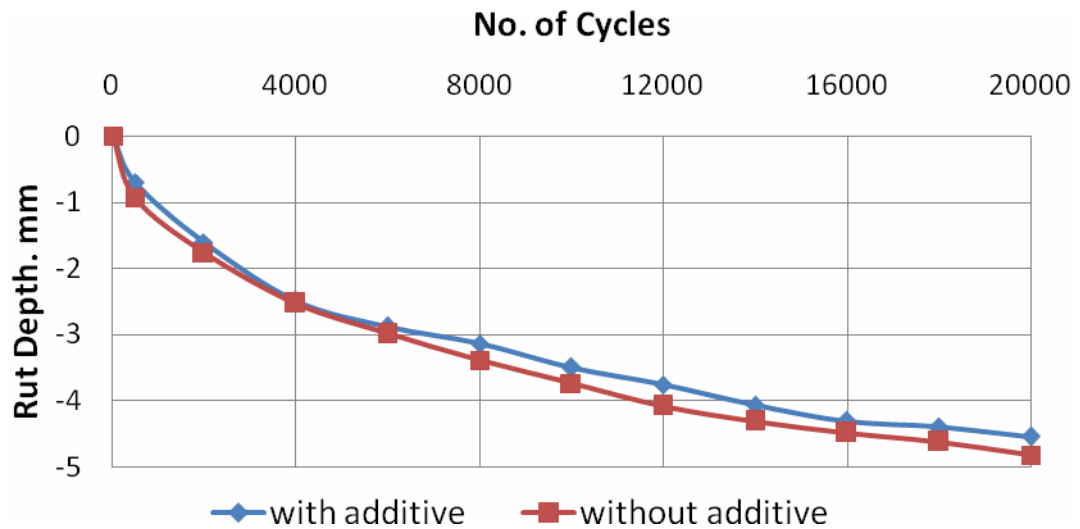


Figure 4-18 Rut depth vs. number of cycles from the APA tests of D6-6G07002A mix (samples prepared at KSU, 50°C wet)

Figure 4-19 presented the measured rut depth vs. number of cycles from the APA tests on samples prepared at KU. It is shown in Figure 4-19 that the use of the additive reduced the rut depth more significantly than that shown in Figure 4-18. More comparison of these results will be presented later. In addition, the curves in Figure 4-19 shows slight stripping inflection points for both samples with and without the additive. It was observed visually that the samples without the additive showed more stripping behavior than those with the additive. However, no stripping point was observed in the test results for other samples made at KU. Therefore, it is not certain whether these points are truly the stripping inflection points.

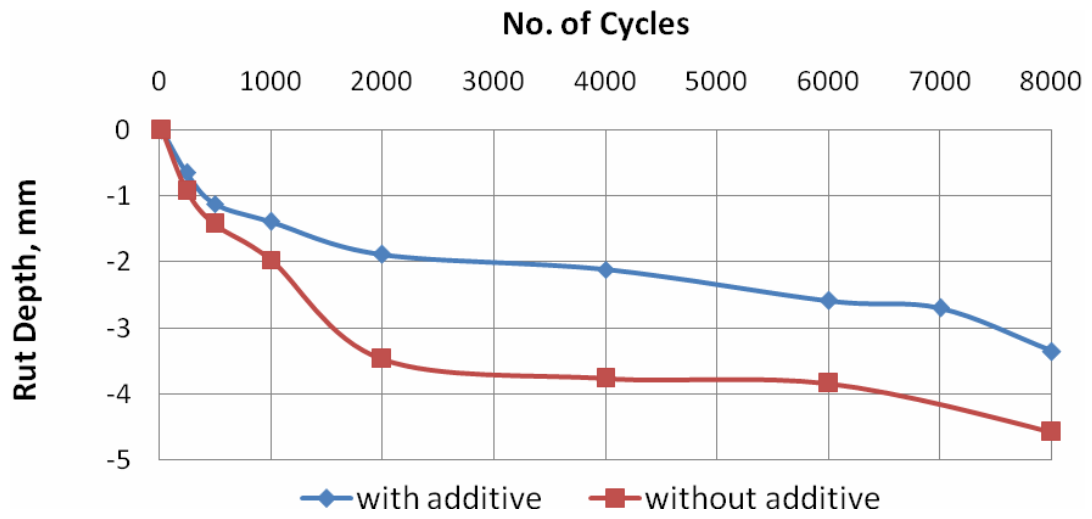


Figure 4-19 Rut depth vs. number of cycles from the APA tests of D6-6G07002A mix (samples prepared at KU, 50°C wet)

HWTD test results

Figure 4-20 presented the measured rut depth vs. number of cycles from the HWTD tests. It is shown that the samples without the additive had a stripping inflection point at approximately 6500 cycles. Samples with the additive did not have any stripping inflection point. Similar to other results, the use of the additive increased the rut depth in a short term but reduced the rut depth in a long term, especially after the inflection point of the sample without the additive.

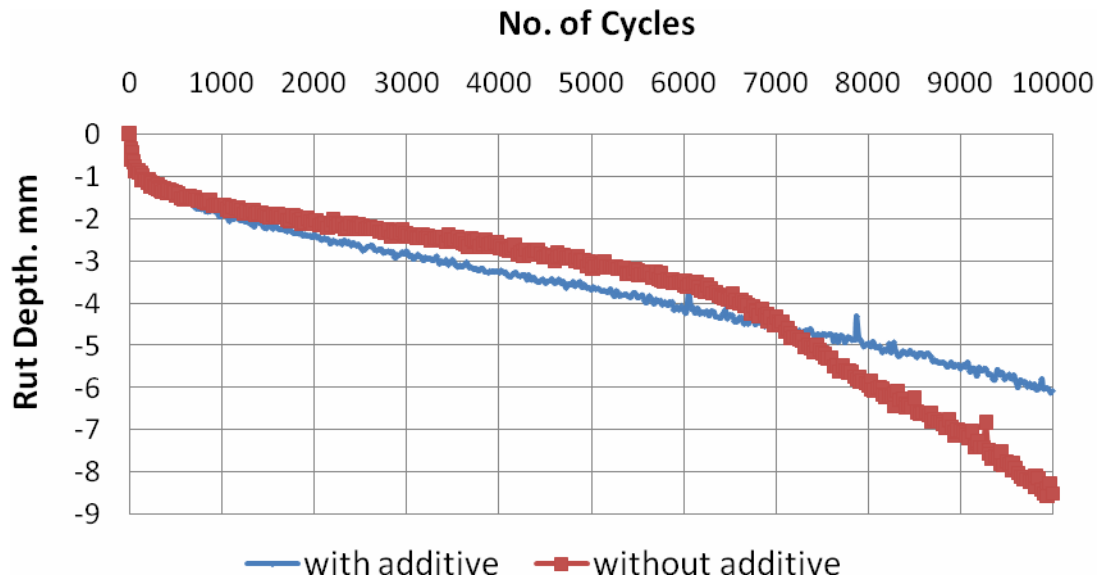


Figure 4-20: Rut vs. number of cycles from the HWTD tests of D6-6G07002A mix (samples prepared at KSU, 50°C wet)

APA vs. HWTD test results

Figure 4-21 presents the results from the APA and the HWTD tests. Visual inspection of this sample showed stripping after the APA tests. Rut depths from both APA and HWTD match reasonably well. The APA did not detect stripping inflection point. However, the HWTD test results show a more obvious stripping inflection point for the samples without the additive. Use of additive has improved the performance of the sample against stripping.

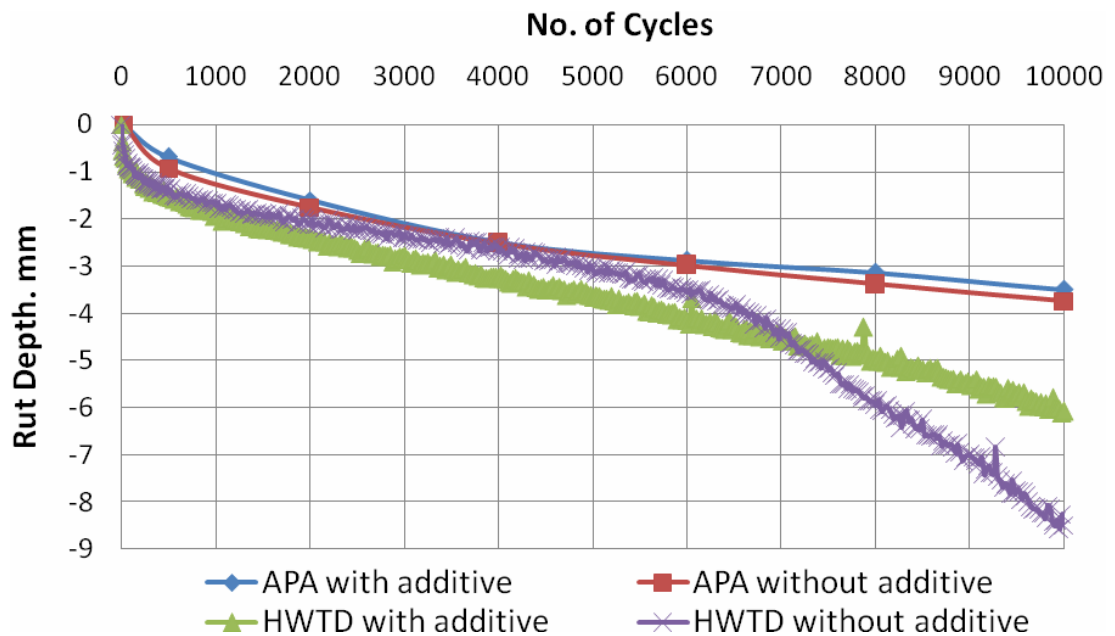


Figure 4-21 Rut depth vs. number of cycles from the APA and the HWTD tests of D6-6G07002A mix (50°C wet)

4.3.7 District 6 (6G07002A -Wet 60°C)

To investigate the temperature effect on the test results, six samples with the additive and six samples without any additive were made at KU. These samples were subjected to 6 min vacuum saturation and one hour soak in water at 60°C before testing. **Figure 4-22** presents the measured rut depth vs. number of cycles from the APA tests. The test results show that the use of the additive reduced the rut depth. However, neither curves had any obvious stripping inflection point. The comparison of the test results for the samples tested at 50°C and 60°C will be presented in the later section.

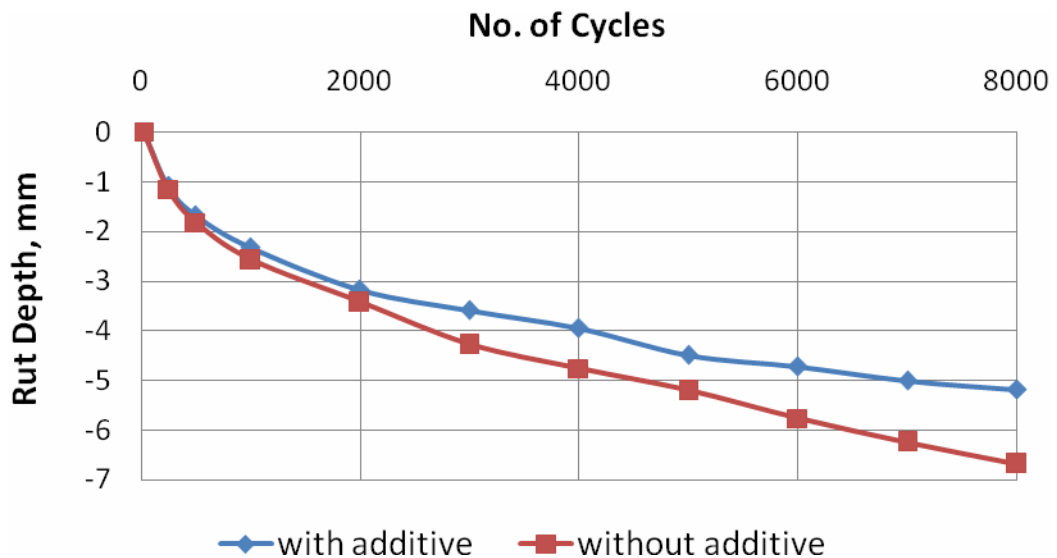


Figure 4-22: Rut depth vs. number of cycles from the APA tests of D6-6G07002A mix (60°C wet)

4.3.8 District 6 (6G07002A -Dry 50°C)

To investigate the preconditioning effect on the test results, six samples with the additive and six samples without the additive were made at KU and tested in a dry condition. The air temperature was raised to 50°C in the APA chamber. **Figure 4-23** presents the rut depth vs. number of cycles from the APA tests. The test results show that the samples without the additive had slightly smaller rut depth than those with the additive. Neither curves had any stripping inflection point as expected for dry samples.

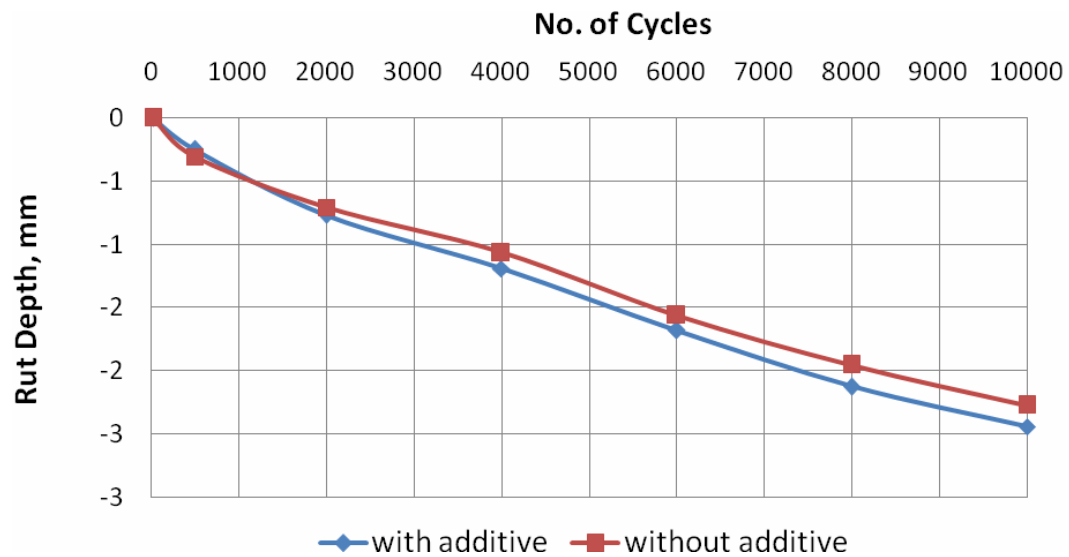


Figure 4-23 Rut depth vs. number of cycles from the APA tests of D6-6G07002A mix (50°C dry)

4.3.9 District 6 (6G07002A –Dry 60°C)

To investigate the combined effect of temperature and preconditioning, six samples with the additive and six samples without the additive were made at KU and tested at a temperature of 60°C in a dry condition. **Figure 4-24** presents the rut depth vs. number of cycles from the APA tests. The test results clearly show the benefit of the additive in the reduction of rut depth. Neither curves had any stripping inflection point as expected for dry samples.

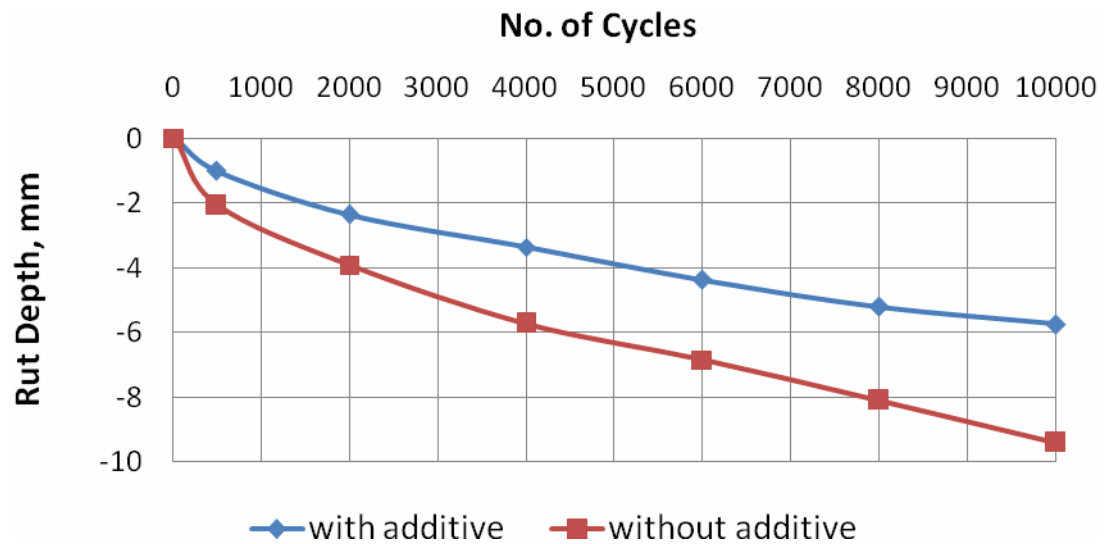


Figure 4-24 Rut depth vs. number of cycles from the APA tests of D6-6G07002A mix (60°C dry)

4.4 Comparisons of Test Results for District 6 - 6G07002A Mix

In this section, the following comparisons are made in terms of rut depths obtained using the APA tests on samples made at KU under different preconditioning and temperature conditions:

- a. Wet vs. dry tests at 50°C
- b. Wet vs. dry tests at 60°C
- c. Wet 60°C vs. wet 50°C
- d. Dry 60°C vs. dry 50°C

4.4.1 Wet vs. dry tests at 50°C

Figure 4-25 presents the test results of the samples tested under wet 50°C vs. dry 50°C, which show that the rut depths are larger in wet tests than in dry tests at 50°C. This finding implies that water has a negative effect on the performance of HMA.

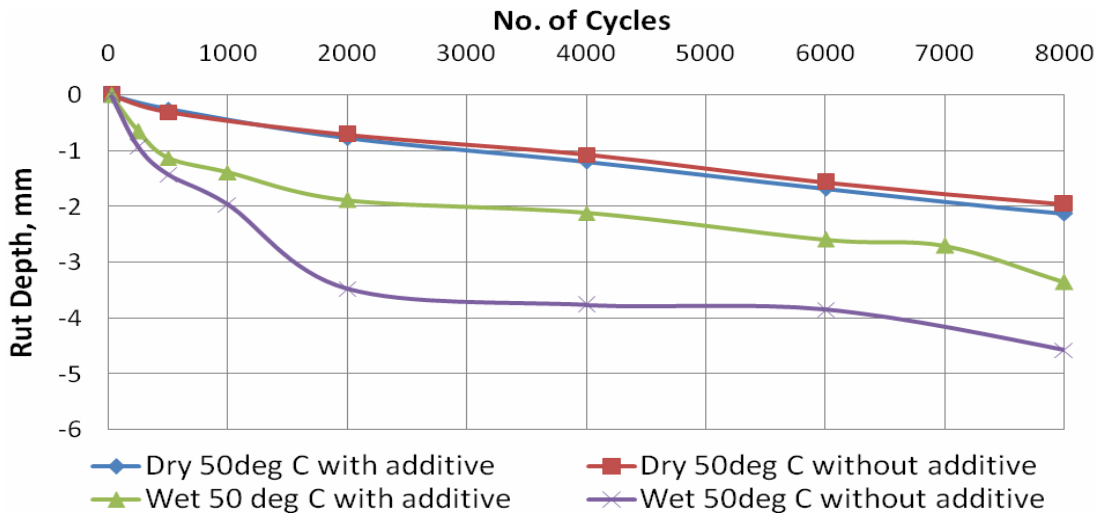


Figure 4-25 Rut depths for samples tested under wet 50°C vs. dry 50°C

4.4.2 Wet vs. dry tests at 60°C

The binder used for this mix was PG 64-22. As compared with Figure 4-21, **Figure 4-22** shows that the samples tested at a higher temperature (60°C) had different behavior from those tested at a lower temperature (50°C).

Interestingly, in the case of samples without any additive, the rut depth was lower in the wet test than in the dry test. In the dry test, the sample showed higher rut depth with heaving on the sides of the wheel path. It was observed during the test that the binder was soft at the higher temperature thus causing more rut depth and heaving on the sides. In the case of the wet test there was no heaving on sides and the rut depth was lower. In the case of the samples with additive, the rut depth was higher in the wet test than that in the dry test.

Another comparison can be made based on the results in **Figure 4-22**. For the wet tests at 60°C, the use of the additive showed slight benefit in the reduction of the rut depth. For the dry tests at 60°C, the use of the additive showed significant benefit in the reduction of the rut depth. This comparison implies that the additive not only improves the performance of HMA against stripping but also reduces the overall rutting deformation under dry and wet conditions.

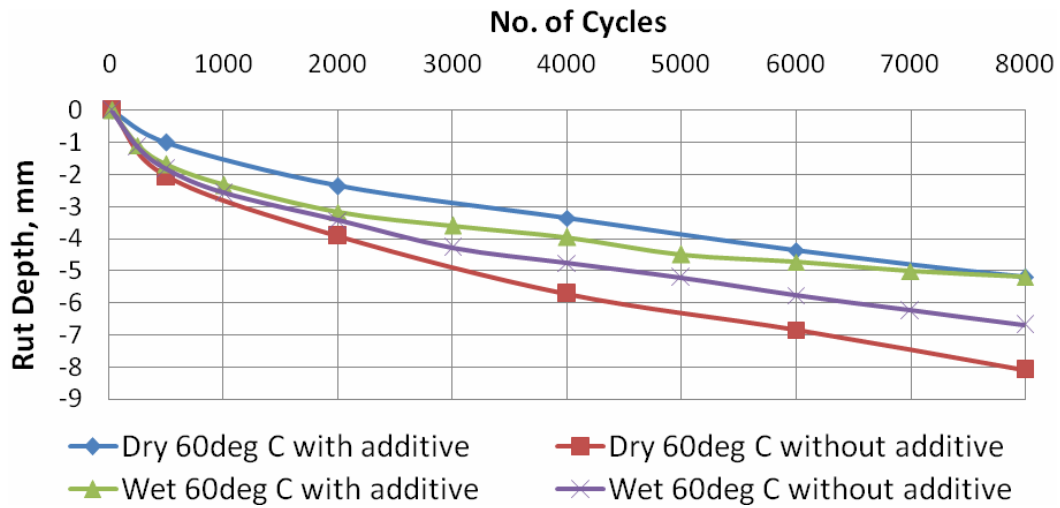


Figure 4-26 Rut depths for samples tested under wet 60°C vs. dry 60°C

4.4.3 Wet tests at 50°C vs. 60°C

Figure 4-27 shows the comparison of the test results obtained by the wet tests at different temperatures. It is quite obvious that the rut depths were larger at 60°C than those at 50°C. Both sets of curves show the benefit of the additive in the reduction of the rut depth.

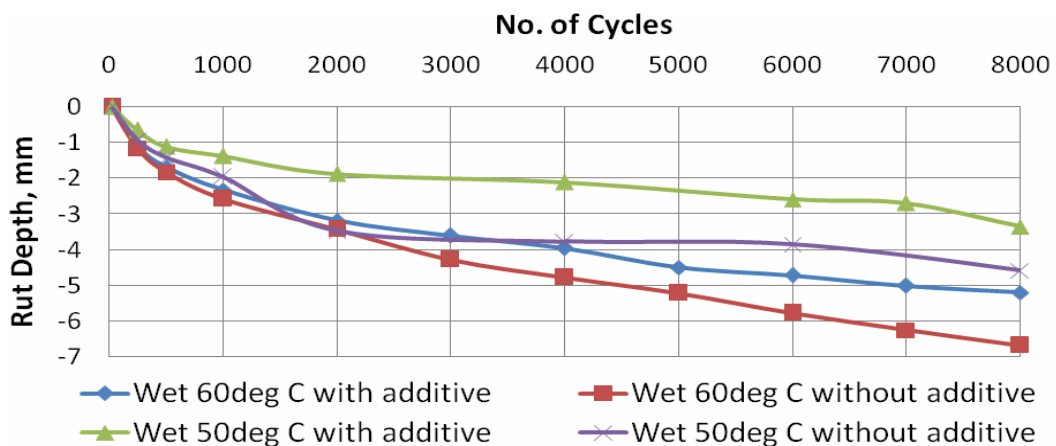


Figure 4-27 Wet tests at 50°C vs. 60°C

4.4.4 Dry tests at 50°C vs. 60°C

Figure 4-28 presents the rut depths obtained for the same mix when tested at different temperatures. It is obvious that the rut depth was larger at 60°C than at 50°C. At the higher temperature, the use of the additive showed more benefit in the reduction of the rut depth.

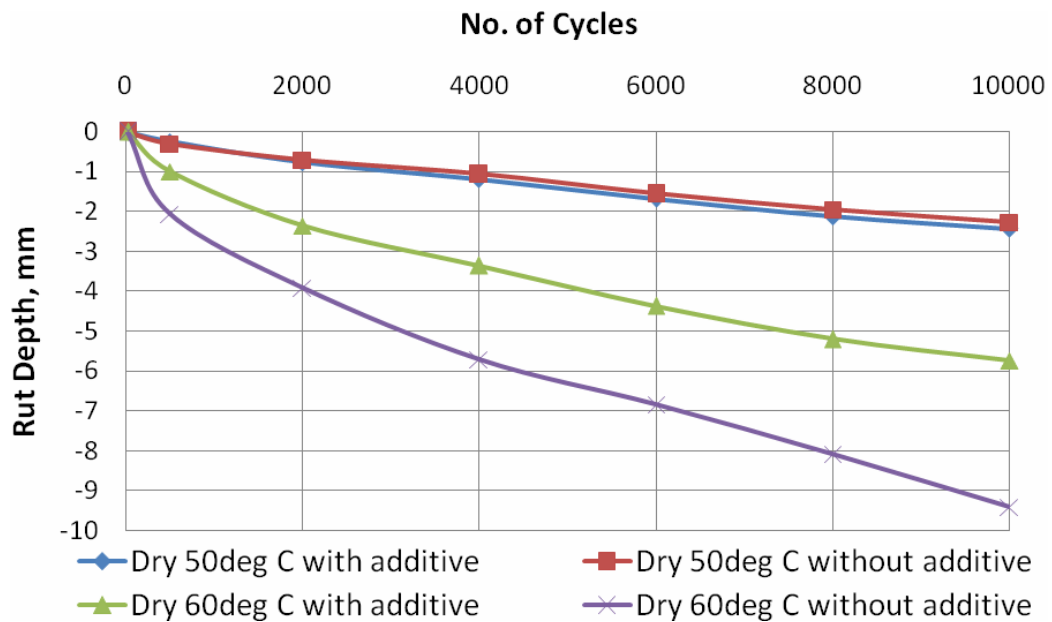


Figure 4-28 Dry tests at 50°C vs. 60°C

4.4.5 Samples prepared at KSU vs. KU

Figure 4-29 presents the APA test results of the samples prepared at KSU and KU, which show some difference for the samples without any additive but negligible

difference for the samples with the additive. However, the overall difference for these test results is not that significant.

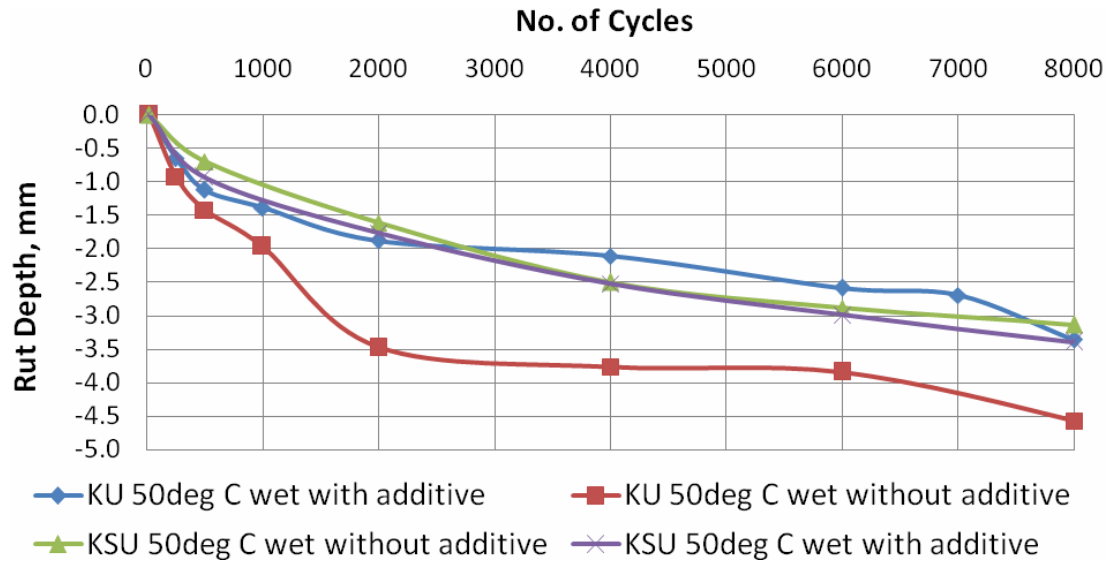


Figure 4-29: Samples made at KSU vs. KU

4.5 Summary of Test Results

Table 4-8 summarizes the test information and results obtained using the APA and the HWTD tests, which includes the district, the project design number, the mix, the lab designation number, the type or conditioning of the test, and the test results.

The comparisons of test results yield the following conclusions:

(1) Wet vs. dry tests at 50°C

- rut depths were larger in the wet test than in the dry test
- visible stripping was shown in the wet test
- benefit of the additive in the wet test was shown but not in the dry test

Table 4-8 Summary of test information and results.

No.	District	Design Number	Mix	Lab Designation Number	Type of test done	APA tests			Hamburg tests	
						Stripping inflection point	Benefit of Additive	Visual inspection of sample	Stripping inflection point	Benefit of Additive
1	2	2G06015A	9.5 A	T3 (w/o additive)	Wet-50°C	Not seen		Stripping, loss of bonding	After about 1500 cycles	
2	2	2G06015A	9.5 A	T5 (w additive)	Wet-50°C	Not seen	Negative impact	No stripping	Not seen	Benefit seen
3	3	3G06020A	SM-19A	T13 (w/o additive)	Wet-50°C	Not seen		Stripping seen	After about 4500 cycles	
4	3	3G06020A	SM-19A	T15 (w additive)	Wet-50°C	Not seen	Not seen	No stripping	Not seen	Benefit seen only at later stage
5	5	5G06016A	9.5 A	T7 (w/o additive)	Wet-50°C	Not seen		Stripping seen	After about 1500 cycles	
6	5	5G06016A	9.5 A	T11 (w additive)	Wet-50°C	Not seen	Negative impact	No stripping	After about 2000 cycles	Slight Benefit
7	6	6G06011A	SM-19A	T18 (w/o additive)	Wet-50°C	Not seen		No stripping	Not seen	
8	6	6G06011A	SM-19A	T20(w additive)	Wet-50°C	Not seen	Negative impact	No stripping	Not seen	Negative impact
9	6	6G07002A	SM-19A	T23 (w/o additive)	Wet-50°C	Not seen		Stripping seen	After about 6000 cycles	

Table 4-8 Summary of test information and results (continued).

No.	District	Design Number	Mix	Lab Designation Number	Type of test done	APA tests			Hamburg tests	
						Stripping inflection point	Benefit of Additive	Visual inspection of sample	Stripping inflection point	Benefit of Additive
10	6	6G07002A	SM-19A	T25 (w additive)	Wet-50°C	Not seen	Slight benefit	No stripping	Not seen	Benefit seen in later stage
11	6	6G06016A	SM-19A	T28 (w/o additive)	Wet-50°C	Not seen		No stripping seen	Not seen	
12	6	6G06016A	SM-19A	T30 (w additive)	Wet-50°C	Not seen	Not seen	No stripping seen	Not seen	Benefit seen
13	6	6G07002A	SM-19A	K1 (w/o additive)	Wet-50°C	Not clear		Shows stripping, loss of bonding	These tests not done in Hamburg Device.	
14	6	6G07002A	SM-19A	K2 (w/o additive)	Wet-60°C	Not seen		No stripping seen		
15	6	6G07002A	SM-19A	K5 (w/o additive)	Dry-60°C	Not seen		No stripping seen, heave on the sides of the load path seen		
16	6	6G07002A	SM-19A	K6 (w/o additive)	Dry-50°C	Not seen		No stripping seen		
17	6	6G07002A	SM-19A	K3 (w additive)	Wet-50°C	Not clear	Benefit seen	No stripping seen		
18	6	6G07002A	SM-19A	K4 (w additive)	Wet-60°C	Not seen	Benefit seen	No stripping seen		
19	6	6G07002A	SM-19A	K7 (w additive)	Dry-60°C	Not seen	Benefit seen	No stripping seen		
20	6	6G07002A	SM-19A	K8 (w additive)	Dry-50°C	Not seen	Slight Benefit	No stripping seen		

(2) Wet vs. dry tests at 60°C

For the samples without the additive

- rut depth was smaller in the wet test than in the dry test
- high rut in the dry test with heaving on sides developed but no heaving on the wet test

For the samples with the additive

- rut depth was larger in the wet test than in the dry test
- no heaving developed on sides
- benefit of the additive was not high in the wet test
- benefit of the additive was higher in the dry test
- additive improved not only stripping resistance but also overall performance of HMA against rutting.

(3) Wet 60°C vs. wet 50°C

- Rut depth was larger at 60°C than at 50°C in the wet test
- Both tests showed benefit of the additive.

(4) Dry 60°C vs. dry 50°C

- rut depth was larger at 60°C than at 50°C
- additive showed more benefit at a high temperature than at a low temperature.

(5) Samples prepared at KSU vs. KU

- both samples had rut depths in the range of 3-4 mm after 8000 cycles
- results matched reasonably well.

5. CONCLUSIONS AND RECOMMENDATIONS

5.1. Conclusions

1. Visual observation showed stripping in four out of six mixes used for the tests. Loss of bonding between aggregate and binder occurred in these samples. Sand particles were washed out of binder in a few stripped samples.
2. None of the APA tests conducted in this study showed a stripping inflection point. However, the HWTD tests did show such a stripping inflection point in all four mixes which showed stripping. The HWTD tests did not show stripping point for two mixes which did not show stripping during visual inspection.
3. The use of the additive showed the benefit in the reduction of the rut depth in some cases of the APA tests but not in all. However, most of the HWTD test results showed the benefit in the later stage of the tests. In the earlier stage, the samples with the additive had larger rut depths than those without any additive. In one mix (D6G06011A), the use of additive showed high negative impact for both APA and HWTD tests.

4. At the higher temperature (60°C for PG 64-22 binder), the rut depths were higher in the dry test than in the wet test. More heaving on the sides of the wheel path was observed in the dry test than that in the wet test. Rutting damage is more critical at higher temperature when the binder becomes soft. At the lower temperature (50°C for PG 64-22 binder), rut depths were higher in the wet test than in the dry test. Stripping was seen in the wet test. Thus stripping has more contribution to rut depth at low temperature than at high temperature.
5. Both the APA and the HWTD tests take around 4-6 hours to complete. These methods are faster than conventional test methods used to determine moisture sensitivity. APA tests can show stripping behavior visually. On the other hand, Hamburg tests can detect stripping behavior in HMA mixes based on rut depth vs. number of cycles curve. Thus the HWTD tests are more effective as a rapid test method in case of determining moisture sensitivity.

5.2. Recommendations

1. This study shows that the HWTD tests can better predict the stripping behavior. More studies and laboratory tests using the HWTD device should be conducted to investigate more influential factors on moisture sensitivity.

2. More studies should be carried out to relate number of passes for stripping inflection point with severity of stripping.

3. Correlating laboratory test data with actual performance in the field would be necessary to verify the test results obtained in this study.

6. REFERENCES

1. Al-Swailmi, S. and Terrel, R. L. (1992). "Evaluation of water damage of asphalt concrete mixtures using the Environmental Conditioning System (ECS)" Journal of the Association of Asphalt Paving Technologists, Vol. 61.
2. Anjelo, J. and Anderson, R. (2003). "Material production, mix design, and pavement design effects on moisture damage", Moisture Sensitivity of Asphalt Pavements, TRB Seminar Paper, 187-201.
3. Aschenbrener, T. (1995). "Evaluation of Hamburg Wheel-Tracking Device to predict moisture damage in hot mix asphalt", Transportation Research Record, 1492, 193-201.
4. Aschenbrener, T. (1996). "Comparison of several moisture susceptibility tests to pavements of known field performance", Asphalt Paving Technology, Association of Asphalt Paving Technologists, Volume 64, 163-208.
5. Bhairampally, R. K., Lytton, R. L., and Little, D. N. (2000). "Numerical and graphical method to assess permanent deformation potential for repeated compressive loading of asphalt mixtures". In Transportation Research Record:

Journal of the Transportation Research Board, No. 1723, TRB, National Research Council, Washington, D.C., pp. 150–158.

6. Castan, M. (1968). “Rising of binder to the surface of an open-graded bituminous mix”. *Bulletin de liaison des laboratoires routiers*, No. 33, pp. 77–84.
7. Cheng, D., Little, D. N., Lytton, R. L., and Holste, J. C. (2002). “Surface energy measurement of asphalt and its application to predicting fatigue and healing in asphalt mixtures”. in *Transportation Research Record: Journal of the Transportation Research Board*, No.1810, TRB, National Research Council, Washington, D.C., pp. 44–53.
8. Coplantz, S. (1988). “Water sensitivity test methods for asphalt concrete mixtures, a laboratory comparison”, *Transportation Research Board*, 1171, 44-50.
9. Cross, S.A. and Voth, M.D. (2001). “Effects of sample preconditioning on Asphalt Pavement Analyzer (APA) wet rut depths”, *Transportation Research Board*, Paper No. 01-0392, 1-20.

10. Curtis, C. W. (1992). "Fundamental properties on asphalt aggregate Interactions adhesion and adsorption". Final Report on Contract A-003B. Strategic Highway Research Program, National Research Council, Washington, D.C
11. Fromm, H. J. (1974). "The mechanisms of asphalt stripping from aggregate surfaces". Association of Asphalt Paving Technologists, Vol. 43, pp. 191–223.
12. Gordon, D.A. (2005). "Combined laboratory ageing/ moisture sensitivity assessment of high modulus base asphalt mixtures" Asphalt Paving Technology: Association of Asphalt Paving Technologists, Issn. No. 0270-2932, 307-345.
13. Gzemski, F. C., McGlashan, D. W., and Dolch, W. L. (1968). "Thermodynamic Aspects of the Stripping Problem". Highway Research Circular 78 HRB, National Research Council, Washington, D.C.
14. Huang, S.H., Robertson, R.E, Branthaver, J.F., and Peterson, J.C. (2005). "Impact of lime modification of asphalt and freeze-thaw cycling on the asphalt-aggregate interaction and moisture resistance to moisture damage." Journal of Materials in Civil Engineering, ASCE, 711-718

15. Hubbard, P. (1938). "Adhesion of asphalt to aggregates in presence of water". Highway Research Board Proceedings, Vol. 18, Part 1, pp. 238—249.
16. Hunter, E. and Ksaibati, K. (2002). "Evaluating moisture susceptibility of asphalt mixes", University of Wyoming, United States Department of Transportation to the Mountain-Plains Consortium (MPC), 1-37.
17. Kandhal, P. (2002). "Premature failure of asphalt overlays from stripping: Case histories", Asphalt Pavement Technology, Association of Asphalt Pavement Technologists, Volume 70, 301-351.
18. Kandhal, P. and Mallick, R. (1999) "Potential of Asphalt Pavment Analyzer (APA) to predict rutting of Hot Mix Asphalt", International Conference on Accelerated Pavement Testing, 1-23.
19. Kennedy, T. W., Roberts, F. L., and Anagnos, J. N. (1984). "Texas Boiling Test for evaluating moisture susceptibility of asphalt mixtures" Research Report 253-5. Center for Transportation Research, University of Texas at Austin, Jan.
20. Kennedy, T. W., Roberts, F. L., and Lee, K. W. (1984). "Evaluating moisture susceptibility of asphalt mixtures using the Texas Boiling Test". In

Transportation Research Record 968, TRB, National Research Council, Washington, D.C., pp. 45—54.

21. Kennedy, T. W., Roberts, F. L., Lee, K. W., and Anagnos, J. N. (1982). “Texas Freeze–Thaw Pedestal test for evaluating moisture susceptibility for asphalt mixtures”. Research Report 253-3. Center for Transportation Research, University of Texas at Austin, Feb.
22. Kiggundu, B. M. (1986). “Effects of Submergence in Distilled Water on the Surface Coloration of Asphalt”. Unpublished data, NMERI.
23. Kiggundu, B. M., and Roberts, F. L. (1988). “The success/failure of methods used to predict the stripping potential in the performance of bituminous pavement mixtures”. Submitted to TRB.
24. Kim, Y.-R., Little, D. N., and Lytton, R. L. (2002). “Fatigue and healing characterization of asphalt mixtures”. Journal of Materials in Civil Engineering, American Society of Civil Engineers
25. Kruz, N.C. (1990). “Relationship between permanent deformation of asphalt concrete and moisture sensitivity”, Transportation Research Record, 1259, 163-168.

26. Little, D. and Jones, D. (2003). "Chemical and mechanical processes of moisture damage in hot mix asphalt pavements", Moisture Sensitivity of Asphalt Pavements, TRB Seminar Paper, 37-70.
27. Lottman, R. P. (1988). "Methods of predicting and controlling moisture damage in asphalt concrete", Transportation Research Record, 1171, 1-11.
28. Lottman, R. P. (1978). NCHRP Report 192: "Predicting moisture-induced damage to asphaltic concrete". TRB, National Research Council, Washington, D.C.
29. Lottman, R. P. (1982). NCHRP Report 246: "Predicting moisture-induced damage to asphaltic concrete: field evaluation". TRB, National Research Council, Washington, D.C.
30. Mack, C. (1964). "Bituminous Materials". Vol. 1 (A. Holberg, ed.), Interscience Publishers, New York.
31. Majidzadeh, K. and Brovold, F. N. (1968). Special Report 98: "State of the Art: effect of water on bitumen-aggregate mixtures". HRB, National Research Council, Washington, D.C.

32. Martin, J., Cooley, L., and Hainin, H. (2003). Moisture Sensitivity of Asphalt Pavements, Topic 6: Production and construction issues for moisture sensitive hot mix asphalt pavements, TRB Seminar Paper, 209-222.
33. Martin, A., Rand, D., Tedford, D., Sebaaly, P., Bressetti, T., and Maupin, G. (2003). Moisture Sensitivity of Asphalt Pavements, Topic 7: Field experiences, TRB Seminar Paper, 229-255.
34. Maupin, G. W. (1982). "The use of anti-stripping additives in Virginia", submitted at the 51st Association of Asphalt Paving Technologists, Kansas City, MO.
35. McCann, M. and Sebaaly, P.E. (2003). "Evaluation of moisture sensitivity and performance of lime in hot mix asphalt – resilient modulus, tensile strength, and simple shear tests." Transportation Research Record 1832, 9-16.
36. Mohamed, H. (1993). "Debonding location in asphalt concrete associated with moisture change", Journal of Materials in Civil Engineering, 4, 497-509.
37. Mohammad N. (2001). "Characterization of HMA mixtures with the Asphalt Pavement Analyzer", ASTM Special Technical Publication, Volume 1412, 16-29.

38. Moulthrop, J., Button, J. and Hejl, F. (2003). Moisture Sensitivity of Asphalt Pavements, Topic 9: Implementation and strategic plan, TRB Seminar Paper, 265-273.
39. NCHRP Report 192 (1978). "Predicting moisture – induced damage to asphaltic concrete". TRB National Research Council, Washington D.C.,
40. Nguyen, T. (2005). "In Situ spectroscopic study of water at the asphalt/siliceous substrate interface and its implication in stripping", Journal of Adhesion, 1, 1-28.
41. Pan, C. (1998). "Evaluation of stripping for asphalt concrete mixtures using accelerated testing methods." Transportation Research Record, 1630, 98-105.
42. Randy, W., Zhang, J., and Cooley, A. (2004). "Evaluation of Asphalt Pavement Analyser for moisture sensitivity testing", National Center for Asphalt Technology (NCAT) Report 04-04, 1-23.
43. Rickards, I. (2003). "Fatigue testing of asphalt to improve the discrimination of moisture sensitivity in aggregate and bitumen systems", Australian Road Research Board, Volume 21, 243-255.

44. Roberts, F., Kandhal, P., Brown, E., Lee, D., and Kennedy, T. (1996). "Hot Mix Asphalt Materials, Mixture Design, and Construction". 2nd Edition. Lanham, Maryland: NAPA Education Foundation
45. Robertson, R. E. (2000). "Chemical Properties of Asphalts and Their Effects on Pavement Performance". Transportation Research Circular 499, TRB, National Research Council, Washington, D.C.
46. Saleh, A. (1992). "Evaluation of water damage of asphalt concrete mixtures using the environmental conditioning system (ECS)", Association of Asphalt Paving Technologists, Technical Session, Volume 61, 405-445.
47. Schmidt, R. J., and Graf, P. E. (1972). "The effect of water on the resilient modulus of asphalt treated mixes". Proc., Association of Asphalt Paving Technologists, Vol. 41, pp. 118– 162
48. Scott, J. A. N. (1978). "Adhesion and Disbonding mechanisms of asphalt used in highway construction and maintenance". Proc., Association of Asphalt Paving Technologists, Vol. 47, pp. 19–48.
49. Shatnawi, S. (1995). "Moisture sensitivity evaluation of binder-aggregate mixtures", Transportation Research Record, 1492, 71-84.

50. Solaimanian, M., Harvey, J., Tahmoressi, M. and Tandon, V. (2003). Moisture Sensitivity of Asphalt Pavements, Topic 3: Test methods to predict moisture sensitivity of hot mix asphalt pavements, TRB Seminar Paper, 77-110.
51. Tarrer, A. R. (1996). "Use of hydrated lime to reduce hardening and stripping in asphalt mixtures". Presented at the 4th Annual International Center for Aggregate Research Symposium, Atlanta, GA.
52. Tarrer, A. R., and Wagh, V. (1991). "The effect of the physical and chemical characteristics of the aggregate on bonding". Strategic Highway Research Program, National Research Council, Washington, D.C.
53. Terrel, R. L., and Shute, J. W. (1989). "Summary report on water sensitivity". SHRP-A/IR-89-003. Strategic Highway Research Program, National Research Council, Washington, D.C.
54. Terrel, R. L., and Al-Swailmi, S. (1994). "Water sensitivity of asphalt-aggregate mixes: Test Selection". SHRP Report A-403. Strategic Highway Research Program, National Research Council, Washington, D.C.

55. Thelen, E. (1958). "Surface energy and adhesion properties in asphalt-aggregate" Systems Bulletin 192, HRB, National Research Council, Washington, D.C., pp. 63-74.
56. Tseng, K. H., and Lytton, R. L. (1987). "Prediction of permanent deformation in flexible pavement materials. Implication of aggregates in design, construction, and performance of flexible pavements", ASTM STP 1016 (Schreuders, H. G. and Marek, C. R., eds.), American Society for Testing and Materials, Philadelphia, PA.
57. Tunnicliff, D. G., and Root, R. E. (1984). Use of Anti-stripping Additives in Asphaltic Concrete Mixtures, NCHRP Report 274, Laboratory phase. TRB, National Research Council, Washington, D.C
58. Williams, R. (2005). "Utilization of an Asphalt Pavement Analyzer for Hot Mix Asphalt laboratory mix design", Journal of ASTM International, 91-105.
59. Yoon, H. J. (1987). "Interface phenomenon and surfactants in asphalt paving materials dissertation", Auburn University.

Appendix – APA Test Data

A 1: D2-2G06015A-T3-WO Additive-Wet 50deg
A 2: D2-2G06015A-T5-W Additive-Wet 50deg
A3: D5-5G06016A-T7-W0 Additive-Wet 50deg
A4: D5-5G06016A-T11-W Additive-Wet 50deg
A5: D3-3G06020A-T13-WO Additive-Wet 50deg
A6: D3-3G06020A-T15-WO Additive-Wet 50deg
A7: D6-6G06011A-T18-WO Additive-Wet 50 deg
A8: D6-6G06011A-T20-W Additive-Wet 50 deg
A9: D6-6G06016A-T28-WO Additive-Wet 50 deg
A 10: D6-6G06016A-T30-W Additive-Wet 50 deg
A11: D6-6G07002A-T23-WO Additive- Wet 50deg
A 12: D6-6G07002A-T25-W Additive- Wet 50deg
A 13: D6-6G07002A-K1-WO Additive-Wet 50deg
A 14: D6-6G07002A-K3-W Additive-Wet 50deg
A 15: D6-6G07002A-K2-WO Additive- Wet 60 deg
A 16: D6-6G07002A-K4-W Additive- Wet 60 deg
A 17: D6-6G07002A-K5-WO Additive- Dry 60 deg
A 18: D6-6G07002A-K7-W Additive- Dry 60 deg
A 19: D6-6G07002A-K6-WO Additive- Dry 50 deg
A 20: D6-6G07002A-K8-W Additive- Dry 50 deg

A 1: D2-2G06015A-T3-Without Additive-Wet 50°C

Cycles	Left Wheel (Sample No.)				Center Wheel (Sample No.)				Right Wheel (Sample No.)				Average	Rut Depth, mm
	1		2		3		4		5		6			
25	800	790	793	793	763	753	775	784	766	766	770	777	777.50	0.00
250	873	858	840	845	817	820	810	816	792	792	793	797	821.08	-1.11
500	840	835	840	840	800	815	830	845	805	800	815	818	823.58	-1.17
1000	865	860	862	870	808	811	831	854	813	808	810	840	836.00	-1.49
2000	900	900	902	909	845	860	880	890	845	840	850	870	874.25	-2.46
3000	920	930	930	940	867	890	890	912	880	880	885	890	901.17	-3.14
4000	940	945	952	957	890	900	910	935	890	890	900	910	918.25	-3.58
5000	970	975	965	995	906	912	930	945	900	896	890	925	934.08	-3.98
6000	980	985	981	994	938	940	945	960	925	928	920	930	952.17	-4.44
7000	980	990	992	1005	940	945	954	964	935	940	940	950	961.25	-4.67
8000	985	1000	1002	1015	940	957	970	980	942	948	955	960	971.17	-4.92
9000	1005	1020	1012	1025	950	975	980	985	955	962	965	970	983.67	-5.24
10000	1025	1030	1020	1060	958	980	990	992	959	974	940	960	990.67	-5.41

A 2: D2-2G06015A-T5-With Additive-Wet 50°C

Cycles	Left Wheel (Sample No.)				Center Wheel (Sample No.)				Right Wheel (Sample No.)				Average	Rut Depth, mm
	7		8		9		10		11		12			
25	777	772	764	777	785	784	775	785	780	767	766	770	775.17	0.00
250	845	825	820	814	815	830	810	817	815	810	810	800	817.58	-1.08
500	855	840	838	830	840	850	832	840	840	830	825	815	836.25	-1.55
1000	894	878	872	855	880	884	870	875	865	880	855	840	870.67	-2.43
2000	950	925	910	960	925	930	905	905	895	890	882	867	912.00	-3.48
3000	975	960	940	940	945	953	910	925	920	900	900	890	929.83	-3.93
4000	1000	985	970	965	965	980	945	940	935	915	920	905	952.08	-4.49
5000	1022	1010	982	970	987	1000	960	955	950	935	932	915	968.17	-4.90
6000	1050	1030	1010	995	1030	1030	975	960	960	935	945	925	987.08	-5.38
7000	1070	1055	1030	1006	1020	1035	985	980	960	965	955	935	999.67	-5.70
8000	1085	1080	1045	1020	1030	1055	995	990	987	965	975	945	1014.33	-6.07
9000	1104	1095	1057	1040	1070	1070	1005	995	995	987	980	955	1029.42	-6.46
10000	1120	1120	1080	1055	1072	1090	1010	1008	1000	995	985	960	1041.25	-6.76
12000	1175	1152	1110	1080	1098	1110	1028	1018	1015	1015	995	995	1065.92	-7.39

A3: D5-5G06016A-T7-W0 Add-Wet 50deg

Cycles	Left Wheel (Sample No.)				Center Wheel (Sample No.)				Right Wheel (Sample No.)				Average	Rut Depth, mm
	1		2		3		4		5		6			
25	540	526	510	510	530	522	524	526	505	510	517	522	520.17	0.00
250	562	556	530	538	562	566	541	550	560	562	560	558	553.75	-0.85
500	585	572	547	542	580	586	562	560	574	570	585	575	569.83	-1.26
1000	594	597	574	577	600	613	580	583	590	595	600	607	592.50	-1.84
2000	622	615	590	604	644	622	597	610	625	635	650	640	621.17	-2.57
3000	645	655	618	635	674	690	623	635	660	650	655	665	650.42	-3.31
4000	655	670	642	660	693	707	656	655	670	680	705	690	673.58	-3.90
5000	676	673	650	660	715	720	680	682	690	700	720	704	689.17	-4.29
6000	700	683	673	680	720	743	693	693	700	710	735	715	703.75	-4.66
7000	705	690	690	665	735	765	700	700	720	735	750	735	715.83	-4.97
8000	710	720	695	685	748	785	710	710	740	740	756	740	728.25	-5.29
9000	720	720	695	695	753	798	710	718	735	750	760	750	733.67	-5.42
10000	720	730	705	705	763	800	715	725	760	775	775	758	744.25	-5.69

A4: D5-5G06016A-T11-W Add-Wet 50deg

Cycles	Left Wheel (Sample No.)				Center Wheel (Sample No.)				Right Wheel (Sample No.)				Average	Rut Depth, mm
	7		8		9		10		11		12			
25	547	548	550	562	525	530	524	530	523	540	548	552	539.92	0.00
250	598	610	600	615	577	573	565	567	575	574	620	625	591.58	-1.31
500	630	635	645	635	605	595	588	590	575	595	660	660	617.75	-1.98
1000	667	675	675	677	630	625	620	625	610	635	705	700	653.67	-2.89
2000	715	715	735	705	677	660	660	678	658	665	775	760	700.25	-4.07
3000	753	763	767	735	698	699	680	694	680	692	805	795	730.08	-4.83
4000	770	775	795	775	700	702	700	714	684	708	835	830	749.00	-5.31
5000	790	800	802	780	703	722	710	718	698	735	870	850	764.83	-5.71
6000	810	820	845	807	725	740	725	735	718	750	910	880	788.75	-6.32
7000	838	840	858	818	735	755	740	745	730	765	920	910	804.50	-6.72
8000	857	858	880	840	745	770	750	760	738	768	967	942	822.92	-7.19
10000	895	890	920	885	780	795	777	790	770	785	1000	980	855.58	-8.02

A5: D3-3G06020A-T13-WO Add-Wet 50deg

Cycles	Left Wheel (Sample No.)				Center Wheel (Sample No.)				Right Wheel (Sample No.)				Average	Rut Depth, mm
	1		2		3		4		5		6			
25	532	508	500	500	500	520	500	495	520	500	505	503	506.92	0.00
250	548	538	544	544	532	540	530	525	540	525	540	530	536.33	-0.75
500	565	560	567	580	540	550	548	540	548	575	560	550	556.92	-1.27
1000	610	598	635	630	567	572	584	580	590	578	587	575	592.17	-2.17
2000	660	655	670	667	595	590	615	615	612	613	613	608	626.08	-3.03
3000	670	690	700	705	618	640	645	672	630	618	652	624	655.33	-3.77
4000	690	710	735	730	680	655	674	685	630	638	658	644	677.42	-4.33
5000	695	730	752	745	680	675	676	706	660	652	676	660	692.25	-4.71
6000	728	744	756	770	692	680	692	740	670	674	692	674	709.33	-5.14
7000	748	759	790	781	680	681	707	745	675	690	690	685	719.25	-5.39
8000	750	763	810	810	687	694	710	760	690	692	710	695	730.92	-5.69
9000	750	770	835	830	693	702	725	775	707	700	720	700	742.25	-5.98
10000	760	780	860	835	700	700	735	775	710	730	720	700	750.42	-6.18

A6: D3-3G06020A-T15-W Add-Wet 50deg

Cycles	Left Wheel (Sample No.)				Center Wheel (Sample No.)				Right Wheel (Sample No.)				Average	Rut Depth, mm
	7		8		9		10		11		12			
25	523	524	520	520	518	528	515	522	532	515	510	510	519.75	0.00
250	580	558	580	565	562	560	558	565	560	558	545	540	560.92	-1.05
500	588	582	604	573	580	578	577	596	578	570	562	555	578.58	-1.49
1000	620	610	640	602	608	607	600	620	593	587	578	578	603.58	-2.13
2000	665	665	680	665	666	642	645	663	624	618	605	602	645.00	-3.18
3000	665	680	705	693	690	670	682	682	625	642	638	628	666.67	-3.73
4000	706	695	735	705	710	688	698	718	655	658	658	648	689.50	-4.31
5000	724	730	744	750	728	700	718	735	670	685	667	660	709.25	-4.81
6000	730	730	770	750	740	734	720	746	678	685	678	672	719.42	-5.07
7000	750	745	788	774	770	740	738	750	694	704	690	680	735.25	-5.47
8000	750	750	804	775	770	745	765	765	700	700	730	690	745.33	-5.73
9000	758	763	810	785	785	765	782	765	708	738	696	690	753.75	-5.94
10000	775	780	812	795	795	770	772	785	718	730	700	698	760.83	-6.12
11000	782	780	835	810	800	794	800	805	720	745	710	705	773.83	-6.45
12000	787	795	840	812	810	794	810	812	735	750	710	710	780.42	-6.62
13000	780	785	850	830	815	800	817	820	740	754	710	710	784.25	-6.72
14000	793	782	862	850	820	800	820	820	730	765	720	720	790.17	-6.87
15000	808	824	870	850	825	813	835	830	747	767	720	726	801.25	-7.15
16000	808	825	880	860	840	820	835	842	760	750	725	735	806.67	-7.29
17000	815	830	892	865	843	830	838	840	763	787	735	738	814.67	-7.49
18000	812	845	898	870	840	830	840	843	770	795	738	735	818.00	-7.58
19000	820	850	890	875	850	835	850	857	772	798	745	740	823.50	-7.72
20000	820	845	897	880	862	845	860	858	770	793	749	743	826.83	-7.80

A7: D6-6G06011A-T18-WO ADD-Wet 50 deg

Cycles	Left Wheel (Sample No.)				Center Wheel (Sample No.)				Right Wheel (Sample No.)				Average	Rut Depth, mm
	1		2		3		4		5		6			
25	410	405	405	425	448	445	438	460	429	410	406	415	426.00	0.00
250	425	422	418	440	463	460	445	474	435	410	410	430	437.00	-0.28
500	425	425	430	450	475	460	450	474	435	410	420	435	442.18	-0.41
1000	440	430	440	465	485	460	453	495	438	418	440	450	452.18	-0.67
2000	445	445	457	485	487	480	480	505	438	420	444	448	462.64	-0.93
3000	453	445	460	505	505	488	490	510	443	435	460	460	472.82	-1.19
4000	453	445	460	520	510	490	496	518	450	440	480	467	479.64	-1.36
5000	462	455	470	530	520	500	495	525	455	450	485	484	488.09	-1.58
6000	462	457	475	540	525	498	508	535	460	455	495	490	494.36	-1.74
7000	465	460	475	540	540	504	515	535	474	455	494	490	498.36	-1.84
8000	468	464	478	550	545	500	520	545	498	454	500	498	504.73	-2.00
9000	472	469	488	550	547	508	520	547	525	455	504	504	510.64	-2.15
10000	475	469	480	558	554	508	525	560	517	457	510	510	513.45	-2.22
11000	480	465	485	555	560	520	534	570	525	470	510	512	518.73	-2.36
12000	480	470	490	565	565	520	540	580	520	470	514	512	522.36	-2.45

A8: D6-6G06011A-T20-W ADD-Wet 50 deg

Cycles	Left Wheel (Sample No.)				Center Wheel (Sample No.)				Right Wheel (Sample No.)				Average	Rut Depth, mm
	7		8		9		10		11		12			
25	490	465	470	470	465	443	450	475	457	445	440	440	456.36	0.00
250	553	490	500	505	500	470	500	530	500	480	470	480	493.18	-0.94
500	543	510	520	535	510	475	535	550	506	515	487	510	513.91	-1.46
1000	580	540	543	570	528	490	560	580	528	530	505	525	536.27	-2.03
2000	642	580	585	612	545	495	625	620	563	550	563	558	572.36	-2.95
3000	670	620	640	660	570	525	640	660	595	563	590	590	604.82	-3.77
4000	710	660	680	685	585	550	695	663	618	612	625	635	637.09	-4.59
5000	740	705	698	705	595	555	725	678	630	630	640	655	656.00	-5.07
6000	770	730	725	720	615	560	750	710	640	672	670	670	678.36	-5.64
7000	780	765	740	730	620	565	755	720	645	710	690	692	693.82	-6.03
8000	800	790	760	730	620	567	780	728	650	728	710	710	706.64	-6.36
9000	818	793	790	757	640	567	782	747	660	710	716	710	715.64	-6.59
10000	825	800	790	755	630	595	790	750	690	720	745	745	728.18	-6.90
11000	830	815	790	765	615	590	765	760	690	720	745	755	728.18	-6.90

A9: D6-6G06016A-T28-WO Add-Wet 50 deg

Cycles	Left Wheel (Sample No.)				Center Wheel (Sample No.)				Right Wheel (Sample No.)				Average	Rut Depth, mm
	1		2		3		4		5		6			
25	495	496	480	490	490	485	480	490	481	490	485	482	486.27	0.00
250	512	508	492	495	500	492	495	504	480	490	515	495	496.91	-0.27
500	512	512	495	500	500	495	500	528	495	493	540	495	504.82	-0.47
1000	515	500	495	500	500	500	498	525	498	495	540	498	504.45	-0.46
2000	520	505	520	505	504	510	505	520	498	495	550	500	510.18	-0.61
3000	520	507	515	510	511	510	505	518	500	495	550	510	511.91	-0.65
5000	525	510	530	525	510	518	508	520	515	504	560	518	519.82	-0.85
7000	535	518	530	535	526	524	518	525	525	512	570	522	527.73	-1.05
8000	535	528	538	540	528	526	520	525	525	512	570	520	530.18	-1.12
10000	535	528	540	541	537	534	520	525	525	512	580	525	533.36	-1.20
12000	538	530	540	540	535	535	530	530	525	515	580	530	535.45	-1.25

A 10: D6-6G06016A-T30-W Add-Wet 50 deg

Cycles	Left Wheel (Sample No.)				Center Wheel (Sample No.)				Right Wheel (Sample No.)				Average	Rut Depth, mm
	7		8		9		10		11		12			
25	485	485	500	480	492	500	482	482	481	478	482	483	485.83	0.00
250	502	491	501	489	499	510	495	490	487	482	486	485	493.08	-0.18
1000	472	485	475	470	480	485	482	495	482	485	500	485	500.00	-0.36
2000	478	490	490	487	500	515	515	518	490	490	518	508	516.92	-0.79
3000	490	498	490	488	503	505	510	510	490	492	515	505	516.67	-0.78
4000	491	498	495	488	520	515	510	517	490	498	516	504	520.50	-0.88
5000	492	498	495	488	500	530	525	545	490	500	515	505	523.92	-0.97
6000	490	502	495	490	510	520	515	535	495	505	530	520	525.92	-1.02
7000	493	500	497	508	510	535	515	535	493	498	522	510	526.67	-1.04
8000	495	505	505	510	535	535	520	537	495	505	520	518	532.00	-1.17
10000	495	505	502	512	535	538	520	540	495	505	518	520	532.42	-1.18
12000	495	503	502	512	535	540	525	540	495	505	515	520	532.58	-1.19

A11: D6-6G07002A-T23-WO ADD- Wet 50deg

Cycles	Left Wheel (Sample No.)				Center Wheel (Sample No.)				Right Wheel (Sample No.)				Average	Rut Depth, mm
	1		2		3		4		5		6			
25	467	467	475	484	470	470	480	478	480	470	482	472	474.58	0.00
500	485	497	552	532	487	490	515	505	510	535	515	512	511.25	-0.93
2000	517	542	617	590	505	517	540	540	507	540	550	562	543.92	-1.76
4000	540	572	662	640	532	545	550	572	535	575	575	590	574.00	-2.53
6000	562	585	698	670	540	542	550	580	548	610	612	610	592.25	-2.99
8000	578	602	715	690	540	573	575	602	576	610	615	620	608.00	-3.39
10000	582	618	740	710	535	575	587	615	615	622	630	635	622.00	-3.74
12000	598	626	760	740	560	595	584	615	610	635	658	642	635.25	-4.08
14000	603	632	775	742	575	595	590	620	610	660	666	665	644.42	-4.31
16000	620	630	807	760	562	606	603	625	597	650	678	675	651.08	-4.48
18000	620	635	820	795	562	585	605	635	595	658	682	685	656.42	-4.62
20000	630	662	850	790	575	585	605	630	597	665	690	695	664.50	-4.82

A 12: D6-6G07002A-T25-W ADD- Wet 50deg

Cycles	Left Wheel (Sample No.)				Center Wheel (Sample No.)				Right Wheel (Sample No.)				Average	Rut Depth, mm
	7		8		9		10		11		12			
25	463	483	485	500	493	498	494	498	507	498	490	505	492.83	0.00
500	524	526	525	512	498	508	518	508	526	530	535	532	520.17	-0.69
2000	580	585	587	575	530	535	522	515	552	560	570	562	556.08	-1.61
4000	610	635	644	630	545	558	565	560	572	584	610	580	591.08	-2.50
6000	630	640	655	640	565	575	577	575	592	618	619	590	606.33	-2.88
8000	640	638	672	664	567	590	587	584	603	630	630	591	616.33	-3.14
10000	648	652	695	678	588	597	595	587	600	645	665	615	630.42	-3.49
12000	662	670	707	687	590	607	604	615	604	650	670	625	640.92	-3.76
14000	680	700	720	710	600	610	602	632	615	660	675	635	653.25	-4.07
16000	690	715	738	710	607	620	614	650	614	665	684	644	662.58	-4.31
18000	687	705	780	720	610	625	610	640	617	670	687	644	666.25	-4.40
20000	694	705	784	740	615	640	610	620	630	665	687	670	671.67	-4.54

A 13: D6-6G07002A-K1-WO Add-Wet 50deg

Cycles	Left Wheel (Sample No.)				Center Wheel (Sample No.)				Right Wheel (Sample No.)				Average	Rut Depth, mm
	1		2		3		4		5		6			
25	752	754	750	751	750	750	748	762	757	750	747	758	752.42	0.00
250	795	801	830	815	776	770	780	780	778	768	770	800	788.58	-0.92
500	822	818	843	825	788	782	806	818	785	795	802	815	808.25	-1.42
1000	845	842	860	853	810	812	840	834	800	810	820	830	829.67	-1.96
2000	892	895	935	950	860	870	910	910	825	845	870	908	889.17	-3.47
4000	915	920	935	950	887	895	930	872	837	882	880	905	900.67	-3.77
6000	920	925	940	940	895	890	935	900	845	878	880	897	903.75	-3.84
8000	940	960	955	980	930	935	957	920	860	915	908	930	932.50	-4.57
9000	995	1004	990	1010	935	950	960	930	855	950	915	950	953.67	-5.11

A 14: D6-6G07002A-K3-W Add-Wet 50deg

Cycles	Left Wheel (Sample No.)				Center Wheel (Sample No.)				Right Wheel (Sample No.)				Average	Rut Depth, mm
	7		8		9		10		11		12			
25	760	760	762	760	756	762	767	768	754	750	750	762	759.25	0.00
250	787	786	802	801	766	773	780	785	770	767	792	806	784.58	-0.64
500	805	809	837	845	785	786	805	810	775	778	798	807	803.33	-1.12
1000	816	822	840	854	787	800	820	832	792	785	806	810	813.67	-1.38
2000	840	845	860	882	795	815	865	867	800	800	815	815	833.25	-1.88
4000	870	860	860	850	820	817	867	905	810	792	822	835	842.33	-2.11
6000	880	875	872	870	824	840	882	910	840	835	850	855	861.08	-2.59
7000	885	875	875	880	826	845	884	910	850	845	850	860	865.42	-2.70
8000	905	908	935	940	860	867	916	940	850	850	860	865	891.33	-3.35

A 15: D6-6G07002A-K2-WO Add- Wet 60 deg

Cycles	Left Wheel (Sample No.)				Center Wheel (Sample No.)				Right Wheel (Sample No.)				Average	Rut Depth, mm
	1		2		3		4		5		6			
25	520	510	520	535	502	498	515	520	516	505	492	503	511.33	0.00
250	580	595	580	585	518	535	580	580	540	535	515	538	556.75	-1.15
500	607	630	598	595	540	572	608	610	568	580	545	548	583.42	-1.83
1000	640	668	635	625	575	618	640	645	575	600	565	568	612.83	-2.58
2000	685	705	680	665	603	668	685	680	605	602	570	608	646.33	-3.43
3000	718	740	720	715	650	705	712	706	625	618	618	630	679.75	-4.28
4000	738	778	732	730	676	715	740	720	648	640	630	640	698.92	-4.76
5000	762	780	762	770	682	730	758	746	660	660	630	655	716.25	-5.20
6000	785	820	790	820	690	752	776	765	670	680	640	670	738.17	-5.76
7000	800	890	795	830	710	765	795	778	698	693	650	682	757.17	-6.24
8000	835	930	832	832	740	778	810	790	685	704	660	695	774.25	-6.68

A 16: D6-6G07002A-K4-W Add- Wet 60 deg

Cycles	Left Wheel (Sample No.)				Center Wheel (Sample No.)				Right Wheel (Sample No.)				Average	Rut Depth, mm
	7		8		9		10		11		12			
25	510	512	515	510	516	520	550	530	517	505	500	510	516.25	0.00
250	545	547	567	547	555	570	605	580	545	557	550	545	559.42	-1.10
500	555	578	610	575	553	593	635	608	560	582	580	562	582.58	-1.68
1000	597	608	645	605	585	615	655	622	575	600	598	590	607.92	-2.33
2000	625	640	682	645	595	645	690	670	602	630	655	618	641.42	-3.18
3000	645	655	705	670	625	665	700	680	617	650	650	632	657.83	-3.60
4000	650	684	722	687	635	677	724	705	625	650	655	648	671.83	-3.95
5000	685	698	740	705	645	690	748	720	628	680	700	680	693.25	-4.50
6000	675	710	755	710	665	705	760	720	642	690	705	688	702.08	-4.72
7000	688	718	778	740	675	715	770	735	648	690	705	700	713.50	-5.01
8000	698	730	785	750	680	720	780	750	660	690	705	700	720.67	-5.19

A 17: D6-6G07002A-K5-WO Add- Dry 60 deg

Cycles	Left Wheel (Sample No.)				Center Wheel (Sample No.)				Right Wheel (Sample No.)				Average	Rut Depth, mm
	1		2		3		4		5		6			
25	499	500	506	500	500	508	500	510	500	495	505	495	501.50	0.00
500	585	605	605	595	540	585	585	590	570	580	570	585	582.92	-2.07
2000	680	690	695	690	600	665	690	660	600	605	625	670	655.83	-3.92
4000	740	760	800	820	670	730	755	715	645	695	675	715	726.67	-5.72
6000	795	785	840	855	670	785	805	765	695	750	735	770	770.83	-6.84
8000	880	920	875	860	700	820	860	820	730	810	760	805	820.00	-8.09
10000	930	940	930	980	780	860	905	860	775	845	815	845	872.08	-9.41

A 18: D6-6G07002A-K7-W Add- Dry 60 deg

Cycles	Left Wheel (Sample No.)				Center Wheel (Sample No.)				Right Wheel (Sample No.)				Average	Rut Depth, mm
	7		8		9		10		11		12			
25	510	505	512	505	510	515	518	510	510	500	510	520	510.42	0.00
500	545	558	558	575	535	545	550	535	545	560	550	545	550.08	-1.01
2000	595	625		628	575	580	610	595	570	625	615	620	603.45	-2.36
4000	635	670	625	655	640	600	635	630	595	675	670	685	642.92	-3.37
6000	665	698	715	700	665	670	675	675	620	670	715	720	682.33	-4.37
8000	685	720	740	730	690	718	700	705	635	730	755	775	715.25	-5.20
10000	708	745	750	750	720	718	718	722	665	755	785	805	736.75	-5.75

A 19: D6-6G07002A-K6-WO Add- Dry 50 deg

Cycles	Left Wheel (Sample No.)				Center Wheel (Sample No.)				Right Wheel (Sample No.)				Average	Rut Depth, mm
	1		2		3		4		5		6			
25	493	485	486	510	515	495	485	485	480	482	480	480	489.67	0.00
500	510	492	510	515	520	510	500	502	490	490	487	495	501.75	-0.31
2000	528	520	532	538	530	528	515	515	500	505	498	502	517.58	-0.71
4000	548	545	566	552	545	548	526	526	502	507	505	510	531.67	-1.07
6000	570	575	598	585	565	570	540	545	510	515	515	525	551.08	-1.56
8000	587	597	620	608	585	590	555	550	515	523	530	540	566.67	-1.96
10000	590	608	632	625	602	605	570	578	520	530	540	550	579.17	-2.27

A 20: D6-6G07002A-K8-W Add- Dry 50 deg

Cycles	Left Wheel (Sample No.)				Center Wheel (Sample No.)				Right Wheel (Sample No.)				Average	Rut Depth, mm
	7		8		9		10		11		12			
25	490	490	490	490	503	500	505	510	500	500	490	503	497.58	0.00
500	505	505	520	500	510	510	508	510	500	505	505	510	507.33	-0.25
2000	524	530	545	530	528	522	525	550	510	520	520	530	527.83	-0.77
4000	550	558	560	545	548	538	535	550	525	540	540	545	544.50	-1.19
6000	572	582	580	558	565	552	558	565	540	560	562	570	563.67	-1.68
8000	588	602	595	575	580	570	560	580	565	580	585	595	581.25	-2.13
10000	602	615	608	585	592	582	587	560	580	602	602	610	593.75	-2.44